Overhanging

Lower Riverbank Slope:

Flat

Moderate

Steep

Vertical

Upper Riverbank Sediment:

Silt/Sand

Rock

Lower Riverbank Sediment:

Silt/Sand

Gravel

Cobbles

Boulders

Rock

Clay

Upper Riverbank Height:

Low

Medium

High

Degree of Upper Riverbank Vegetation:

Heavy

Moderate

Sparse

None to very sparse

Lower Riverbank Vegetation:

Heavy

Moderate

Sparse

None

Mass Wasting:

Little/None

Little/None

Little/None

Some

Some

Extensive

Extensive

Extensive

Erosion Type:

None

Notching

Overhanging bank

Undercut Toe

Slide

APPENDIX D – RED HEN SYSTEMS GEO-REFERENCED VIDEO MAPPING

Red Hen Systems Geo-Referenced Video Mapping

VMS-HD Complete System Bundle Includes:

- Red Hen VMS Hardware
- Convergent Design nanoFlash HD/SD Digital Video Recorder/Player
- Desktop GIS Software: MediaMapper 5.3*
- GPS Antenna/Receiver
- Feature Trigger (on board)
- 4" Microphone Jack Cable
- Power Adapter with International Plugs
- Hirose Power Cable
- Flash Card Reader/USB Cable
- Pelican Case
- Manuals

Convergent Design nanoFlash HD/SD Digital Video Recorder/Player

Introducing the World's smallest high quality HD/SD-SDI / HDMI Recorder/Player. The nanoFlash by Convergent Design is the most versatile Recorder/Player in the World in terms of bit-rates, recording options and formats. By adding the nanoFlash , one can meet the acquisition requirements, 50 Mbps, for many networks. The nanoFlash is a state-of-the-art miniature CompactFlash HD/SD SDI and HDMI Recorder/Player. Red Hen Systems is pleased to have been selected as the premier Spatial Multimedia Reseller and GIS Integration partner for the nanoFlash by Convergent Design.

- Improves the image quality of most cameras as the HD/SD-SDI and HDMI outputs are before the compression stages.
- Many cameras only record highly compressed 4:2:0 while outputting 4:2:2 over HD-SDI or HDMI.
- The nanoFlash uses these high-quality uncompressed 4:2:2 images to produce higher quality recordings.

The nanoFlash offers a dramatically better image, free from motion artifacts and other image problems, such as mosquito noise. Typically the nanoFlash offers a better image, even from many high-end cameras.

Wide Range of Bit-Rates

- 4:2:2 Long-GOP from 50 to 180 Mbps Long-GOP
- 4:2:2 I-Frame Only from 100 to 280 Mbps
- 4:2:0 Long-GOP from 18 to 35 Mbps
- SD 5/6/7/8/9 Mbps

Wide Range of Frame Rates

- Supports HD-SDI, SD-SDI and HDMI inputs
- Works with most any camera with HD/SD-SDI or HDMI outputs HD/SD-SDI and HDMI outputs active simultaneously
- Long, Uninterrupted Recording Times

Records in:

- Native Quicktime for Final Cut Pro
- Native MXF for Avid, Sony Vegas, Edius, others
- MPG Format in SD for quick same day creation of DVD's
- MPG Format in HD - Realtime Rendering of Blu-Ray disks
- No Mandatory Transcoding - Drag and Drop Editing

- All Solid-State - No Moving Parts - No Fans - No Noise - Field Proven Rugged - Withstands Extreme Temperatures - High Humidity - High Altitudes - High Vibration - High G-Forces
- Camera Mountable - 0.85 Pounds - 1/4" x 20 Tripod Thread
- Very Low Power - 5.6 Watts maximum, 0.2 watts standby Wide Voltage Range - 6.5 to 19.5 Volts DC - Uses most any battery type - International AC Power Supply included

- Supports Timecode and Audio embedded in HD/SD-SDI
- Supports Audio embedded in HDMI
- Supports Analog Audio, 24-Bit/48K, with up to 44 dB of gain via 3.5 mm audio input, compatible with tape-out signals
- One Channel balanced audio consumer line level / mic, orT
- Two Channel unbalanced audio consumer line level / mic

All audio recorded at 24-Bit/48K Uncompressed
Headphone / Consumer line-level outputs

2 CompactFlash card slots - Records seamlessly from one card to the next
The image quality produced by the nanoFlash is exactly the same as the Flash XDR.

VMS-HDII

Our easy-to-use digital camera accessories and GPS video digital recorders let you collect video imagery - along with essential location information. Our GIS software lets you process the imagery and generate multimedia maps that bring vital information to the eyes and fingertips of decision-makers. With the click of a button you know where something is, as well as what it looks like. And you can share the maps with others over the Internet.

This system combines Red Hen's VMS-333 with the nanoFlash recorder from Convergent. Completely customizable, now add up to 4 channels of recording for UltraViolet, Infrared, Standard Definition, and/or High Definition. Expand the information in your data collect for more comprehensive results. In our most portable, light-weight size yet, the HDII is especially suited to collect geo-tagged "path" HD video from all mobile platforms, such as aircraft, ground vehicles and marine vessels.

Features:

- Format: Record in High-Definition or standard definition
- Recording: All video and GPS data encapsulated in a single file on compact flash card, seamlessly switches recording from card 1 to card 2
- GPS: WAAS-enabled for greater location accuracy in the US; supports international SBAS (Satellite Based Augmentation System) in Europe and Asia
- Feature Trigger: Allows you to "mark" points of interest for quick analysis
- Photo Capture: Automatically capture geo-referenced still photos from High-Definition video
- Analysis: MediaMapper 5.3 software allows for subject matter experts to create electronic work products

Benefits:

- Competitive price, with unprecedented High-Def and multimedia mapping functionality
- Light weight, portable — easily switch between aircraft and vehicles, or carry on foot
- Removable compact flash cards allow for archiving of original recording — ideal for law enforcement
- All Solid-State design - Ideal for Extreme Environments

Supported Video Input Formats:

· 1920x1080i @ 60, 59.94, 50 Hz
· 1920x1080p @ 30, 29.97, 25, 24, 23.98 Hz
· 1920x1080psf, @ 30, 29.97, 25, 24, 23.98 Hz
· 1280x720p @ 60, 59.94, 50 Hz
· 720x486 @ 29.97 Hz
· 720x576 @ 25 Hz

.mts & .m2ts file types may not work correctly and therefore are not supported.

Appendix E – Previous data and information for Adult American shad

Bibliography for Adult Shad Movement Studies at the Turners Falls Complex In Chronological Order

Northeast Utilities Service Company. (1985). *The Movements and Behavior of Migratory American Shad in the Turners Falls Project Power Canal. Radio Telemetry and Hydroacoustic Studies*. Hartford, CT: Author.

Biosonics, Inc. (1985). Hydroacoustic Studies of Adult American Shad in the Cabot Station Power Canal, Turner's Falls, Massachusetts. Draft Report, prepared for Northeast Utilities Service Co., Harford, CT: Author.

Environmental Research and Consulting, Inc. (ERC) (1987). *Radiotelemetry Study of American Shad in the Turners Falls Power Canal*. Prepared for the Northeast Utilities Service Company. Hartford, CT: Author.

Sullivan, T., Haro, A., & Castro-Santos, T. (2001). *Passage of American Shad at Turners Falls Fishways: PIT Tag Evaluation* (CAFRC Internal Report No. 2002-01). Turners Falls, MA: S.O. Conte Anadromous Fish Research Center.

S.O. Conte Anadromous Fish Research Center. (2003). *Preliminary Results: Turners Falls Fish Passage Studies*. Author

S.O. Conte Anadromous Fish Research Center. (2004). *Preliminary Results: Turners Falls Fish Passage Studies*. Author.

Sullivan, T.J. (2004). *Evaluation of the Turners Falls Fishway Complex and Potential Improvements for Passing Adult American Shad*. (M.S. Thesis). University of Massachusetts, Amherst.

Haro, A. & Castro-Santos, T. (2005). *Turners Falls Fish Passage Studies 2005*. S.O. Conte Anadromous Fish Research Center.

Haro, A. & Castro-Santos, T. (2009). *Turners Falls Gatehouse Telemetry Studies, 2009 Interim Report*. S.O. Conte Anadromous Fish Research Center.

Haro, A. & Castro-Santos, T. (2010). *Synopsis of 2010 Gatehouse Fishway Telemetry Studies*. S.O. Conte Anadromous Fish Research Center.

Appendix F – Turners Falls Upstream Fish Passage CFD Modeling of Gatehouse Entrance

Turners Falls Upstream Fish Passage CFD Modeling of Gatehouse Entrance

By:

Songheng Li, Ph.D., P.E.

George E. Hecker, P.E.

Andrew E. Johansson

Submitted to:

First Light Power Resources

20 Church Street

Hartford, CT

February 2013

1115TFCFD-R1

ALDEN RESEARCH LABORATORY, INC

TABLE OF CONTENTS

LIST OF TABLES

LIST OF FIGURES

This page left blank purposefully

ABSTRACT

Observation of 2010 fish passage revealed that only about 50% of Shad in the power canal passed the Turners Falls gatehouse fishway. Various modifications had been made over a number of years to improve passage, including the construction of an additional entrance in the canal and internal changes to the original ("old") canal entrances. To better understand the effects on the hydraulics of the modifications made to date, to improve flow and velocity conditions in the fishway at the old entrance, and to develop concepts for possible further enhancements at the old entrance, Alden was contracted by FirstLight to model the gatehouse ladder and its canal entrances from the upstream pool to the downstream junction with the spillway ladder. This model included the gate house with all its gates and the upstream end of the canal.

In order to achieve the objectives, a three-dimensional (3D) computational fluid dynamics (CFD) model was first developed for the available canal bathymetry and present (2012) fishway structures, using Flow3D by Flow Science. The model was then validated using field data from 3/16/2006 (head gates operating without fishway flow) and 5/27/2009 (both fishway and head gates operating). Following these validation cases, the model was run for two additional field scenarios corresponding to conditions on 5/24/2008 (low flow) and 5/20/2009 (moderately high flow). For both of the additional scenarios, both the head gates and fishway were in operation.

The CFD results of the validation cases showed good agreement with the field data indicating that the model was accurately reproducing the hydraulic conditions of interest. Further, the validation cases as well as the base low and moderately high flow scenarios revealed some flow conditions that can be improved for fish passage in the fishway, at the old entrances and in the canal downstream of the gatehouse.

Based on the results of the CFD model with the existing geometric configuration, it was decided to investigate modifications that would enhance fish passage. The first modification considered, Modification 0 (abbreviated as Mod 0), was the design of an additional section of fish ladder extending from the remaining old entrance into the canal. Design parameters included a flow rate

of 180 cfs and a total water drop of 2.5 ft. After some consideration, it was concluded that this new ladder may be less effective than Modification 1 (discussed below) and therefore no CFD simulations were conducted for Mod 0.

Modification 1 (abbreviated as Mod 1) focused on the region inside the old entrance in the sloped diffuser area to achieve a design flow rate of 180 cfs through the old entrance. Modifications included: 1) adding a vertical concrete wall to create a channel separating the flow to the old entrance (left) from that flowing to the new entrance and spillway ladder (right); 2) closing the existing three upstream openings in the floor of the fish way just upstream of the diffuser; 3) keeping a left diffuser opening of 18 ft and closing the remaining part of the left diffuser; 4) adding two single slotted weirs in the left channel; 5) adding an orifice at the entrance of the left tunnel to the diffuser; 6) cutting down the sill at the old entrance from El. 168.2 ft to El. 166 ft and removing the stop-logs. A CFD simulation was conducted with Modification 1 using Validation Case 2 flow conditions but with new gate openings.

Lastly, Mod 1 was further refined to arrive at Modification 2 (abbreviated as Mod 2) which included: 1) adding a baffle at the right side of the new left channel; 2) narrowing the slot width of the added upstream slot in Mod 1; 3) removing the existing baffle at the left side of the old entrance and adding a new wider baffle at the right side of the old entrance ; 4) re-aligning the angled wooden diffuser in the left channel; 5) enlarging the orifice at the entrance of the left tunnel . Mod 2 was then tested with new gate openings and pond water level.

1. INTRODUCTION

1.1 Background

With the old and new entrances operating, following the last round of operational and structural improvements, even with the latest changes, only about 50% of the fish in the power canal passed through the gatehouse fishway in 2010. In order to better understand the effects on the hydraulics of the modifications made to date, to improve flow and velocity conditions in the fishway at the old entrance, and to develop concepts for possible further enhancements at the old entrance, FirstLight contracted Alden Research Laboratory (Alden) to conduct a Computational Fluid Dynamics (CFD) model study of the modified Tuners Falls gatehouse fishway including gatehouse ladder, its entrances to the upper end of the spillway ladder.

1.2 Project Description

The Turners Falls Gatehouse is located at the upstream end of the Cabot Station power canal in Turners Falls, MA. The gate house has 14 operating gates and one gate opening plugged with concrete during the renovation of the gatehouse for the Northfield pumped storage project. Width and height of each gate opening is listed in Table 1. Each gate is operated independently and field experience has indicated a generally preferred operating sequence to control canal flow patterns and water levels.

The power canal between the Turners Falls Dam Gatehouse and Cabot Station is approximately 2.2 miles in length. The canal width varies. The width at the gatehouse is approximately 180 ft while 360 ft downstream of the gatehouse the width decreases to 120 ft. From this point downstream, the width increases and opens out into the forebay of Cabot Station. The unlined canal is excavated in rock and concrete walls are constructed from the top of the rock to the top of the canal, some of the rock above the top of the canal is exposed. Canal walls south of the railroad bridge are rock lined embankments.

The Turners Falls Pond level varies between El. 184.0 and El. 176.0 ft when fishway is operating and not flood flows. The power canal water level at the downstream side of the gatehouse varies.

The level on the left side of the canal commonly gets down to 173.5 ft (ever lower at times), and doesn't exceed 175 ft very often. The right side of the canal may be somewhat higher than the left side, but not much at medimum to low canal flow. Due to the bend in the canal immediately downstream of the gatehouse, the canal water surface tends to be super elevated across the downstream face of the gatehouse, with higher water level on the right side of the canal looking downstream.

The Turners Falls Fish Passage Facilities consist of three separate structures: the Cabot fishway, Gatehouse fishway, and Spillway fishway. The Cabot Fishway, located at Cabot Station, enables upstream migrating fish to ascend to the power canal from the river. Once in the power canal, the fish swim two miles to reach the Turners Falls Gatehouse. The Spillway Fishway, located at the spillway of the Turners Falls Dam, permits any fish which have by-passed Cabot Station and arrived at the base of the dam, to ascend up into the Gatehouse Fishway where they can continue their upstream migration. The Gatehouse Fishway enables fish to swim from the power canal, through the south end of the Gatehouse and up into the Turners Falls Pond.

There are two entrances to the Gatehouse fishway. The original entrance is located on the left end of the gatehouse (looking downstream) and originally utilized three 5 ft wide openings each with a sill elevation of 170.0 ft. Currently, two of the three entrances are closed (to provide the required attraction flow to the new fish entrance) and only the southwestern most entrance is used for passage. Internal changes were also made to better guide the flow to the old entrance and for the remaining flow to turn 90 degrees into the gatehouse gallery. The new second entrance is located near the right end of the gatehouse and canal, looking downstream, immediately adjacent to the top of the spillway fish ladder.

1.3 Prior Studies

Hydraulic model studies of portions of the spillway and gatehouse fishways at Turners Falls were performed at Alden in 1975 (Pennino and Hecker 1975). The objective of that study was to locate the spillway fish ladder entrance in relation to spillway flow over the dam so that flows from the entrance would be effective in attracting fish. Model testing of the gatehouse fishway with the slotted weirs showed that a wall parallel to the shoreline would allow satisfactory flow pattern at the fishway exit. Testing also showed that an increase from six to seven weirs would beneficially reduce the average head drop across the weirs and the maximum velocities at the additional slots.

1.4 Study Scope

The scope of work for the current study included the followings:

1.4.1 Model Development

The proposed model simulations were conducted using the commercial code FLOW-3D by Flow Science. Setup of a FLOW-3D model requires development of solid models to represent the canal bed, fishways, gatehouse gallery geometry, etc. The canal bottom was based on the available bathymetric data. The model included the area downstream of the existing sluice and gate structures, the gatehouse fishway, the spillway fish ladder, the entrance gallery and all related internal geometry that would affect flow patterns, and the spillway fishway attraction water entrance geometry. The model initially represented the existing field configuration.

A computational mesh was applied to the model with structured variable grid spacing. The model was tested for numeric stability and to ensure the grid resolution is sufficient.

1.4.2 Model Validation

Model validation was completed using available field data related to flow and water level. Water level information for selected low and moderately high flow conditions was used to validate and potentially calibrate the numeric model such that observed and predicted water surface profiles are in agreement.

1.4.3 Base Model Runs

The model was run at two operating conditions of interest, selected with FirstLight, to evaluate existing hydraulic conditions and to be used as a basis for development of potential modifications. These flow conditions, not necessarily the same as used in the model validation task, were envisioned to include unique combinations of canal water level, gate opening and total flow. These simulations bounded the performance of the fishway entrances and provide a basis upon which modifications were considered and evaluated. Consequently, there are two model runs using the base (existing) geometry and varying only the site flow conditions.

For each simulation, a series of plots were created showing horizontal and vertical planes colored by water velocity and showing velocity vectors in selected planes at the entrances and within the fishway and gallery. A series of plots showing vertical planes through the power canal were created to show the water velocity and depth along the length of the canal. Plots of pathlines were created to show the general flow patterns throughout the model domain. Animations were used to help visualize flow patterns.

1.4.4 Fishway Modifications and Simulations

Three modifications to the gatehouse fishway geometry were included to improve hydraulic conditions at the fishway entrances and in the entrance gallery. Two geometric modifications were evaluated at flow conditions studied in base model runs or other selected flow condition. Comparisons were made between the geometric modifications to select the most promising option.

1.5 Objectives

The main objective of the modeling is to study and improve the hydraulic conditions for upstream passage of American Shad at the original gatehouse fish entrance (the old entrance). Specifically, topics of interest include flow patterns in the canal approaching the fishway entrance and the water level drop(s) and internal flow patterns at the old entrance.

2. CFD MODEL

2.1 Model Description

Prior to the development of the model, the following principal aspects need to be considered:

- The three dimensional (3D) complex geometry and the complicated 3D dynamic features of flow require a full 3D model for this study.
- Water is the working fluid in this study and the changes in water density are sufficiently small to be ignored, therefore, the flow was modeled as an incompressible fluid.
- Water is a Newtonian fluid. Its shear stress is essentially linearly related with strain by a coefficient of viscosity.
- Is the flow inviscid or viscous? In viscous flow, fluid friction has significant impacts on the fluid motion. The Reynolds number is usually used to evaluate whether viscous or inviscid equations are appropriate. Using the flow rate of about 8000 cfs (5/27/2009 data of Validation 2) and the average canal width of 180 ft and water depth of 18.5 ft, the flow Reynolds number, defined as $Re = \rho U D_H/\mu$, in which U=mean velocity, ρ=water density, μ=dynamic viscosity, $D_H = 4A/P_W$ =hydraulic diameter, A=area, P_W = wetted perimeter, is found to be in the order of $1.4\text{x}10^7$. This is much higher than the value of 2000 that is usually used to determine the transition from laminar to turbulent flow. Although the high flow Reynolds number indicates that inertial forces are much more significant than the viscous (friction) forces, however, the presence of solid boundaries does require that fluid viscosity be included. The "no-slip" condition (velocities relative to solid walls are zero) can generate a thin boundary layer with large strain rate (velocity gradient), which will affect the outer fully-developed turbulent flow and generate internal eddies and losses. Therefore, viscous flow was used for this study.
- Laminar or turbulent flow. Turbulence can usually be characterized by random eddies with different length scales. In turbulent flow any instantaneous quantity can be mathematically expressed as the summation of an average (mean) and a fluctuating term by the so-called Reynolds decomposition. Turbulent flow can be well described by the Navier-Stokes equation which is derived from Newton's Second Law of Motion. Judging from the flow Reynolds number of $1.4\text{x}10^7$, the flow in the present study is turbulent. This Reynolds number is too high for application of a Direct Numerical Simulation (DNS) due to the lack of current computer power. However, only the mean flow features are of interest in real-life engineering problems. Substituting the Reynolds decomposition into the instantaneous Navier-Stokes equations yields the Reynolds-Averaged-Navier-Stokes (RANS) equations. The averaging process creates a new term,

the so-called Reynolds stress, in the equation system. The RANS equations used in this study combined with turbulence modeling provides an effective way to simulate the effects of turbulent flow.

- Steady (no variations with time) or unsteady (time varying) flow. Unsteady-state flow refers to the flow condition where flow properties (such as velocities, pressure, temperature) at any point in the system do change over time. Free surface flow is the most important characteristic of flow in this study. For such kind of flow with sharp surface formation a necessary approach is to solve the RANS equations with time variation, seeking the results when the flow is developed close to a steady-state situation.
- Fluid temperature. Change of water temperature through the entire computational domain is negligible. There was no need to include the internal energy (or temperature) equation.

Based on the above consideration, the governing equations to be solved are the RANS and turbulence modeling equations for 3D, transient, Newtonian, incompressible, viscous flows without heat transfer.

The commercial CFD code FLOW-3D by Flow Science was used. FLOW-3D solves the fully three dimensional Navier-Stokes equations on a structured hexagonal grid. Several turbulence models are included in the solver for computing the creation, transport and dissipation of turbulent kinetic energy.

The Boussinesq hypothesis is used to relate the Reynolds stress tensor in the RANS equations proportionally to the mean strain rate tensor via a scalar property called eddy viscosity μ_t. This eddy viscosity becomes an unknown parameter and needs to be calculated. The turbulence model serves this purpose. There is no single turbulence model that is best for all kinds of flow problems. Selecting a turbulence model is based on the physics of the problems to be solved, the level of accuracy required, available computer resources, allowed computing time, even personal preference and established practice for a specific class of flow problems. Therefore, it is usually a challenging task to select a suitable turbulence model for hydraulic flow simulations. It is necessary to choose a more refined turbulence model to predict more complex flow patterns such as separating flows, rotating flows, and flows strongly affected by secondary-flows. The common choices for this kind of complex flows are the two-equation turbulence models which are widely used in real-life engineering problems. This usually includes the standard k-ε model, Renormalization-group (RNG) k-ε model, Realizable k-ε model, standard k-ω model, shear-stress transport (SST) k-ω model, etc. Two-equation turbulence models usually overproduce turbulent energy within regions with strong velocity gradients, and different models behave differently in these regions. It has been shown that the k-ε model is useful for free-shear layer flows with relatively small pressure gradients. Relatively speaking, the standard k-ε is probably the worst choice, its variant models (RNG and Realizable k-ε models) may behave better. For this application, the Renormalized Group (RNG) k-ε model was used.

FLOW-3D model uses the Fractional Area/Volume Obstacle Representation (FAVOR) for the modeling of solid obstacles, such as topology, structure members. The FAVOR method allows complex shapes to be simulated without resorting to stair stepping the boundaries. The location of the free surface is computed using the Volume of Fluid (VOF) method. This formulation consists of a scheme to describe the shape and location of the free surface, a method to track the evolution of the shape and location of the free surface through time and space, and a means for applying boundary conditions to the free surface.

2.2 Assumption and Limitation

Impact of air motion above the water surface to the water flow is assumed negligible. Therefore, air movement was not included in the simulation and only water flow was simulated. This simplification yields a considerable reduction in required computational resources and is reasonable for this application.

The Weber number of flow is defined as: $We = \rho V^2 L/\sigma$, in which σ=surface tension of water, V=velocity, ρ=water density, L=characteristic length. Using the mean canal velocity of 2.4 ft/s (for Validation 2 data) and hydraulic diameter for characteristic length L=62 ft, water density ρ=62.37 lbm/ft^3, and σ=5.04x10^{-3} lbf/ft (60F degrees of water), the calculated Weber Number (We) =4419, which is much larger than 1. Therefore, effect of the water surface tension is negligible.

2.3 Geometry and Computational Mesh

Based on the geometry information provided, a solid model was created of the bathymetry and structures in AutoCAD, and STL format files were output. Then the STL files were imported into FLOW-3D model for mesh generation.

Figure 1 shows the general 2D view of the CFD model with the current geometry and structure configuration. The coordinates (X, Y, and Z) are in unit of foot throughout the report. The model consists of several main parts:

- **The whole length of the upstream slotted weir channel (see** Figure 2**)**: Initially it was proposed to just model a couple of the downstream slotted weirs (#7 and #6). However, the lack of suitable data at weir #6 made it impossible to set up the appropriate boundary condition at this location. Practically this location is not ideal for a boundary for a free surface flow problem. Therefore, the model at the slotted weir area needed to be extended all the way upstream to the pond. Including all the seven weirs and the entire channel to the pond facilitated the upstream boundary condition.
- **Attraction water tunnel:** The attraction water tunnel is underneath the slotted weir channel except the most upstream inlet portion which turns at an angle. The flow into the attraction tunnel is through and controlled by two separated adjustable gates AGW 15 and AGW 16 (see Figure 2). The openings of the gates are adjusted to provide the attraction flow that maintains the desired water surface elevation difference between the galley and the canal. This elevation difference can be varied by the operator.
- **Sloped floor diffuser (**Figure 3): Figure 4 shows a zoom-in view of the sloped floor diffuser channel. Attraction flow from the tunnel underneath passes the sloped diffuser to join the flow from the slotted weir channel above, providing fish passage attraction flow to the old entrance and gallery to the new entrance and spillway ladders. At the upstream end of the sloped diffuser, there are three separated openings connecting the underneath attraction flow tunnel to the slotted weir channel above.
- **Gatehouse:** In total, there are 15 individual gates, as shown in Figure 5. Gate 6 is plugged with concrete. The opening of each gate is determined by the operating condition being simulated.

- **Gallery Turning Vanes:** There are turning vanes to the new entrance in the gallery which will impact the flow patterns in the gallery.
- **New entrance:** The whole length of the new entrance was modeled, as shown in Figure 3.
- **Power Canal**: At the right side canal bank downstream of the new entrance there are two gates (AWG 27 and AWG 28, see Figure 6) to control attraction flow to the spillway fish ladders. The CFD model downstream boundary is located at about 700 ft upstream of Keith Bridge. This location was selected to assure the boundary was far enough from the gatehouse so as not to affect results but not too far downstream (to reduce necessary computational cells and computational time). To account for the impact of the roughness of the canal bathymetry to the flow field, the canal bed was divided into several zones with different roughness heights, and couple runs were tested to determine the roughness heightness, as shown in Figure 7. Basically the roughness height is about 2 ft at the right side of the canal, 1 foot at the left side of the canal, and 1 foot in the downstream section of the canal. For Validation 2, there was a rock ramp just downstream from the old entrance, the roughness height for which was set to 2 ft.

Grid generation included the creation of multiple structured mesh blocks over the entire model domain. Cell spacing varied along the three coordinate directions, however, variations in the grid spacing are required to be carried through the entire mesh block. The ability of the model to accurately reproduce the flow field is dependent on the grid resolution in the area of interest. A finer grid requires more computational time to arrive at a final solution. Often, multi-block meshing is used to reduce the overall size of the model domain. In a multi-block mesh flow passes from one mesh block to another at the mesh block interface where the computational mesh of the two neighbor blocks is not required to match. Much finer mesh was required at the slotted weir channel, gallery, and new entrance area. Due to the meshing considerations above it was not practical to model the turning vanes to the new entrance in the gallery as thin plates. A commonly used approach which has little impact on the simulation results is to model the vanes as zero thickness baffles (blockage). Since Flow3D uses a Cartesian mesh these zero thickness baffles need to be located along a cell face. Hence the curved portion of the vanes was approximated using small straight segments as shown in Figure 8. This approximation does not have an impact on the bulk flow patterns created by the turning vanes. The resulting model meshes for the existing and modified geometries included about 3.6 million and 4.5 million active cells, respectively.

2.4 Boundary Conditions

There are six side face boundaries in each single structured mesh block that require boundary conditions to conduct the simulation. At the interface connecting the neighbor mesh blocks, a symmetry boundary condition was usually applied. Special attention was needed for model boundaries and these are prescribed as follows:

- At the pond side, a pressure boundary condition was applied by specifying the appropriate water level where the flow entered the upstream slotted weir channel, the attraction flow tunnel, and the gatehouse gates. It should be pointed out that the gatehouse gates and attraction water gates are not model boundaries where boundary condition should be applied, but internal flow restrictions where an appropriate opening was set up for each gate.
- For the downstream spillway attraction flow at the right bank downstream of the new entrance, based on the fact that the flow from underneath the control gates AWG 27 or AWG 28 is free discharge, an extension mesh block was built to cover about 5 times the length of the gate width, a pressure boundary condition was specified at the most downstream mesh boundary by specifying a water depth less than the height of the gate opening to assure a free discharge from the gate.
- At the downstream canal boundary of the model, a pressure boundary condition was applied by specifying the appropriate water level. Since there was no readily available water level data at this boundary but water level was available at Keith Bridge, an interpolation was required to obtain the water level at the model downstream boundary.
- At the downstream end of the gallery, a pressure boundary condition was applied by specifying an appropriate water height above the weir top.

The boundary conditions for all the runs are shown in Table 2. Table 2 also lists the openings of the adjustable gates to the attraction flow tunnel, downstream spillway attraction flow, and the adjustable weir at the downstream end of the gallery.

3. RESULTS

For each simulation, a complete presentation of the results was provided to FirstLight, and is included in a CD as an appendix of this report.

3.1 Model Validation

3.1.1 Validation Case 1

Validation Case 1 (3/16/2006 data) was selected to represent a moderately high flow condition (about 12,100 cfs) prior to installation of the new entrance. There was no fishway flow and only head gate flow. Results of the CFD simulation are discussed below. Figure 9 and Figure 10 show the total velocity contours and in-plane velocity vectors at elevations 172 and 163 ft. Elevation 172 ft represents shallow water depth (close to water surface) and elevation 163 ft deep water depth. Figure 11 and Figure 12 show the same content but in vertical planes through some of the gate centerlines. Flow pathlines downstream of the gatehouse are shown inFigure 13. Higher velocities are seen in the center of the canal as a result of the gate settings and more flow passing through the middle gates. The velocity vectors and 3D pathlines clearly indicate swirling flow downstream the gatehouse. The flow from the right side gates, particularly Gates 2 and 3, impinges on the right side bank walls and climbs up from deep water to the surface, forming a swirl moving toward the left bank. A counter-clockwise eddy is formed at the left bank downstream of the old entrance. These general flow patterns have been confirmed by the field observation.

Figure 14 shows an overall view of the water surface elevations in the canal. It can be seen that the water level is higher along the right side and lower along the left side of the canal. This coincides with the field observation. Figure 15 shows a zoom-in view of the water level downstream of the gate house. Water levels were measured at points A and B at the old entrance and points C through F along the right bank. CFD calculated and field measured water surface elevations at these points are listed in the figure. Comparison of the water surface elevation at these points is listed in Table 3. The CFD model predicted water surface elevations varied from the measured field data by about 0.1 to 0.3 ft with exception of point C, which showed a difference of about 0.5 ft. It was noticed that flow in the area of point C and its vicinity is unsteady and turbulent, making measurement of water level difficult. Therefore, higher variability and differences in the measurements in this region would be expected.

The canal bed was initially simulated as hydraulically smooth. However, the corresponding simulation results showed lower water level than the measured field data. The exposure of the canal bed when dewatered in the pictures provided by FirstLight suggested that the effect of the roughness of the canal bed to the water level cannot be ignored. Therefore, different values for canal bed roughness were tested to determine the final roughness distribution as shown in Figure 7. This roughness distribution was fixed for all the remaining runs.

3.1.2 Validation Case 2

Validation Case 2 (5/27/2009 data) was selected to represent a mid-range flow condition (about 7500 cfs) with the fishway in operation. Results of the CFD simulation are discussed below.

Figure 16 shows an overall view of the velocity magnitude contours and in-plane velocity vectors at elevation 172 ft. A zoom-in view in the vicinity of the old entrance at elevation 172 ft is shown in Figure 17. Figure 18 shows the same content but in vertical planes through centerlines of gates. A zoom-in view through the centerlines of the old and new entrance is shown in Figure 19. Flow pathlines are shown in Figure 20. Similar to validation case 1, higher velocity flow is seen in the center of the canal as a result of gate settings and more flow passing through the middle gates. The swirling flow, similar to Validation Case 1, is from the right side toward left side downstream of the gatehouse. The flow from the old entrance was apparently deflected by the counter-clockwise eddy at the left bank downstream the old entrance.

Figure 21 shows the velocity in plane at elevation 172 ft at the gallery and slotted weirs. Symmetrical flow patterns are seen through the slotted weirs. In the fishway channel through the gatehouse, there is higher velocity close to the right side channel wall after exiting the last slotted weir (#7). Part of the flow turns right to follow the gallery to the new entrance and spillway ladder, and part of the flow turns left to approach the old entrance. A large counter clockwise back flow eddy was formed at the left side of the fishway channel between the old entrance and the last slotted weir.

Velocities in the attraction flow tunnel are shown in Figure 22 (at elevations 163 and 162 ft) and Figure 23 through Figure 25 (vertical planes through the Sloped diffuser). Some flow patterns can be improved:

- Flow approaches the sloped diffuser at velocity about 3 ft/s which may be considered attractive to fish, fish may be misled by this flow and possibly delay the migration to upstream;
- Back flow occurs above the sloped diffuser in the left channel;
- Flow moves into the tunnel from above through the floor openings upstream of the sloped diffuser in the left channel;
- Flow moves from the tunnel to above through the floor opening upstream the sloped diffuser in the middle channel;
- Flow moves from above into the tunnel with high velocity through the floor opening upstream of the sloped diffuser in the right channel.

Figure 26 shows a zoom-in view of the water surface elevation in the canal downstream of the gate house near the old and new entrances. The water level is higher at the new entrance side compared to the old entrance side. Figure 27 shows the water surface elevation near the old entrance where water levels were measured at points A and B. CFD model predicted and field measured water surface elevations at these points are shown in the figure and compared in Table 4. The comparison shows that the CFD model results are in good agreement with the field measurements (within 0.1 ft).

3.2 Base Conditions

3.2.1 Base 1: Low Flow

A CFD simulation was conducted for Base Case 1, a low flow condition (about 4900 cfs) with both the old and new entrances in operation corresponding to field conditions on 5/24/2008.

Figure 28 shows the total velocity contours and in-plane velocity vectors in plane at elevation 172 ft. Figure 29 shows a zoom-in view in the vicinity of the old entrance. Velocities in vertical planes through centerlines of the gates are shown in Figure 30, and a zoom-in view through the centerlines of the old and new entrances are shown in Figure 31. Figure 32 shows the 3D flow pathlines. Higher velocity flow can be seen in the center of the canal as a result of gate settings and more flow passing through the middle gates. The swirling flow from right side toward left side downstream of the gatehouse is significantly weaker compared with the intensity in the validation cases. A large counter-clockwise eddy is seen at the left bank downstream the old entrance. As a result, the attraction flow from the old entrance is deflected toward the center of the canal.

Figure 33 shows the velocity at elevation 172 ft in the gallery and slotted weirs. As expected, flow through the slotted weirs is symmetrical. In the fishway channel through the gatehouse, higher velocity flow is seen near the right side channel wall after exiting the last slotted weir. A large counter clockwise eddy forms along the left side of the fishway channel between the old entrance and the last slotted weir.

Velocities in the attraction flow tunnel are shown in Figure 34 (at elevations 163 and 162 ft) and Figure 35 through Figure 37 (vertical planes through the sloped diffuser). Some flow patterns similar to Validation Case 2 exist in the fish way channel through the gatehouse. Figure 38 shows a zoom-in view of the water surface elevation in the vicinity of the old and new entrances downstream the gate house in the canal. The water level is higher near the new entrance when compared to the old entrance side. Figure 39 shows the water surface elevation in the vicinity of the old entrance. Water levels were measured at points A and B. The CFD calculated and measured water surface elevations at these points are listed in the figure. Comparison of the CFD model predicted and field measured water surface elevations at these points is listed in Table 5. The differences between the CFD model and field data are within 0.1ft.

3.2.2 Base 2: High Flow

Another CFD simulation was also conducted (Base 2) for a moderately high flow condition (about 13,800 cfs) with both the old and new entrances in operation corresponding to field conditions on 5/20/2009.

Contours of velocity magnitude and in-plane velocity vectors at elevation 172 ft are shown in Figure 40. A zoom-in view in the vicinity of the old entrance is shown in Figure 41. Velocities in vertical planes through gate centerlines are shown in Figure 42, and a zoom-in view through the centerlines of the old and new entrances are shown in Figure 43. 3D flow pathlines are shown in Figure 44. Higher velocities are observed in the center of the canal. The swirling flow from the right side toward the left side downstream the gatehouse persisted. The counter-clockwise eddy along the left bank downstream the old entrance is significantly reduced when compared to previous simulations. The attraction flow from the old entrance moves straightly downstream. Backflow can be seen at the right side near the old entrance.

Velocity contours in the slotted weirs and gallery at elevation 172 ft are shown in Figure 45. Flow patterns in the upstream slotted weirs and fish way channel through the gatehouse are similar to that of the Base 1 Low Flow condition.

Velocities contours of the attraction flow are shown in Figure 46 (at elevations 163 and 162 ft) and Figure 47 through Figure 49 (vertical planes through the sloped diffuser). Again, some flow patterns similar to the Base 1 Low Flow case are observed in the fishway channel between the old entrance and the last slotted weir.

A zoom-in view of the water surface elevation in the vicinity of the old and new entrance downstream the gate house in the canal is shown in Figure 50. The water level is higher at new entrance side than at the old entrance. Figure 51 shows the water surface elevation contours in the vicinity of the old entrance. Water surface elevations were measured at points A and B. CFD calculated and measured water levels at these point are shown in the figure and compared in Table 4. The CFD model predicted water surface elevations are higher than the measured data by 0.2 to 0.3 ft.

3.3 Modifications

Based on the results of the validation and base cases, some flow patterns in the fishway channel through the gatehouse can be further improved and are summarized as follows:

- The velocity approaching the sloped diffuser is high and uneven. The high velocity may be delaying upstream movement;
- Back flow exists above the sloped diffuser in the left channel between the old entrance and the last slotted weir;
- Flow moves from above into the tunnel through the floor opening upstream of the sloped diffuser in the left and right channels;
- Flow moves from the tunnel to above through the floor opening upstream of the sloped diffuser in the middle channel;
- The water drop through the old entrance is too high. The near surface velocity is too high (about 13 ft/s) downstream the old entrance for Base 2.

3.3.1 Mod 1

Mod 0, as shown in Figure 52, was considered less effective than Mod 1 and therefore not considered for any further CFD simulations. Mod 1 was developed, as shown in Figure 53 and Figure 54. Mod 1 focused on the region inside the old entrance in the sloped diffuser area to achieve a design flow rate of 180 cfs through the old entrance. Modifications included:

- Adding a vertical concrete wall sitting on the existing left separation wall of the sloped diffuser to create a channel separating the flow to the old entrance from that flowing to the new entrance and spillway ladder;
- Closing the existing three upstream openings in the floor of the fish way just upstream of the diffuser (these openings were blocked for the 2012 season);
- Keeping a left diffuser opening of 18 ft at its downstream end and closing the remaining part of the left diffuser to form an extended floor for the left channel;
- Adding two single slotted weirs in the left channel between the 1st upstream slotted weir to the beginning of the opening of the left diffuser at about 10 ft spacing;

- Adding an orifice (3 ft wide by 4 ft high) at the entrance of the left tunnel to the diffuser to better control the desired flow (about 80 cfs) from the tunnel to the left channel through the reduced diffuser opening;
- Cutting down the sill at the old entrance from El. 168.2 to El. 166 and removing the stop-logs.

A simulation was conducted using the Mod 1 geometry with modified gates openings and Validation Case 2 flow conditions (Table 1), both the old and new entrances in operation. The purpose of modifying the gate openings was to try to reduce or eliminate the back eddy that formed on the left side of the canal in Validation Case 2 and Base Case 1. After discussion of limitations and alternatives, FirstLight suggested that the simplest arrangement was to open gates 14 and 15 by 6 ft, with the remaining gates open 3 ft. After discussion of the proposed gate arrangement, ALDEN suggested that Gate 2 be closed and Gate 13 opened 6 ft to compensate for closing Gate 2 (Table 1). Previous model runs indicated that the outflow from Gate 2 hits the right canal bank corner at about 45 deg toward the left, causing cross flow in the canal. Closing Gates 1 and 2 was intended to help minimize the cross flow to the left of the canal. It was also suggested that Gate 15 be opened no more than 6 ft. If opened greater than 6 ft, the flow quantity (momentum) would be high compared to flow from the old entrance, resulting in high velocity gradients and a larger back eddy.

Figure 55 shows the velocity magnitude contours and in-plane velocity vectors at elevation 172 ft. A zoom-in view in the vicinity of the old entrance is shown in Figure 56. Velocity in vertical planes through centerlines of gates 12 to 15 is shown in Figure 57, and a zoom-in view through the centerlines of the old and new entrance is shown in Figure 58. Figure 59 shows 3D flow pathlines downstream of the gatehouse. Flow with higher velocity is in the center of the canal. The swirling flow from right side toward left side downstream of the gatehouse is still clearly shown. A counter-clockwise eddy forms along the left bank downstream of the old entrance. The flow from the old entrance is significantly deflected by this eddy.

Velocities at elevation 172 ft within the gallery and slotted weirs is shown in Figure 60. Flow patterns in the upstream slotted weirs are similar to Validation Case 2. The new division wall separates the fishway between the old entrance and the existing last slotted weir into two channels: the right side, unchanged from the existing configuration, and the left side, with separate channel and additional slotted weirs. Flow exits the right slot of the last slotted weir toward the division wall, forming a small counter-clockwise eddy zone at the left corner and a clockwise eddy at the right side of the right channel. Flow smoothly follows the dividing wall and the transition connecting the dividing wall and left gallery wall. In the new left channel, flow passes through the two new slots and approaches the old entrance fairly uniformly.

Velocities contours of the attraction flow are shown in Figure 61 (at elevations 163 and 162 ft) and Figure 62 through Figure 64 (vertical planes through the sloped diffuser). Flow from the orifice in the attraction water tunnel is toward the left wall of the left diffuser channel, forming a high velocity zone along the left wall, the flow is a fairly uniform approaching the sloped diffuser, except for an area of higher flow at the upper corner of the sloped diffuser. Flow in the middle and right diffuser channels is fairly uniform.

Figure 65 shows the water surface elevation contours in the vicinity of the old and new entrances downstream of the gate house in the canal. The water level is higher at new entrance side than at the old entrance side. Figure 66 shows the water surface elevations in the modified area of the fish way. The averaged water drops along the pools are shown in Figure 67. Averaged water drops are about 0.8 ft between the 5th and 4th pools, 1.2 ft between 4th and 3rd pools, 0.4 ft between 3rd and 2nd pools, 1 foot between 2nd and upstream portion of 1st pool, and 0.1 ft between the downstream portion of 1st pool and the canal downstream of the old entrance. The water surface elevation is about 176.4 ft in the right side channel.

The flow rates through various locations is listed in Table 7. For a general clarification, the CFD calculated flow rates for the validation and base cases and Mod 2 are also listed in the same table. If the referred flow in the table does not apply for the case, a N/A (not available) note is shown. The calculated total gate flow is about 7940 cfs, the upstream slotted weir flow is 254 cfs of which 112 cfs passes through the new left channel and 142 cfs passes through the right channel. The attraction flow is 188 cfs of which 105 cfs passes through the left diffuser channel (through the orifice) and 83 cfs passes through the middle and right diffuser channels. The flow through the old and new entrance is 217 cfs and 185 cfs, respectively. The flow to the adjustable weir downstream of the gallery at the top of the spillway fishway is 40 cfs. The downstream spillway attraction flow is 228 cfs.

3.3.2 Mod 2

Based on the CFD results with Mod 1 the following conclusions are drawn:

- With the proposed modifications flow patterns inside the fishway were improved;
- The eddy on the left side of the canal side was not eliminated by more uniform gate openings. The main reason for the persistent eddy is that there is no flow from the gatehouse between the left bank of canal and Gate 15 (Gate 15 is about 30 ft away from the left bank of the canal), therefore, there is no reason to remove the rocky outcrop of the left bank. The eddy was minimized in Base 2 for the high flow condition;
- Refinement of the geometry is necessary to further improve flow conditions.

Building on Mod 1 results, additional refinements were made which resulted in Mod 2, shown in Figure 68 through Figure 70. Mod 1 was further refined to arrive at Mod 2 which included:

- Rev. 2.1: Adding a 1.5 ft wide baffle at the right side of the new left channel;
- Rev. 2.2: Narrowing the slot width of the added upstream slot in Mod 1 from 1 foot 9 inches in Mod 1 to about 1 foot 4 inches;
- Rev. 2.3: Removing the existing 1 foot wide baffle at the left side of the old entrance (which exists in all the simulations of Validation Case 1, Validation Case 2, Base 1, Base 2, and Mod 1) and adding a new 2.7 ft wide baffle at the right side of the old entrance to form a 3.3 ft opening;
- Rev. 2.4: Re-aligning the angled wooden diffuser in the left channel below the fishway to the end of the new extended fishway floor;
- Rev. 2.5: Enlarging the orifice at the entrance of the left tunnel to 4 ft wide by 4 ft high from 3 ft wide by 4 ft high.

Mod 2 was then tested under a pond level of 181.5 ft with a new gate openings provided by FirstLight (Table 8). The new gate openings were based on field observation of the canal at flows similar to the flow tested in Mod 2. Following this gate sequence and maintaining the total opening area as used in Mod 1, the final gate openings for Mod 2 are shown in Table 1.

Contours of velocity magnitude and in-plane velocity vectors at elevation 172 ft are shown in Figure 71. Figure 72 is a zoom-in view of the same content in the vicinity of the old entrance in the canal. Velocity in vertical planes through centerlines of gates 12 to 15 are shown in Figure 73, and a zoom-in view through the centerlines of the old and new entrances is shown in Figure 74. Figure 75 shows 3D flow pathlines in the canal. In general, flow shows a pattern of low velocity along the left side of the canal, then a high velocity zone, then a low velocity zone, and then high velocity along the right side of canal. This general canal flow pattern reflects the gate opening distribution. The swirling flow from the right side toward the left side downstream of the gatehouse is weakened. An upwelling is seen roughly in the middle of canal and at about 40 ft downstream from the gallery. Closer to the old entrance, a counter-clockwise eddy is formed along the left bank. The flow from the old entrance is initially oriented toward the left bank and straight downstream. The deflection by the back eddy of the flow from the old entrance has been reduced significantly.

Velocity contours at elevation 172 ft of the gallery and slotted weirs are shown inFigure 76. Flow patterns in the upstream slotted weirs, the right channel, and the gallery are similar to that of Mod 1. In the left new channel, flow passes through the two new slots and two baffles and approaches the old entrance fairly uniformly.

Velocities contours of the attraction flow are shown in Figure 77 (at elevations 163 and 162 ft) and Figure 78 through Figure 80 (vertical planes through the sloped diffuser). In the left diffuser channel, flow from the orifice is toward the left wall of the left diffuser channel, forming a high velocity zone along the left wall; but the flow adjusted fairly quickly to uniformly approach the re-oriented sloped diffuser. Although some higher velocity regions are still seen at the upper portion of the sloped diffuser, the velocity is significantly lower than in the flow from the slotted weir. Therefore, fish would not be attracted by the diffuser flow. Flow in the middle and right diffuser channels is fairly uniform.

Figure 81 shows the water surface elevations in the vicinity of the old and new entrance downstream of the gate house in the canal. The water level is higher at the new entrance side than at the old entrance side. Figure 82 shows the water surface elevation in the modified area of the fish way and Figure 83 shows the averaged water drops along the pools. The water surface elevation is about 176.4 ft in the right side channel. The averaged water drop is about 0.7 ft between the 5th and 4th pools, 0.7 ft between the 4th and 3rd pools, 0.7 ft between the 3rd and 2nd pools, 0.6 ft between the 2nd and upstream portion of 1st pool, 0.5 ft between the upstream portion and the downstream portion of 1st pool, and 1.2 ft between the downstream portion of the 1st pool and the canal downstream from the old entrance.

Flow distribution between various locations is listed in Table 7 and illustrated in Figure 84. The calculated total gate flow is Q3=7230 cfs. The upstream slotted weir flow is Q1=232 cfs, of which Q6=99 cfs through the left new channel and Q7=133 cfs to the right channel. The attraction flow is Q2=195 cfs of which Q4=102 cfs through the left diffuser channel through the orifice and Q5=93 cfs through the middle and right diffuser channels. The flow through the old entrance is Q8=201 cfs, the gallery flow is Q9=226 cfs which is split into the new entrance flow Q10=194 cfs and the adjustable weir (spillway) flow Q11=31 cfs. The spillway ladder flow Q11 is less than that of Mod 1 because the top of the weir was increased from El. 173.7 ft for Mod 1 to 174.5 ft for Mod 2. In Mod 1 simulation, the upstream water level is 175.7 ft and the adjustable weir top elevation is 173.7 ft, the corresponding water depth over the weir is 2 ft which is deeper than the normal water depth of 1.2 ft. During the meeting on 5/7/2012 with FirstLight, it was decided to raise the weir top elevation to 174.5 ft to have 1.2 ft water over the weir for Mod 2 simulation. The downstream spillway attraction flow is Q12=220 cfs.

4. CONCLUSIONS AND DISCUSSION

CFD modeling was used to better understand the characteristics of flow inside the fishway at the Turners Falls Gatehouse and derive conceptual modifications for improving the hydraulic condition for more efficient fish passage through the fishway. A 3D CFD model was developed for the existing geometry and structure configuration. The model was first validated using two flow conditions for which field data existed and then tested for two additional flow conditions.

The validations showed that the model was accurately reproducing the hydraulic conditions of interest. Based on the results of these simulations, three conceptual modifications (Mod 0, Mod 1, and Mod 2) were proposed. Geometric changes to the CFD model were then made to incorporate Mod 1 and Mod 2 and additional simulations were conducted to evaluate the effectiveness of the modifications. The model results of the currently existing (2012) configuration revealed flow patterns inside the fishway and in the canal that could be improved. In summary, this includes: 1) high and uneven approach velocities to the sloped diffuser which may be attractive to fish causing possible delay of migration, 2) a large eddy above the sloped diffuser at the left channel, 3) exaggerated flow complexity due to flow through the three floor openings upstream of the sloped diffusers, 4) larger than desired water drop through the old entrance, 5) a counter-clockwise eddy at the left bank of the canal downstream the old entrance deflecting the flow from the old entrance, and 6) cross flow from right to left side of the canal.

Results of Mod 1 can be summarized as follows: 1) the modifications showed improvement to the flow patterns inside the fishway, 2) further improvements were needed to lower the water drops between the upstream portion of the 1st pool and 2nd pool, and between the 3rd pool and the 4th pool inside the fishway, 3) the back eddy along the left side of canal downstream of the old entrance had significant impact on the flow from the old entrance and that eddy was not eliminated by more uniform gate openings.

Results of Mod 2 can be summarized as follows: 1) Flow patterns inside the fishway and in the canal downstream of the old entrance and gatehouse were further improved compared to Mod 1, 2) averaged water drop was about 0.7 ft between the 5th and 4th pools, 0.7 ft between the 4th and 3rd pools, 0.7 ft between the 3rd and 2nd pools, 0.6 ft between the 2nd and upstream portion of the 1st pool, 0.5 ft between the upstream portion and downstream portion of the 1st pool, and 1.2 ft between the downstream portion of the last section of pool and the canal downstream of the old entrance, 3) flow from the old entrance is affected less by the back eddy on the left side of the canal, 4) A gate operating sequence was developed to improve the flow pattern in the canal. The back eddy persisted at the left side of the canal downstream from the old entrance and the eddy was not eliminated by manipulations of different gate openings. However, its impact on the flow from the old entrance was limited with the Mod 2 configuration and flow conditions.

CFD modeling results indicate that Mod 2 would provide enhanced hydraulic condition for fish passage. Some fine tuning and optimization of this concept may be conducted in the field.

5. REFERENCES

Bruce J. Pennino and George E. Hecker, 1975 "Model Studies of the Proposed Turners Falls Fish Passage Facilities for Northeast Utilities Service Company", Alden Research Laboratory, Worcester Polytechnic Institute, Holden, Massachusetts.

Table 1 Width and Height and Openings of Each Gate for CFD Simulations

Gate	Number	15	14	13	12	11	10	9	8	7	6	5	4	3	2	1
	Width ft	8	8	8	8	8	8.7	9.25	8.5	8.5	8.5	8.5	8.5	8.5	8.5	8.5
	Height ft	10	10	10	10	10	10	12	12	12	12	12	12	12	12	12
Openings ft	Validation 1	8.7	9.3	5.9	9.6	9.4	9.7	11.3	8.2	closed	Blocked	3	3	3	2.9	Closed
	Validation 2	0.3	Closed	Closed	4.9	9.5	9.2	2.9	3	3.3	Blocked	3	3	3	3	Closed
	Base 1	0.3	Closed	Closed	Closed	Closed	7.8	3	2.9	3	Blocked	3	3	3	3	Closed
	Base 2	8.9	8.9	9.4	10	9.5	9.2	10.5	3	3.1	Blocked	2.9	3	2.9	3	Closed
	Mod 1	6	6	6	3	3	3	3	3	3	Blocked	3	3	3	Closed	Closed
	Mod 2	10	10	2	2	2	2	2	2	2	Blocked	2	2	7	closed	Closed

Table 2 Boundary Conditions

	Pond Water Level	Keith Bridge Water Level	CFD Downstream Boundary Water Level	Spillway Adjustable Weir		AWG 15 Opening	AWG 16 Opening	AWG 27 Opening	AWG 28 Opening
				Upstream Water Level	Weir Top El.				
	ft	ft	ft	ft	ft	ft	ft	ft	ft
Validation 1	180.2	173.9	174.1	Not Operating					
Validation 2	182.0	173.7	173.8	175.7	173.7	Closed	2.1	Closed	1.9
Base 1	182.2	173.7	173.7	175.1	173.4	1.0	Closed	Closed	1.4
Base 2	181.5	173.6	173.6	176.0	173.8	2.7	Closed	Closed	2.0
Mod 1	182.0	173.7	173.8	175.7	173.7	Closed	2.1	Closed	1.9
Mod 2	181.5	173.7	173.8	175.7	174.5	Closed	2.1	Closed	1.9

Table 3 Water Surface Elevation Comparison of Validation Case 1

Point	Water Surface Elevation (ft)		
	Measured	CFD	Difference
A	174.2	174	0.2
B	174.1	174	0.1
C	175.1	174.6	0.5
D	175	174.7	0.3
E	174.9	174.8	0.1
F	175.1	174.9	0.2

Table 4 Water Surface Elevation Comparison of Validation Case 2

Point	Water Surface Elevation (ft)		
	Measured	CFD	Difference
A	173.5	173.5	0.0
B	176.0	175.9	0.1

Table 5 Water Surface Elevation Comparison of Base 1 Low Flow

Point	Water Surface Elevation (ft)		
	Measured	CFD	Difference
A	173.5	173.6	0.1
B	175.2	175.3	0.1

Table 6 Water Surface Elevation Comparison of Base 2 High Flow

Point	Water Surface Elevation (ft)		
	Measured	CFD	Difference
A	173.8	174.0	0.2
B	176.1	176.4	0.3

Table 7 Calculated Flow Distribution

	Q1	Q2	Q3	Q4	Q5	Q6	Q7	Q8	Q9	Q10	Q11	Q12
Validation 1	N/A	N/A	13,400	N/A	N/A	N/A	N/A	N/A	N/A	N/A	N/A	N/A
Validation 2	254	202	7,732	N/A	N/A	N/A	N/A	260	196	162	34	218
Base Case 1	271	105	5,605	N/A	N/A	N/A	N/A	228	148	132	16	180
Base Case 2	208	327	12,562	N/A	N/A	N/A	N/A	320	215	184	31	258
Mod 1	254	188	7935	105	83	112	142	217	225	185	40	228
Mod 2	232	195	7230	102	93	99	133	201	226	194	31	220
Note: 1) Flow rate in cfs; 2) Refer to Figure 84 for locations. Q1: Upstream slotted weir flow; Q2: Upstream attraction flow; Q3: Gate flow; Q4: Orifice flow; Q5: Middle and right diffuser flow; Q6: Left new channel flow; Q7: Right channel flow; Q8: Old entrance flow; Q9: Gallery flow; Q10: New entrance flow; Q11: Adjustable weir flow; Q12: Spillway attraction flow												

Table 8 A New Set of Gate Openings Provided by FirstLight

Step	Action	Step	Action
1	Open gate 15 through 3 two ft, starting with gate 15 towards gate 3;	13	Open Gate 7 seven ft;
2	Open Gate 15 all the way;	14	Open Gate 13 all the way;
3	Open Gate 14 all the way;	15	Open Gate 12 all the way;
4	Open Gate 3 seven ft;	16	Open Gate 4 all the way;
5	Open Gate 13 six ft;	17	Open Gate 11 all the way;
6	Open Gate 12 six ft;	18	Open Gate 10 all the way;
7	Open Gate 4 seven ft;	19	Open Gate 5 all the way;
8	Open Gate 11 six ft;	20	Open Gate 9 all the way;
9	Open Gate 10 six ft;	21	Open Gate 8 all the way;
10	Open Gate 5 seven ft;	22	Open Gate 7 all the way;
11	Open Gate 9 seven ft;	23	Open Gate 3 all the way;
12	Open Gate 8 seven ft;	24	Open Gate 2 all the way.
Closing gates should be in reverse order.			

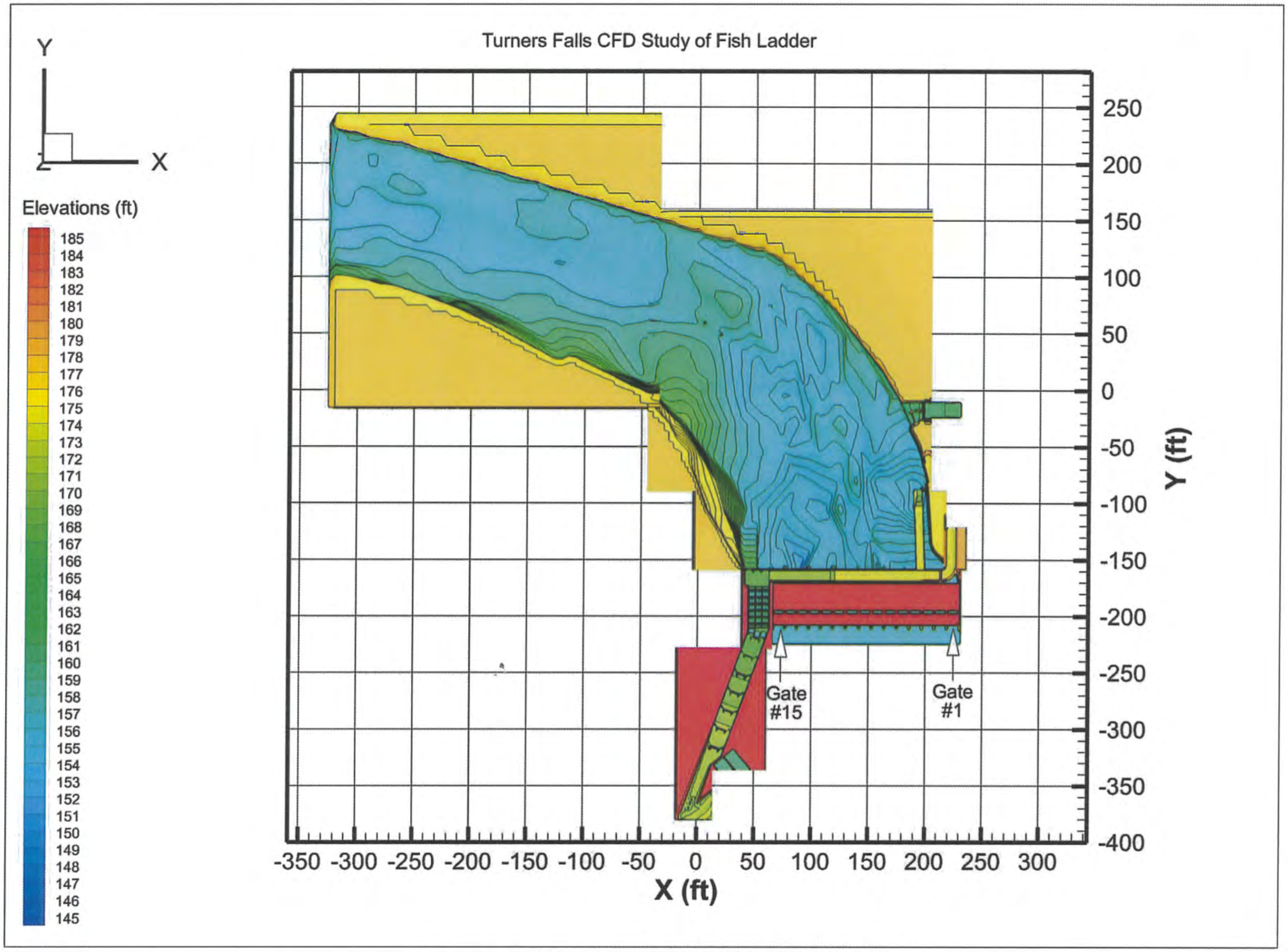

Figure 1 Plan View of the CFD Model

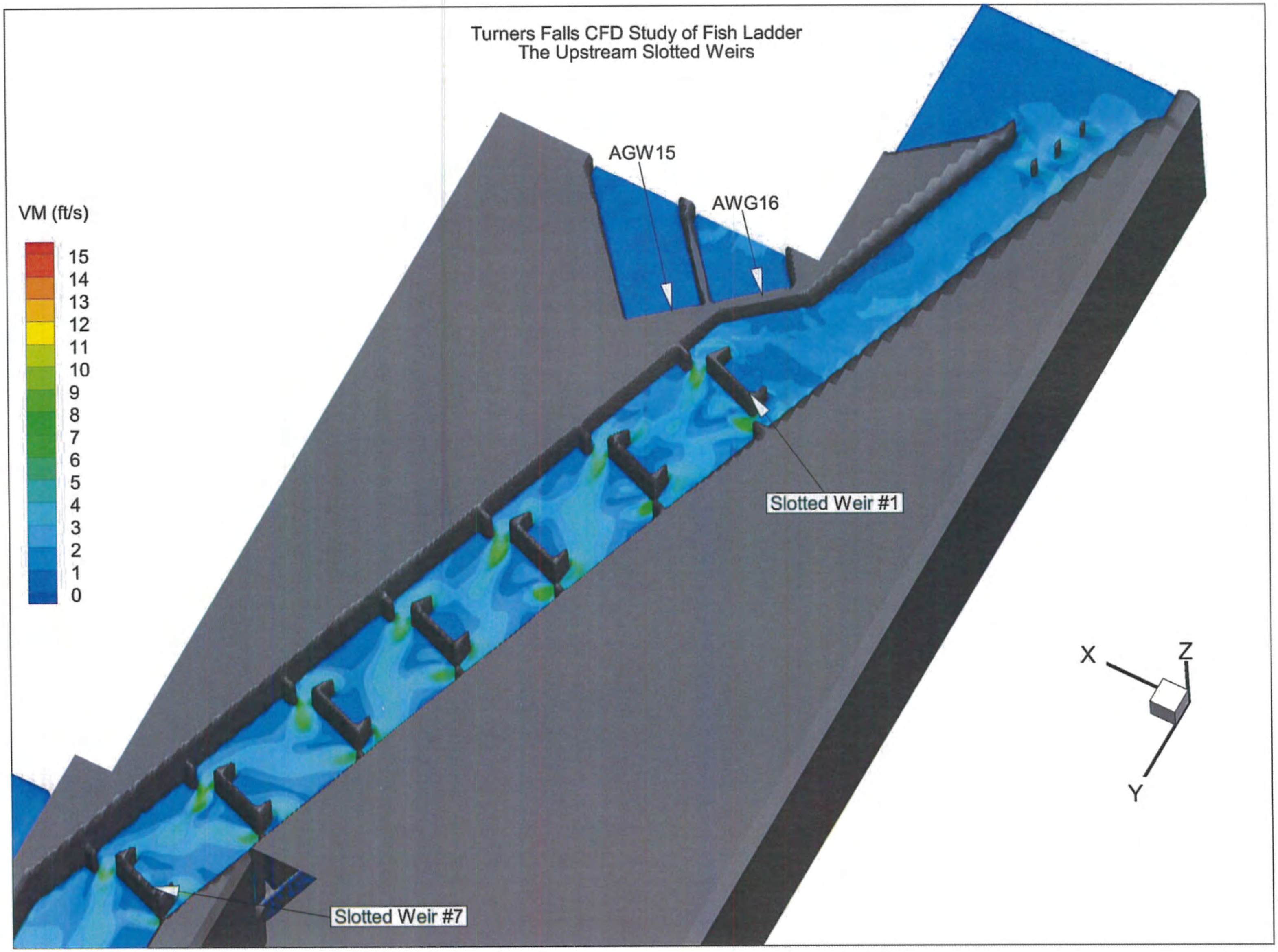

Figure 2 Zoom-in View of the Upstream Slotted Weirs

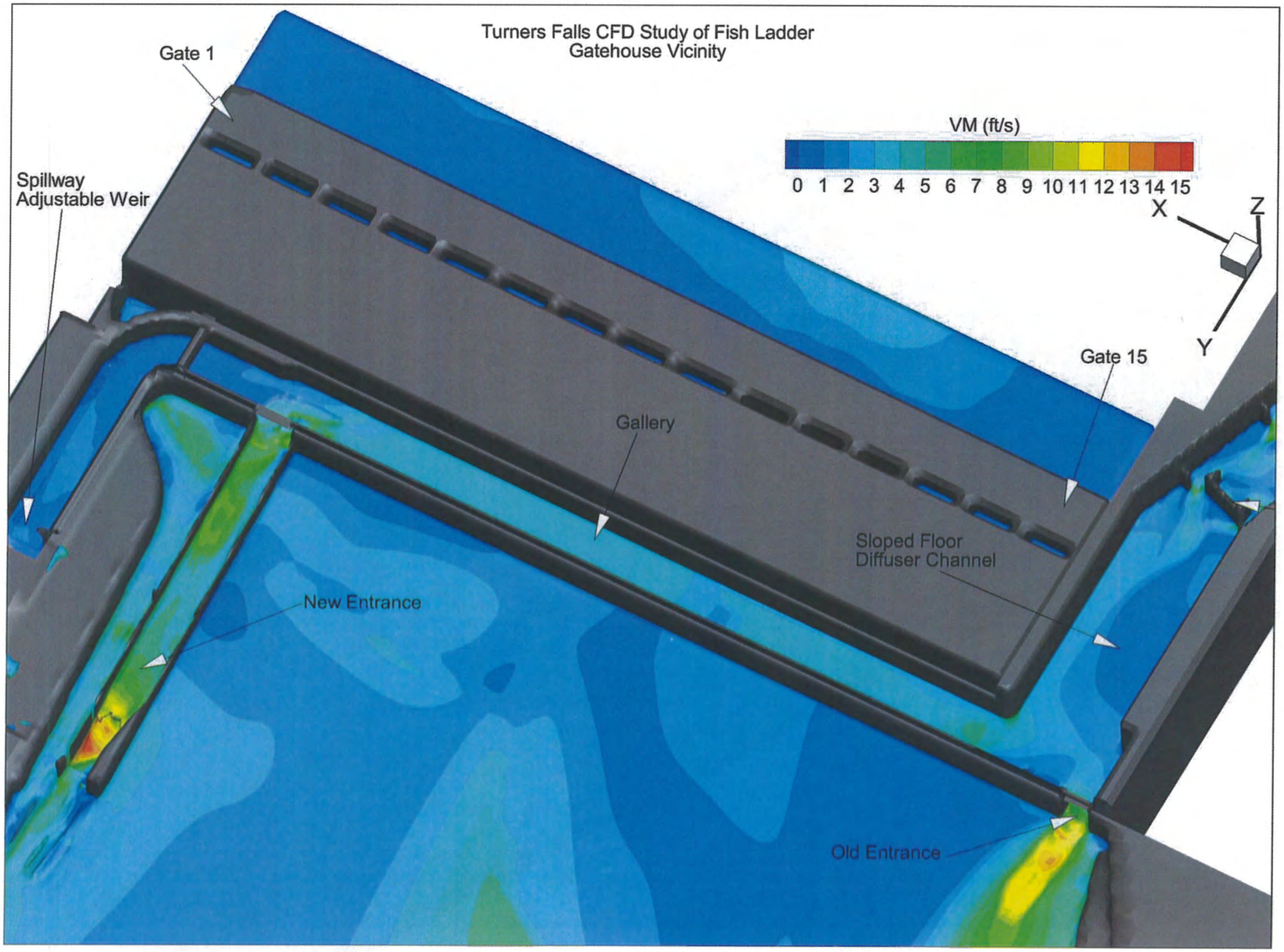

Figure 3 Zoom-in View of the Gatehouse and Vicinity

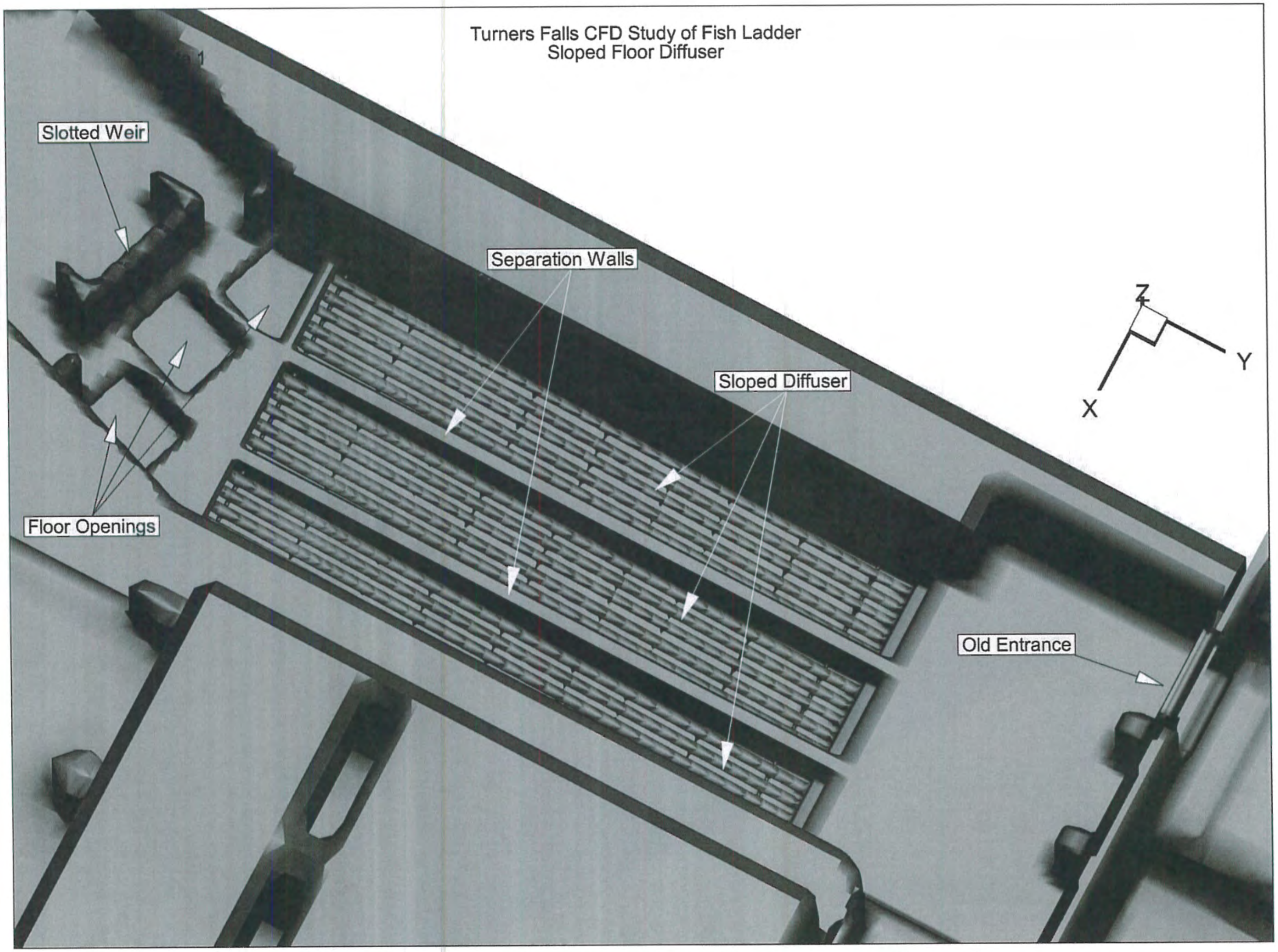

Figure 4 Zoom-in View of the Sloped Floor Diffuser Channel

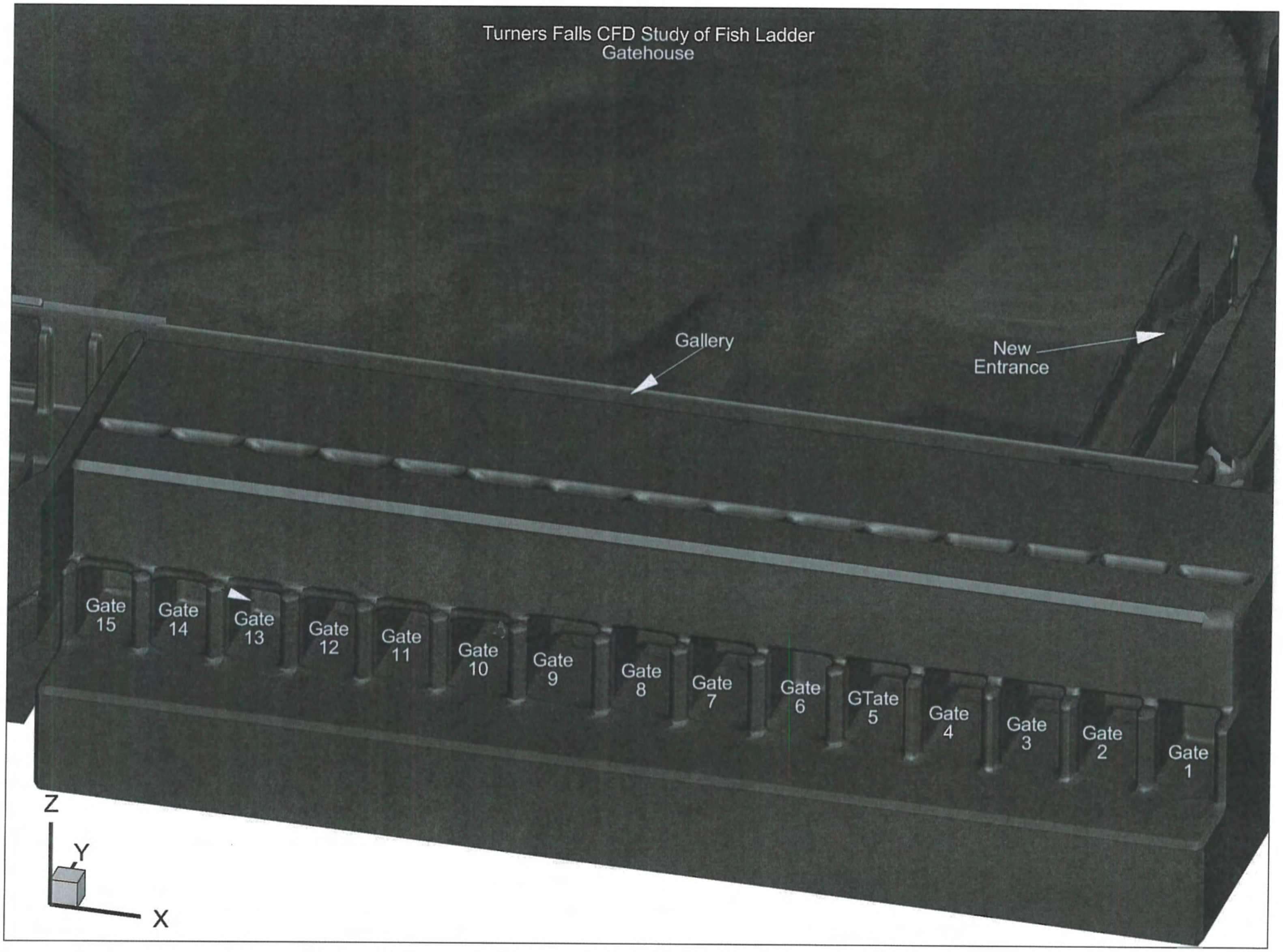

Figure 5 Zoom-in View of the Gatehouse Gates and Vicinity

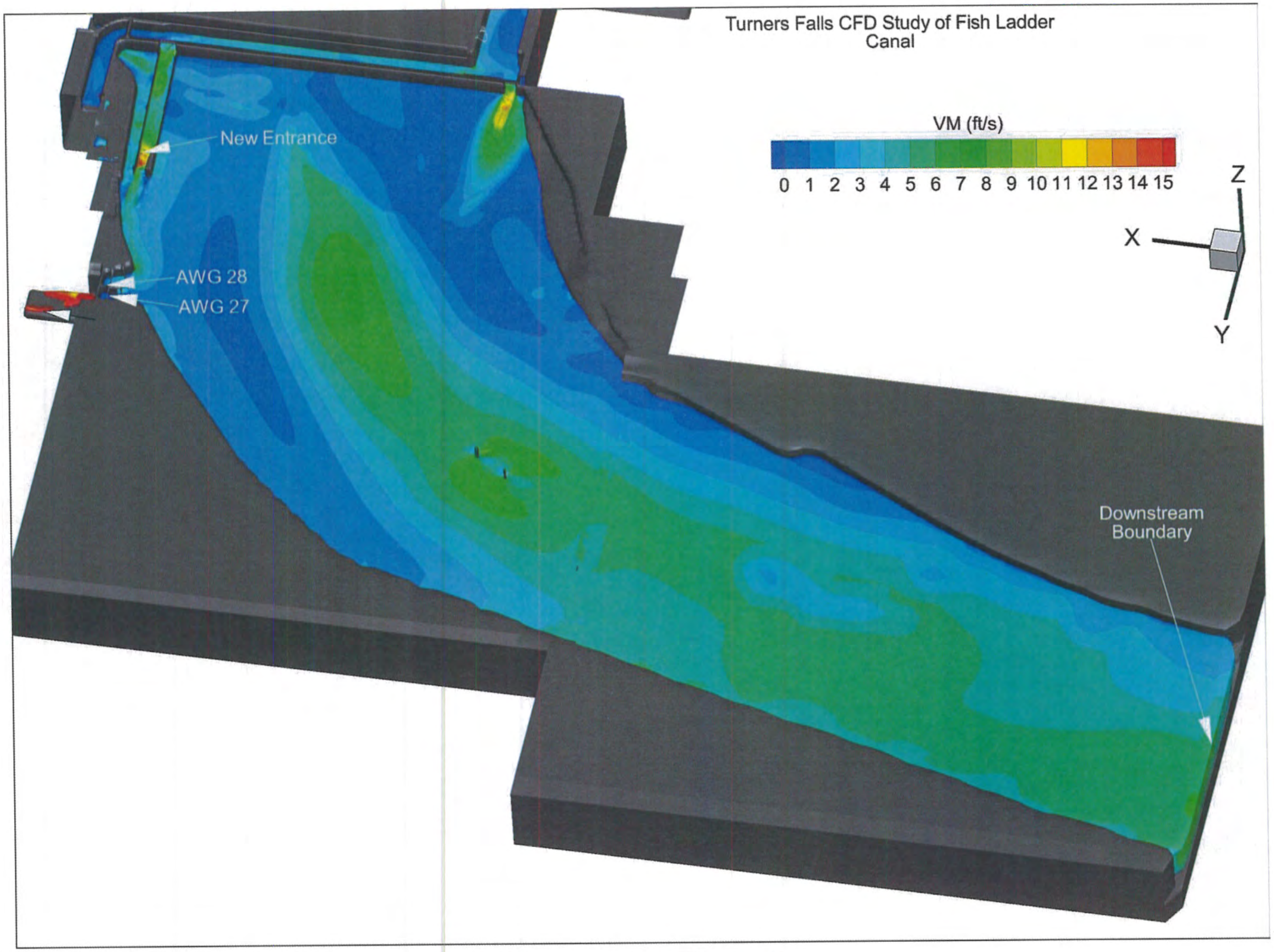

Figure 6 Canal Channel

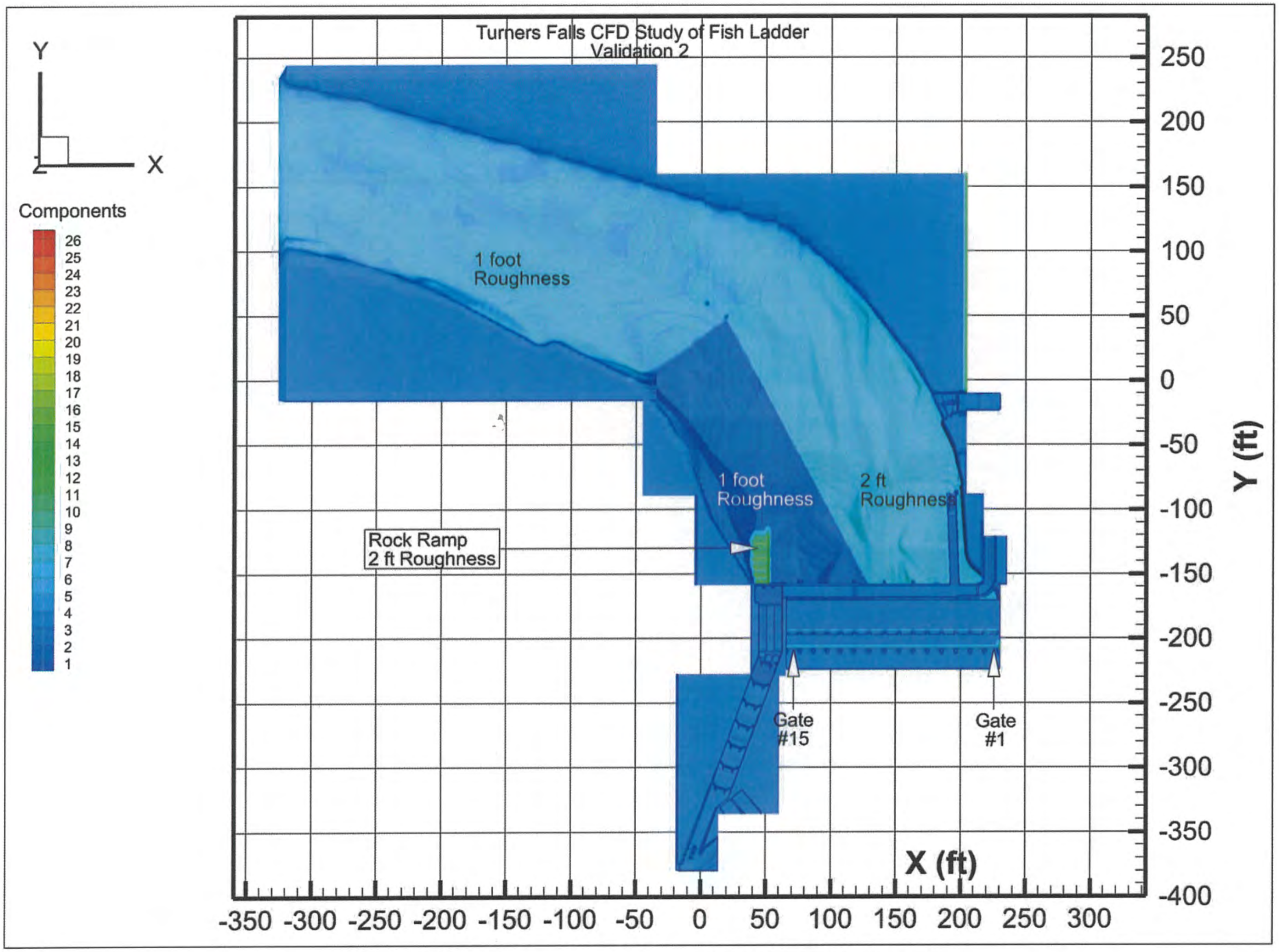

Figure 7 Roughness Height Distribution in the Canal

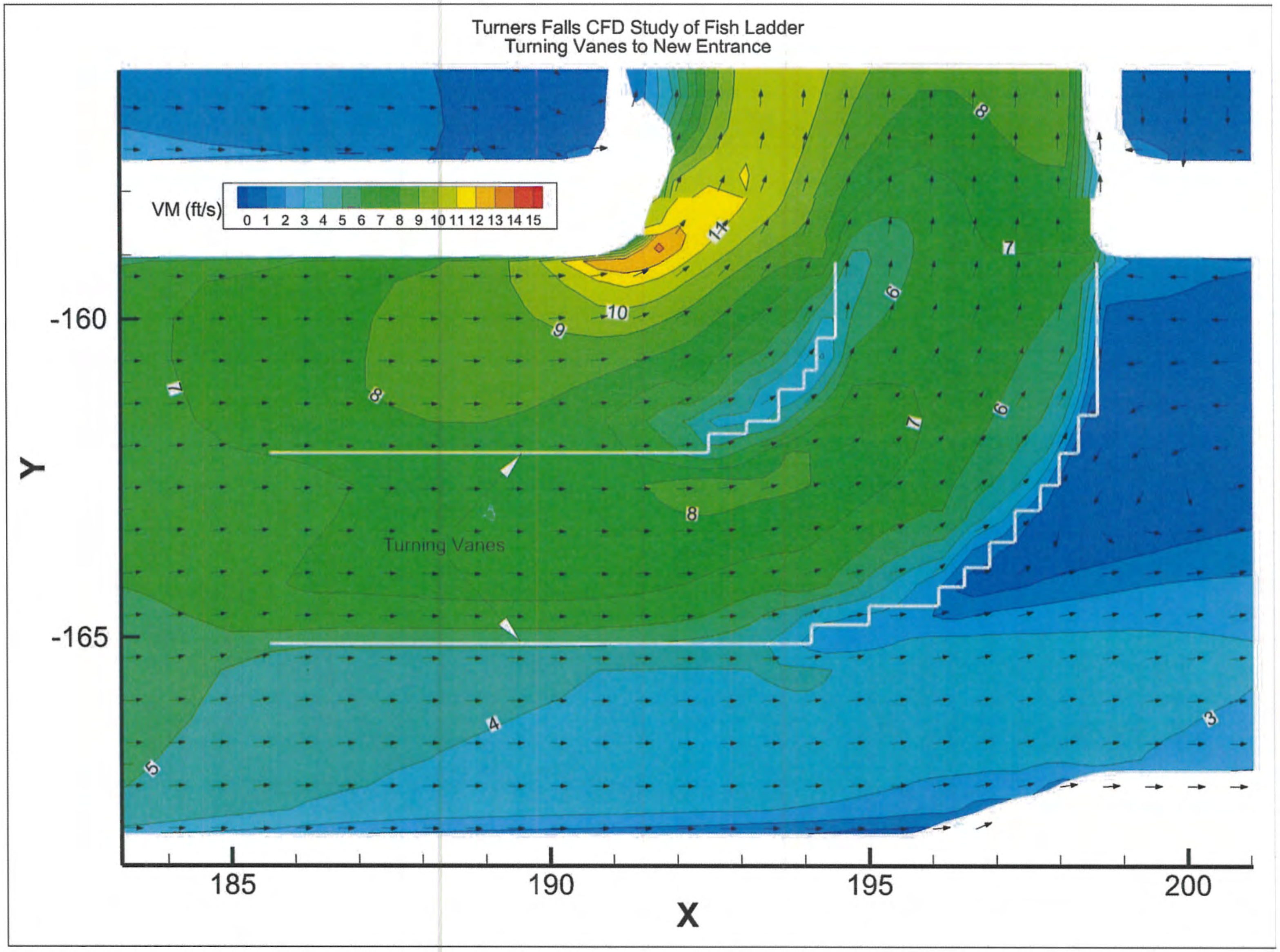

Figure 8 Simplification of Turning Vanes to New Entrance in the Gallery

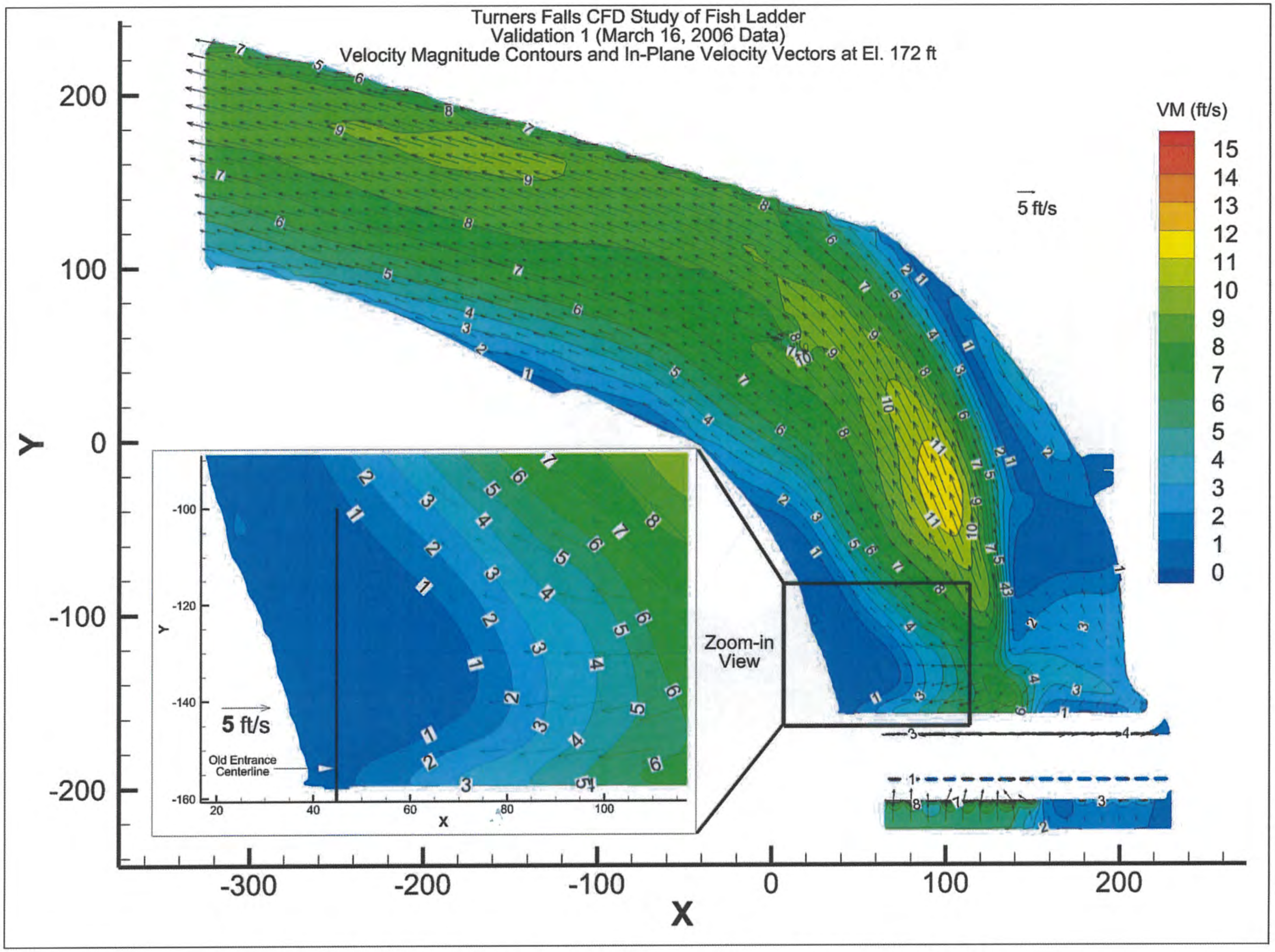

Figure 9 Validation Case 1: Velocity in Plane at Elevation 172 ft

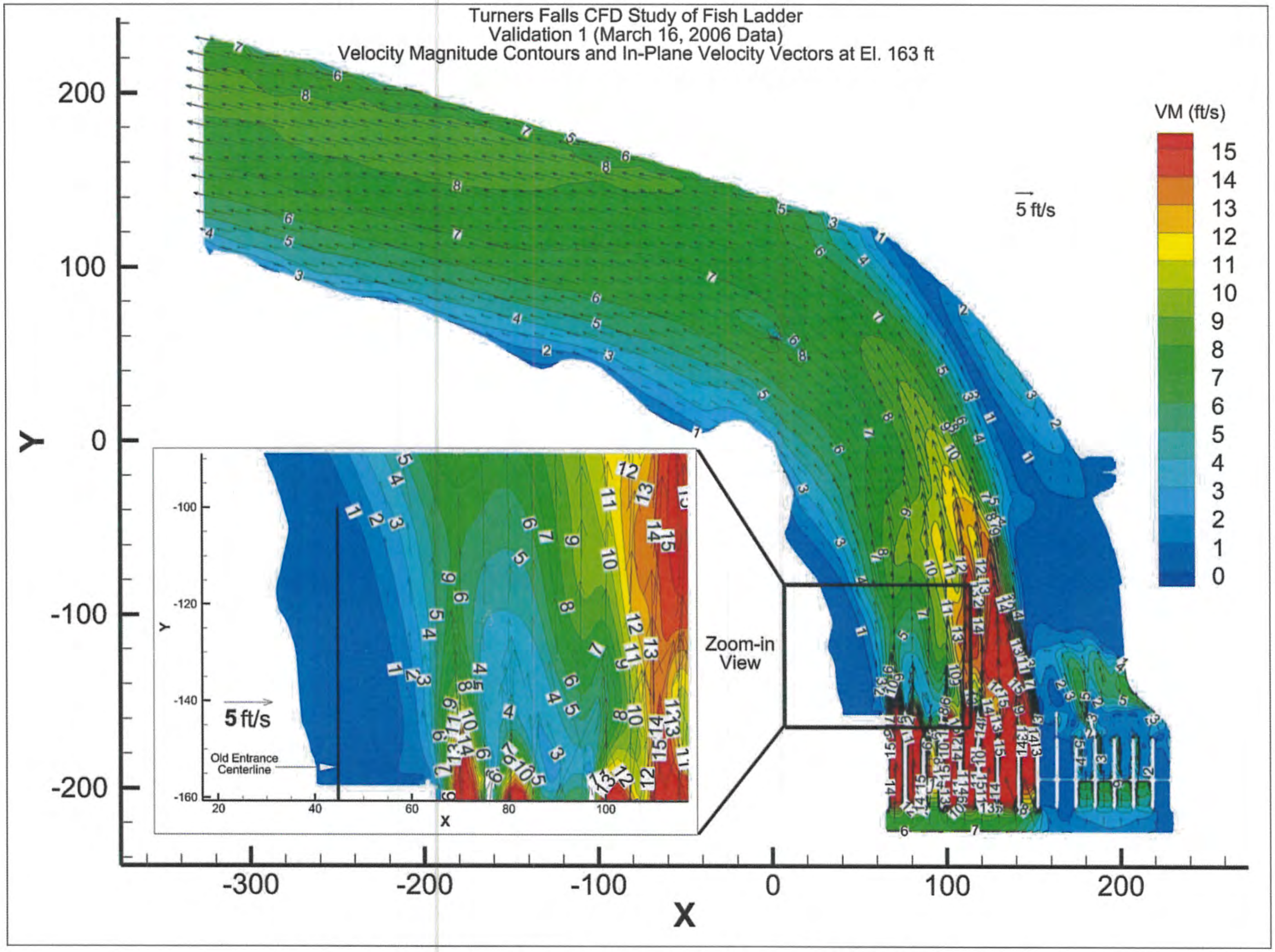

Figure 10 Validation Case 1: Velocity in Plane at Elevation 163 ft

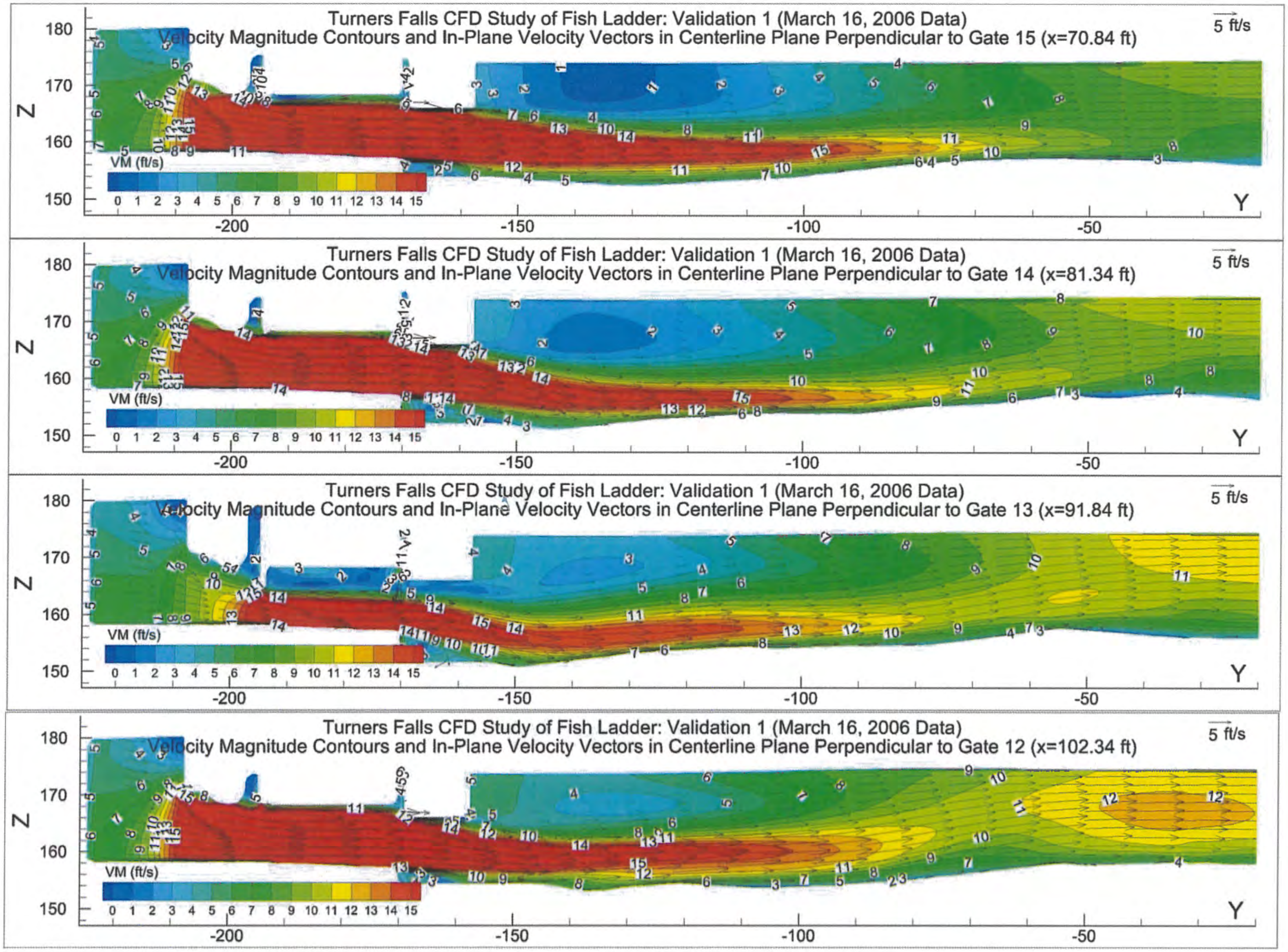

Figure 11 Validation Case 1: Velocity in Sectional Planes (Gates 12 through 15)

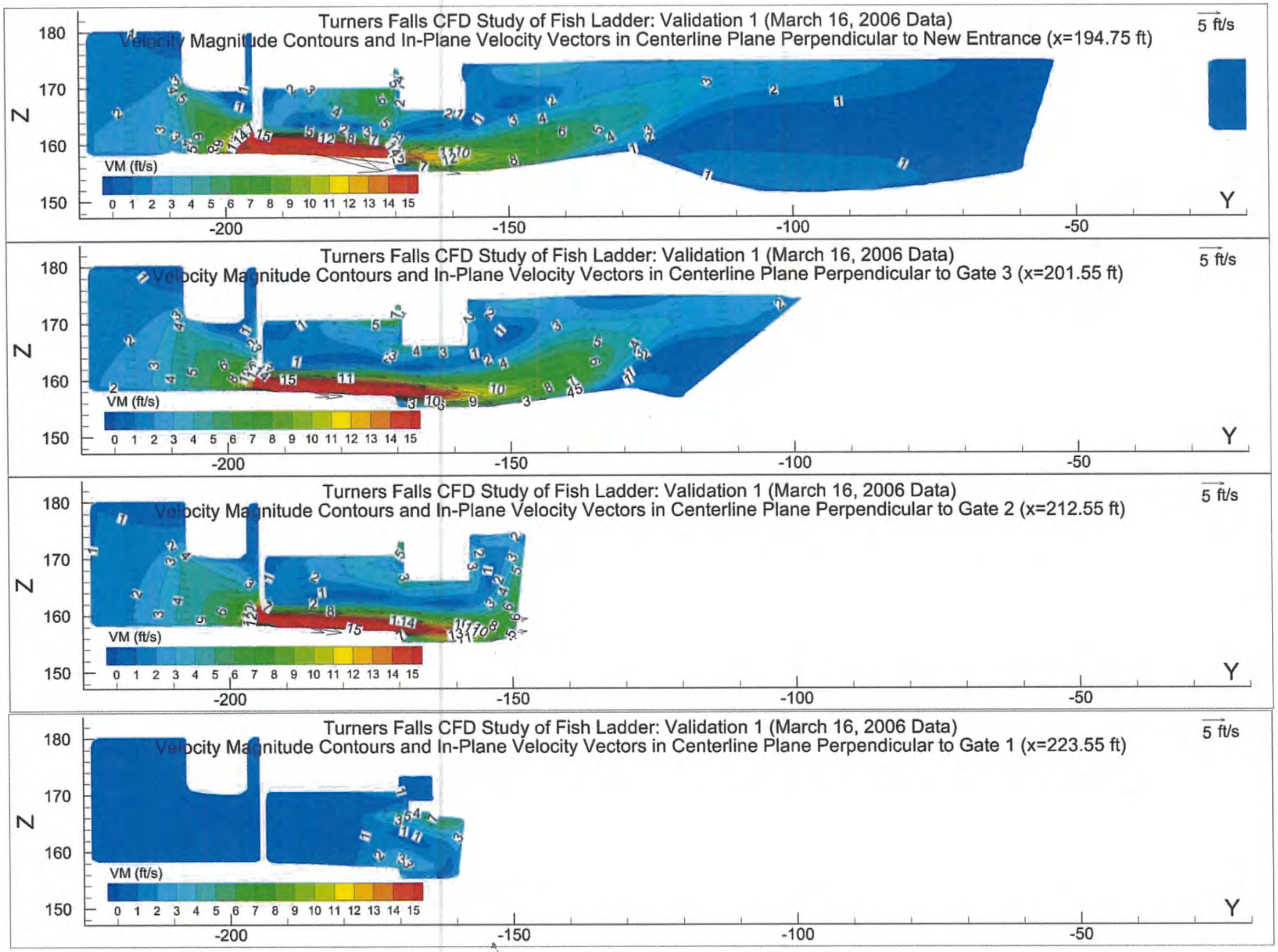

Figure 12 Validation Case 1: Velocity in Sectional Planes (Gates 1 through 3 and New Entrance)

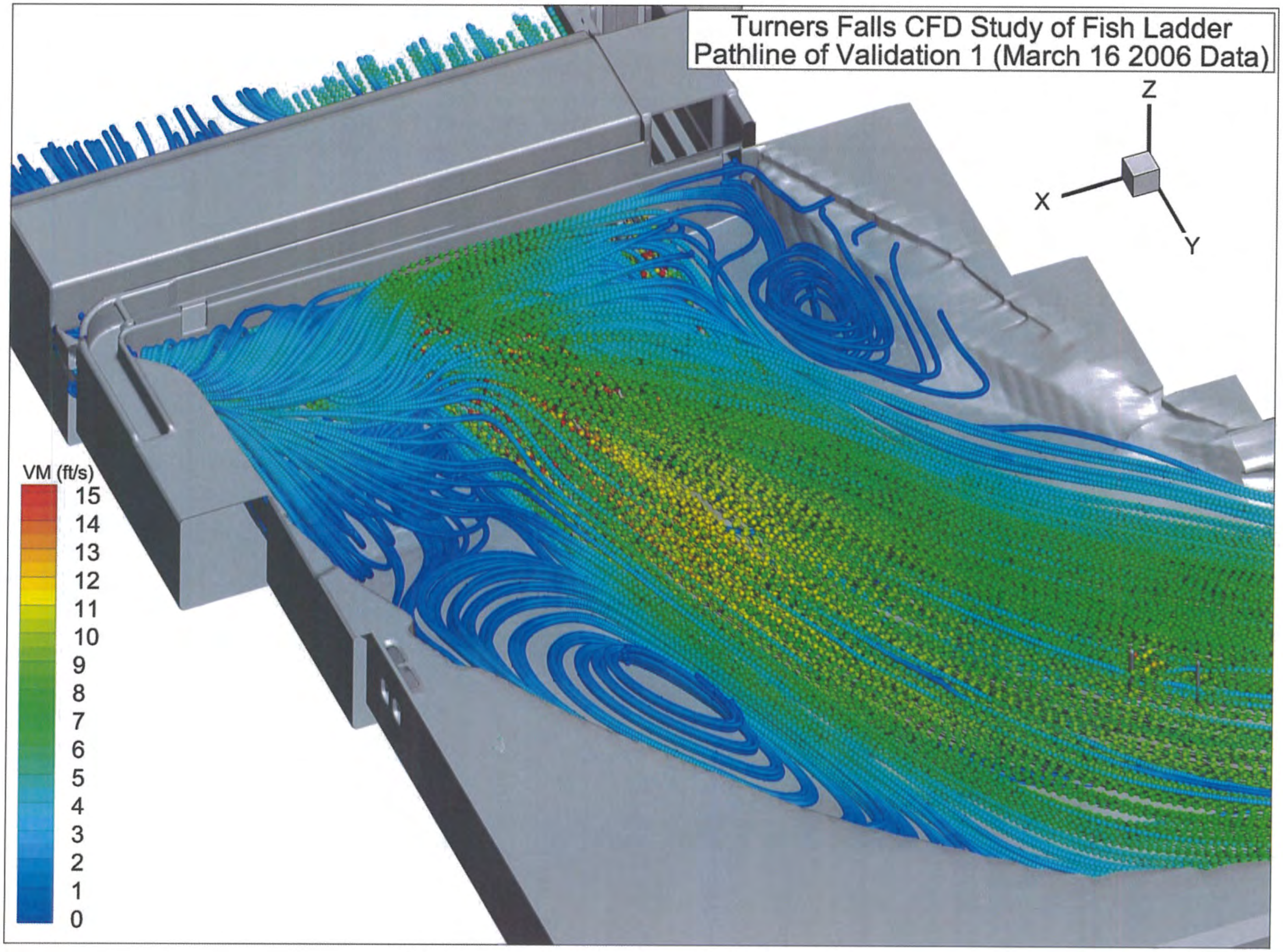

Figure 13 Validation Case 1: 3D Pathlines

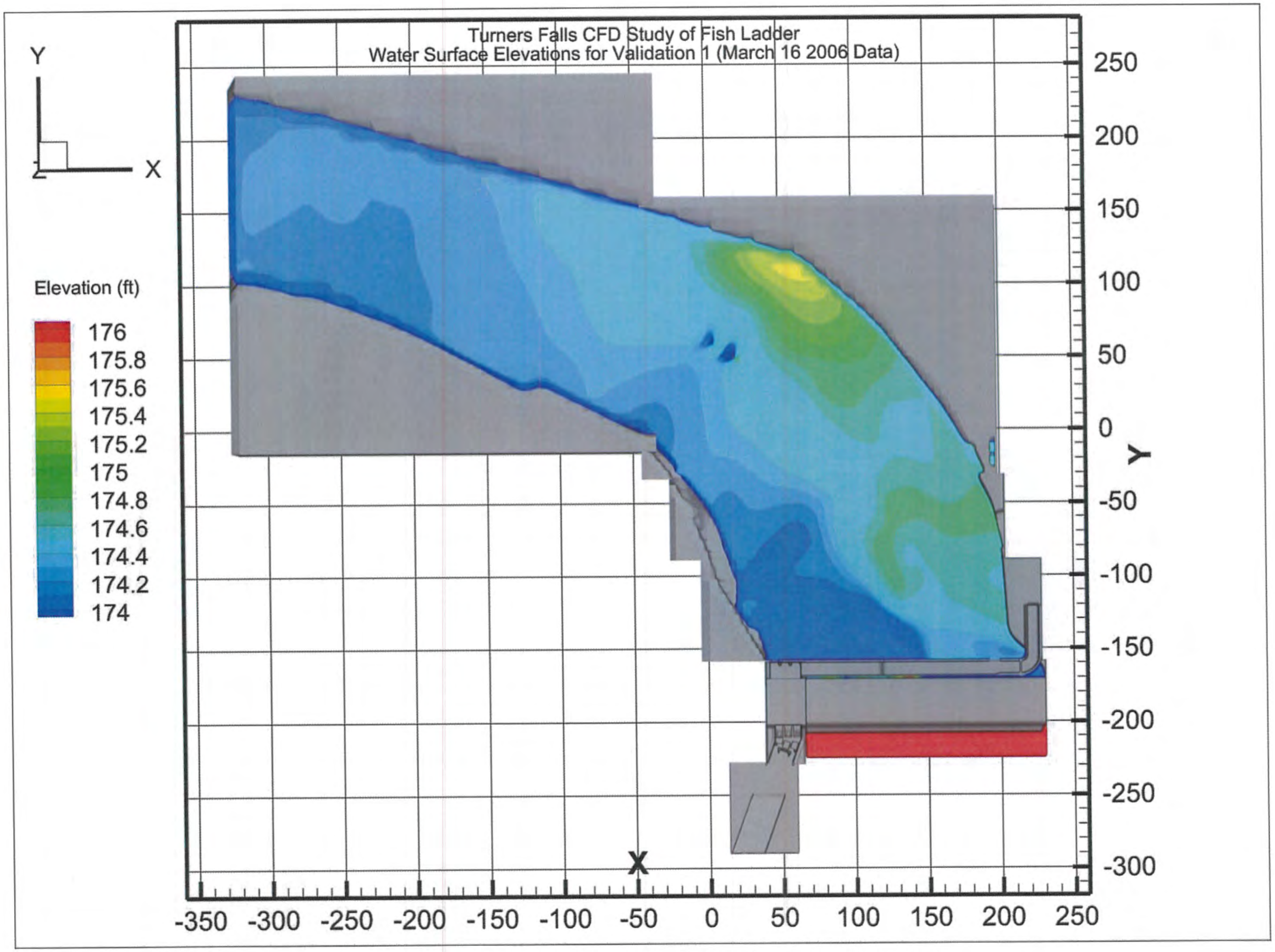

Figure 14 Validation Case 1: Water Surface Elevation

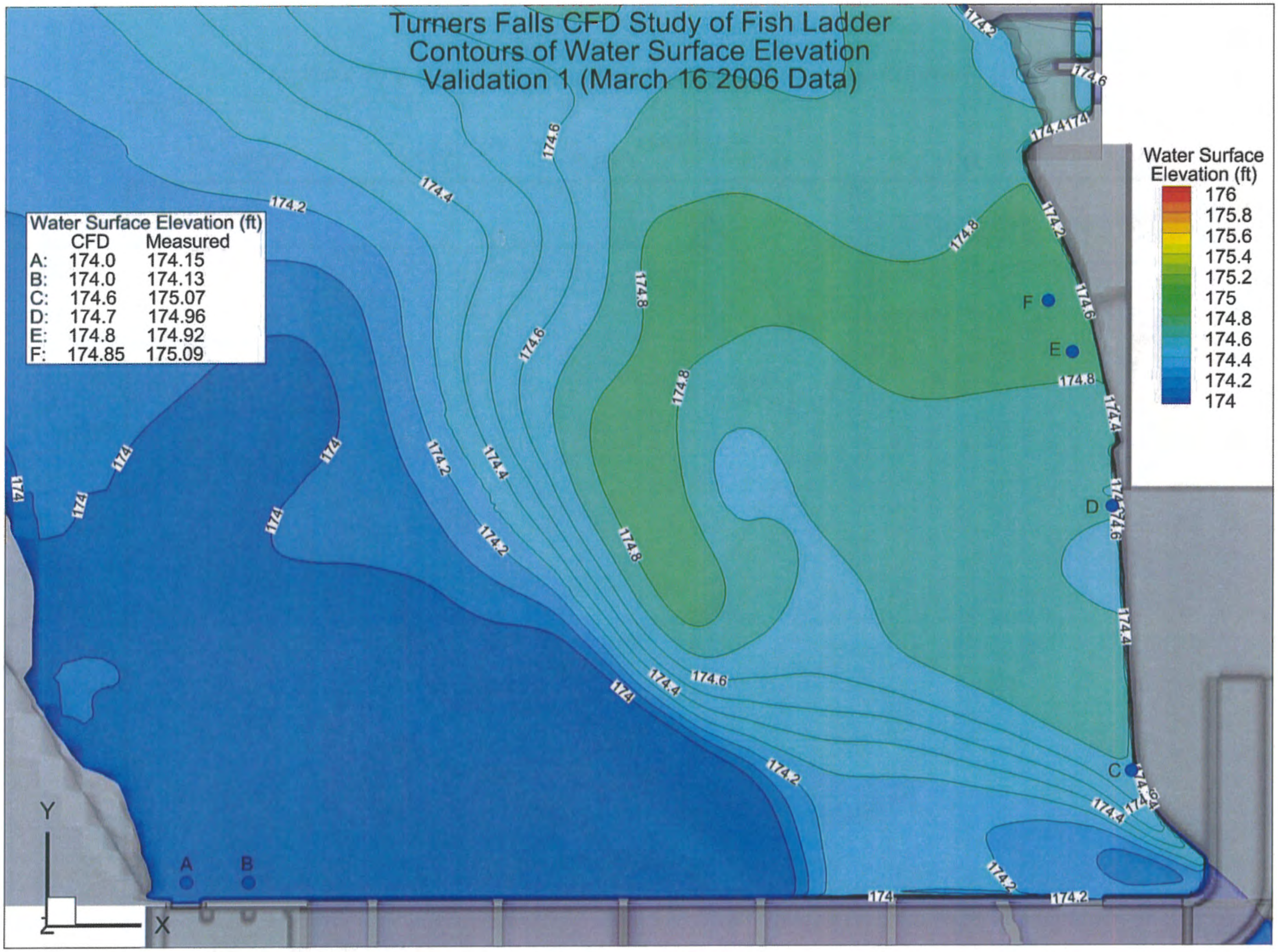

Figure 15 Validation Case 1: Water Surface Elevations and Measurement Points

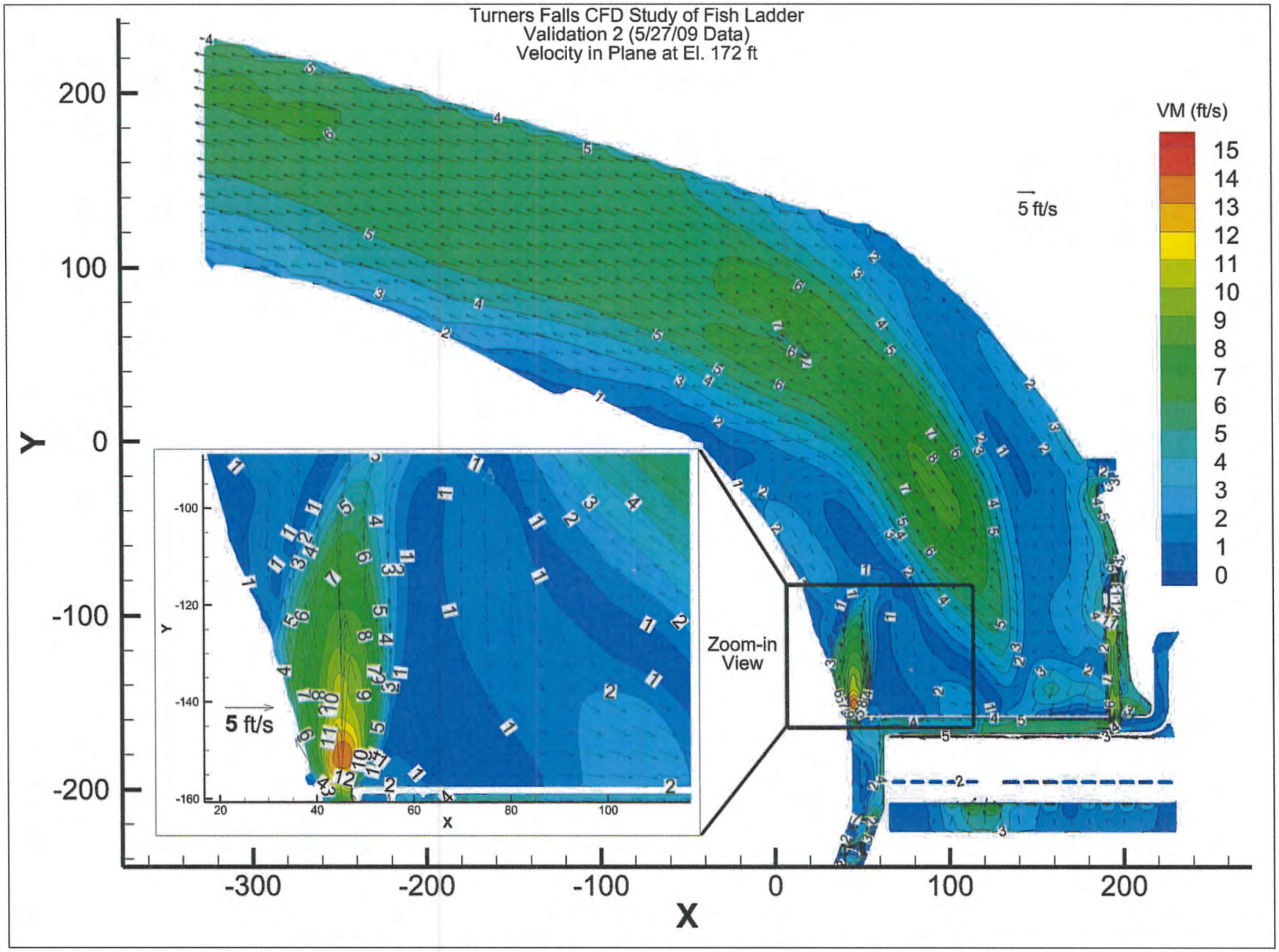

Figure 16 Validation Case 2: Velocity in Plane at Elevation 172 ft

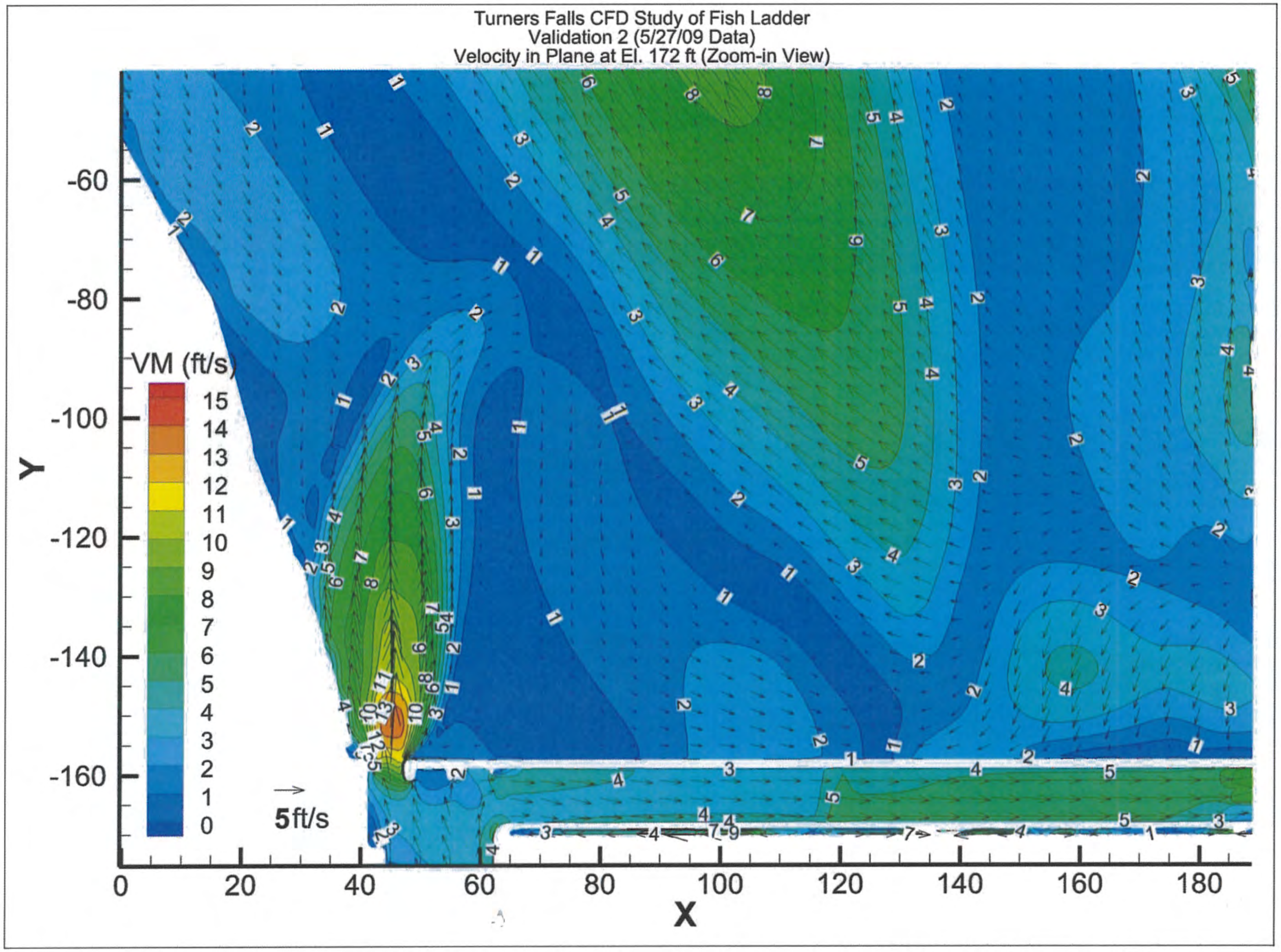

Figure 17 Validation Case 2: Velocity in the Vicinity of Old Entrance in the Canal in Plane at El. 172 ft

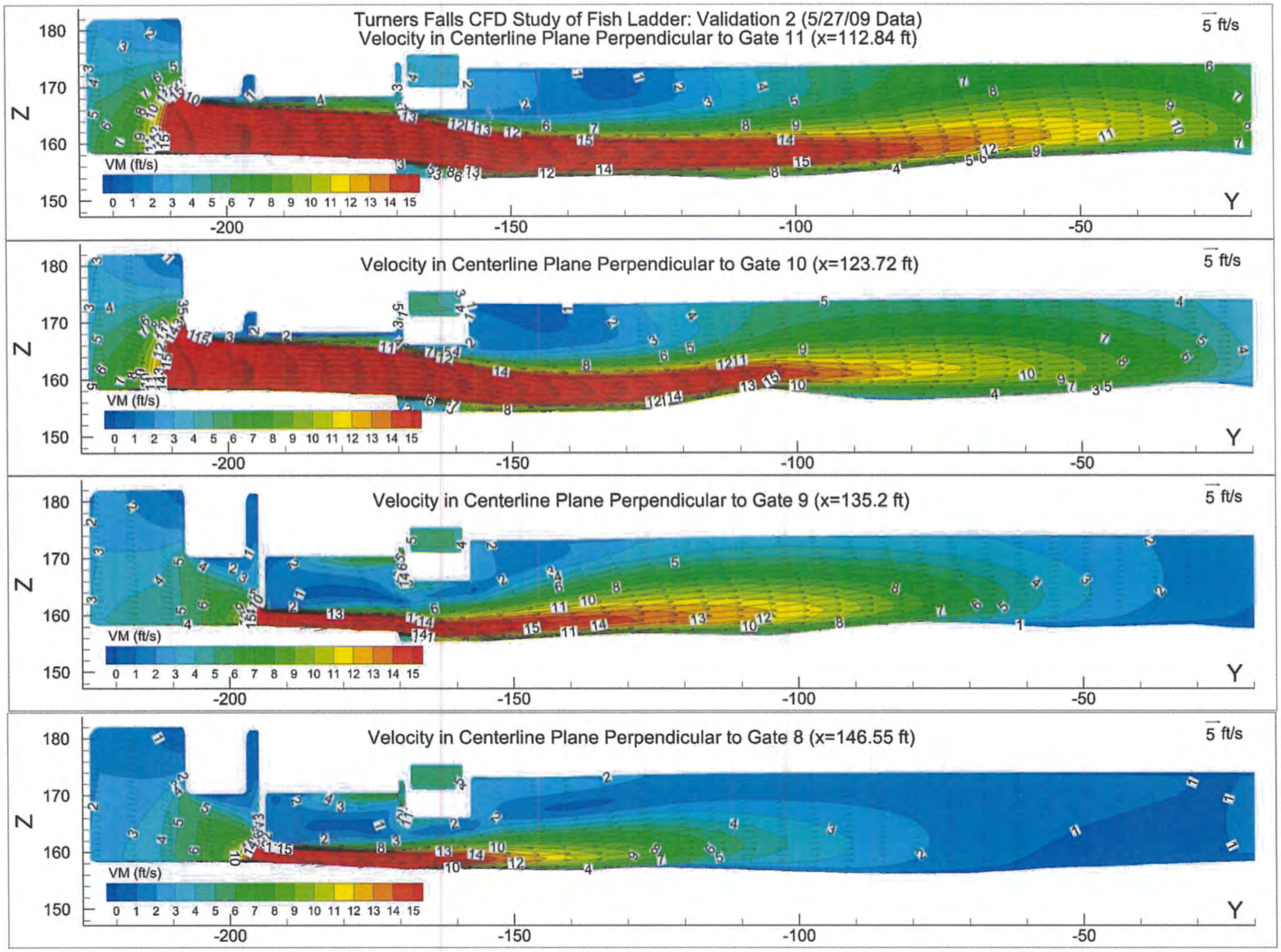

Figure 18 Validation Case 2: Velocity in Centerlines Planes of Gates 8 through 11

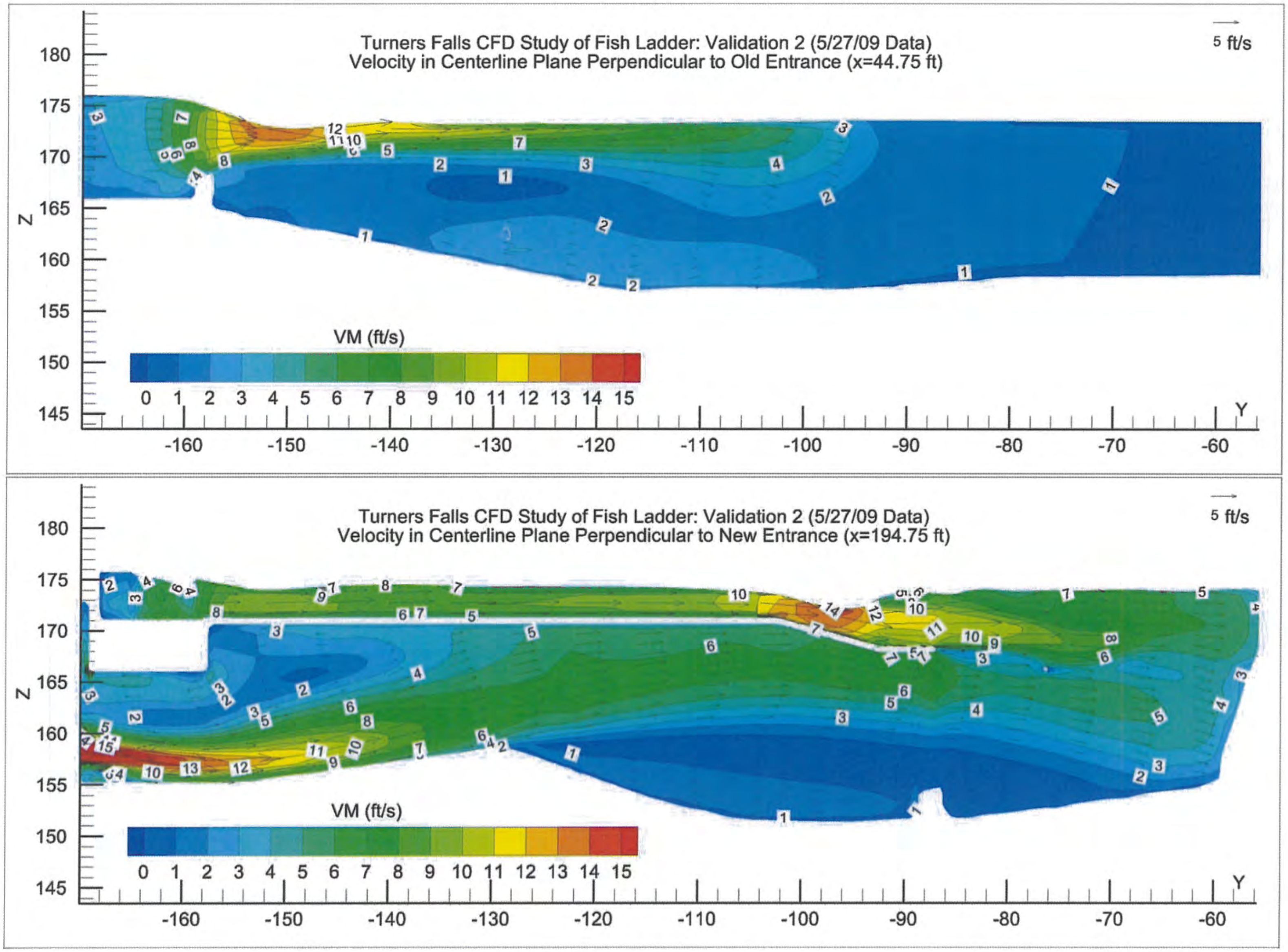

Figure 19 Validation Case 2: Velocity in Centerline Planes of Old and New Entrances

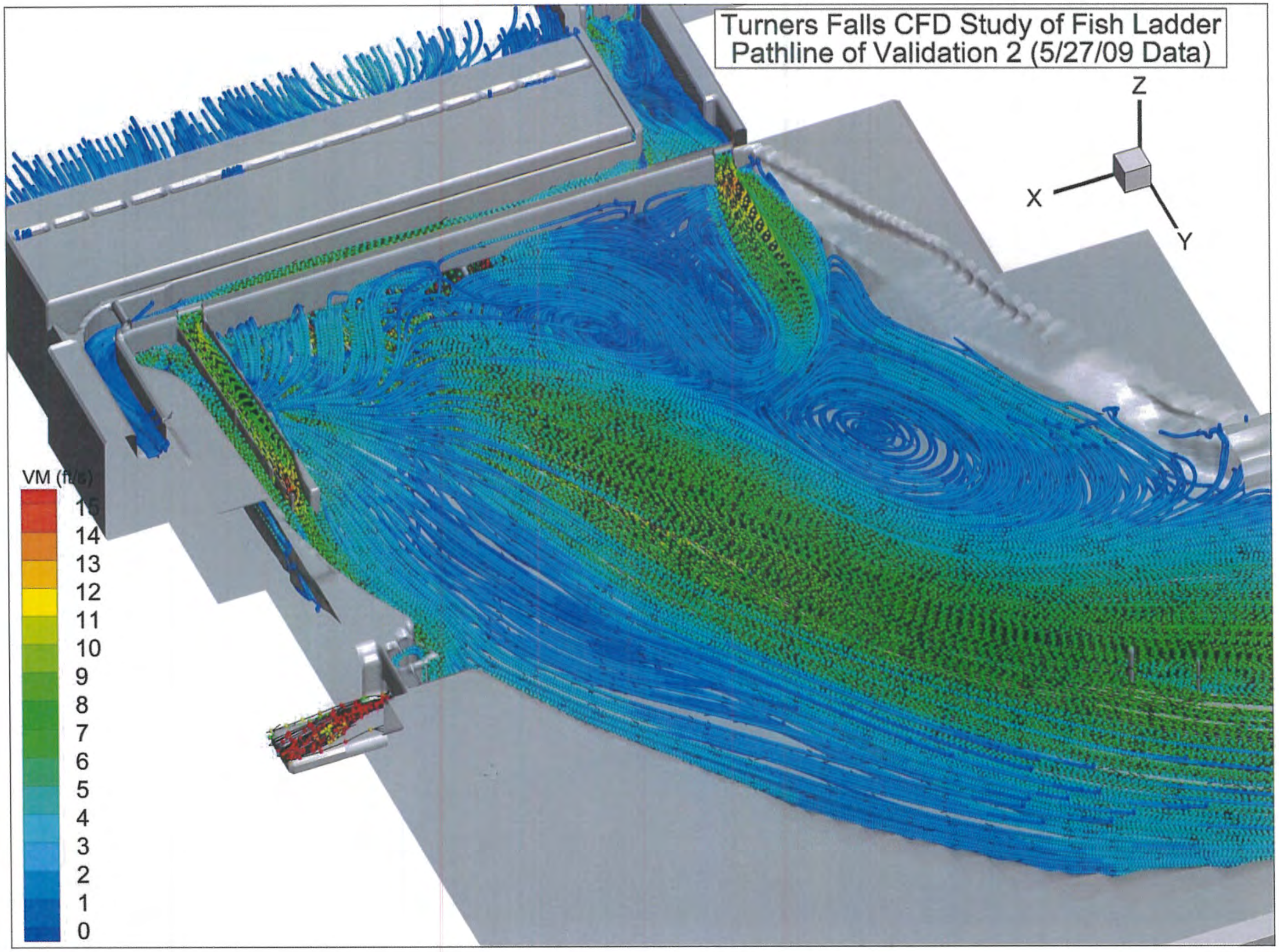

Figure 20 Validation Case 2: 3D Pathlines

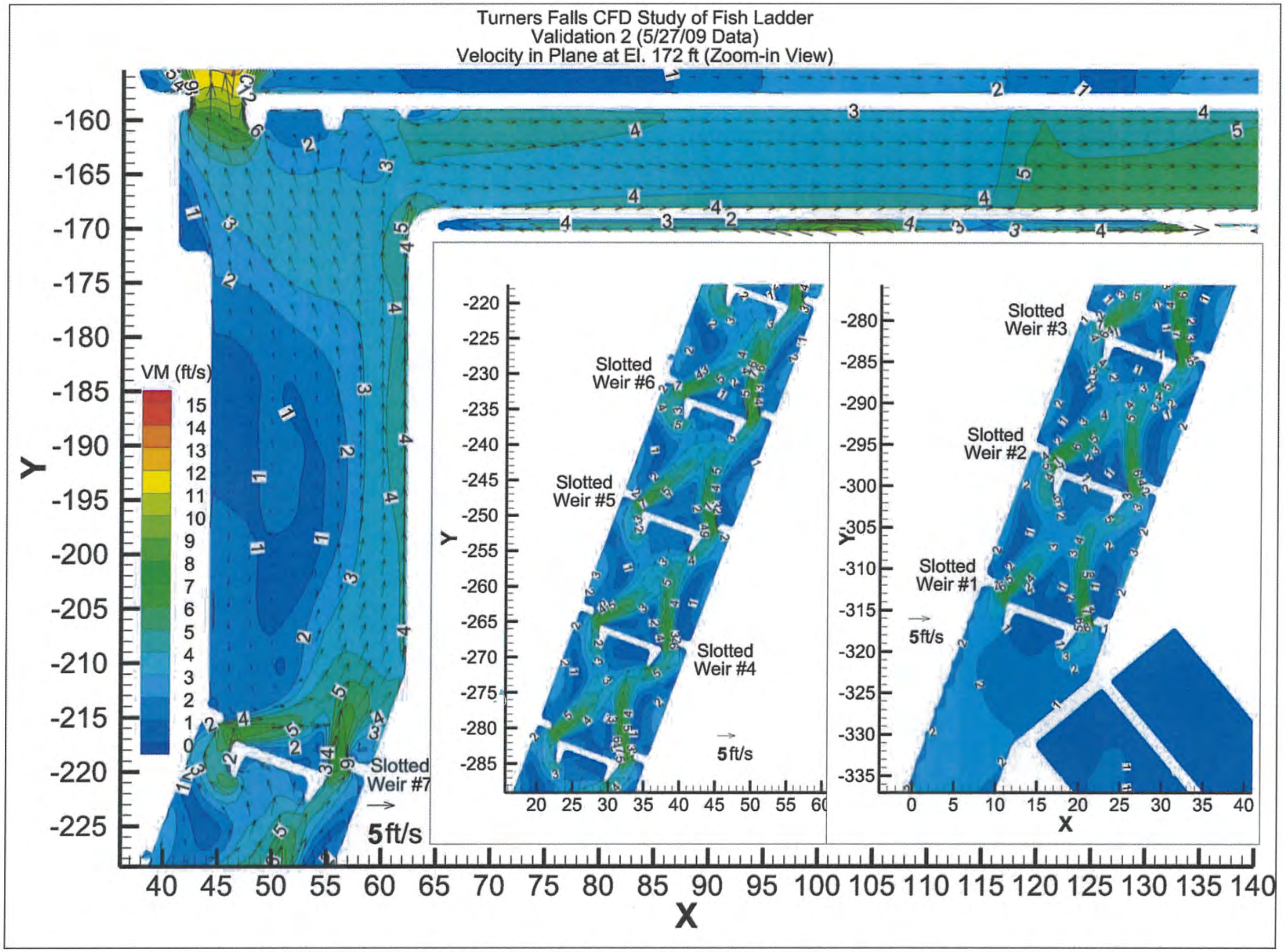

Figure 21 Validation Case 2: Velocity in the Gallery and Slotted Weirs in Plane at El. 172 ft

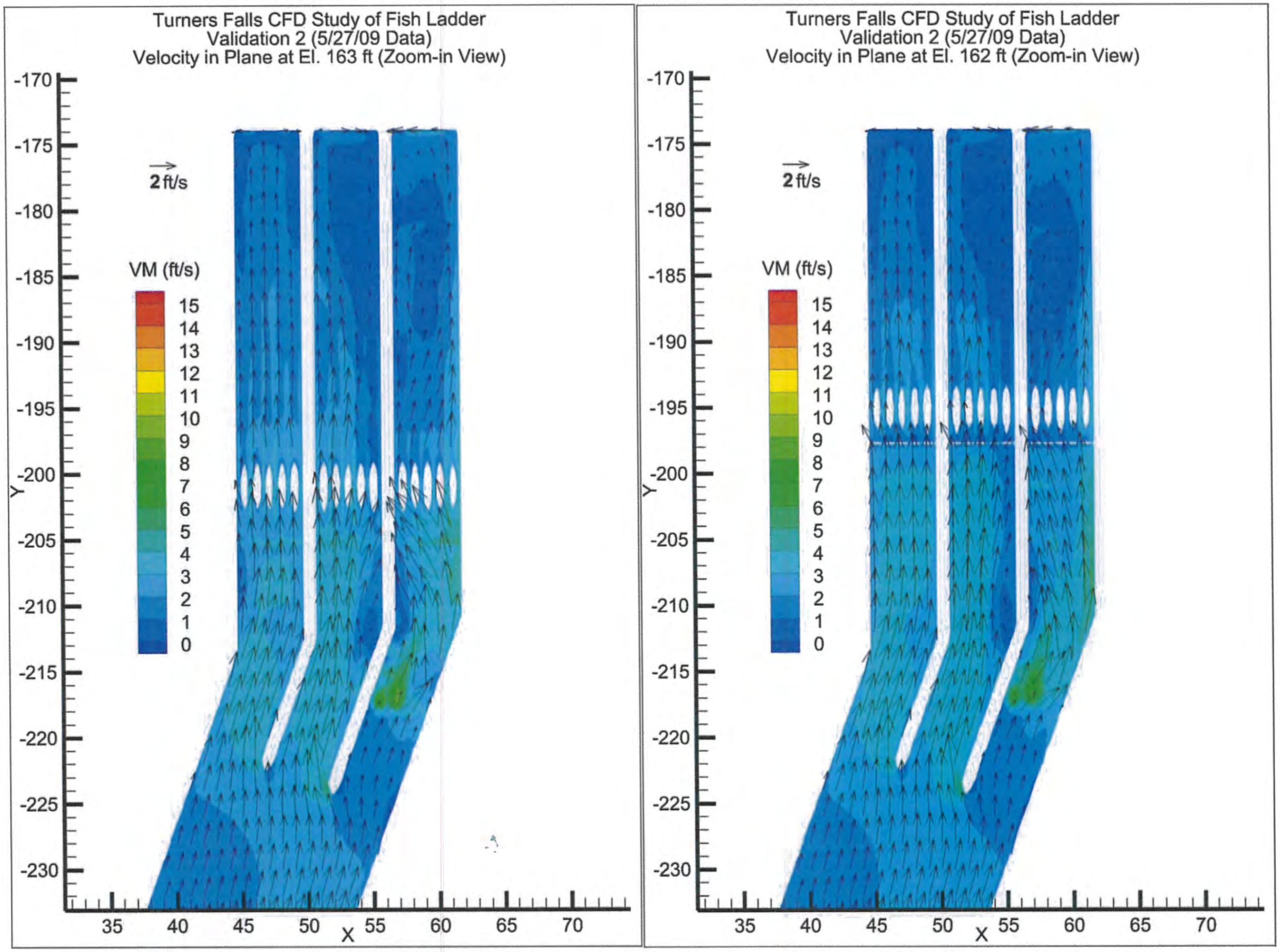

Figure 22 Validation Case 2: Velocity in Fish Way Channel through Gatehouse in Planes at El. 163 and El. 162 ft

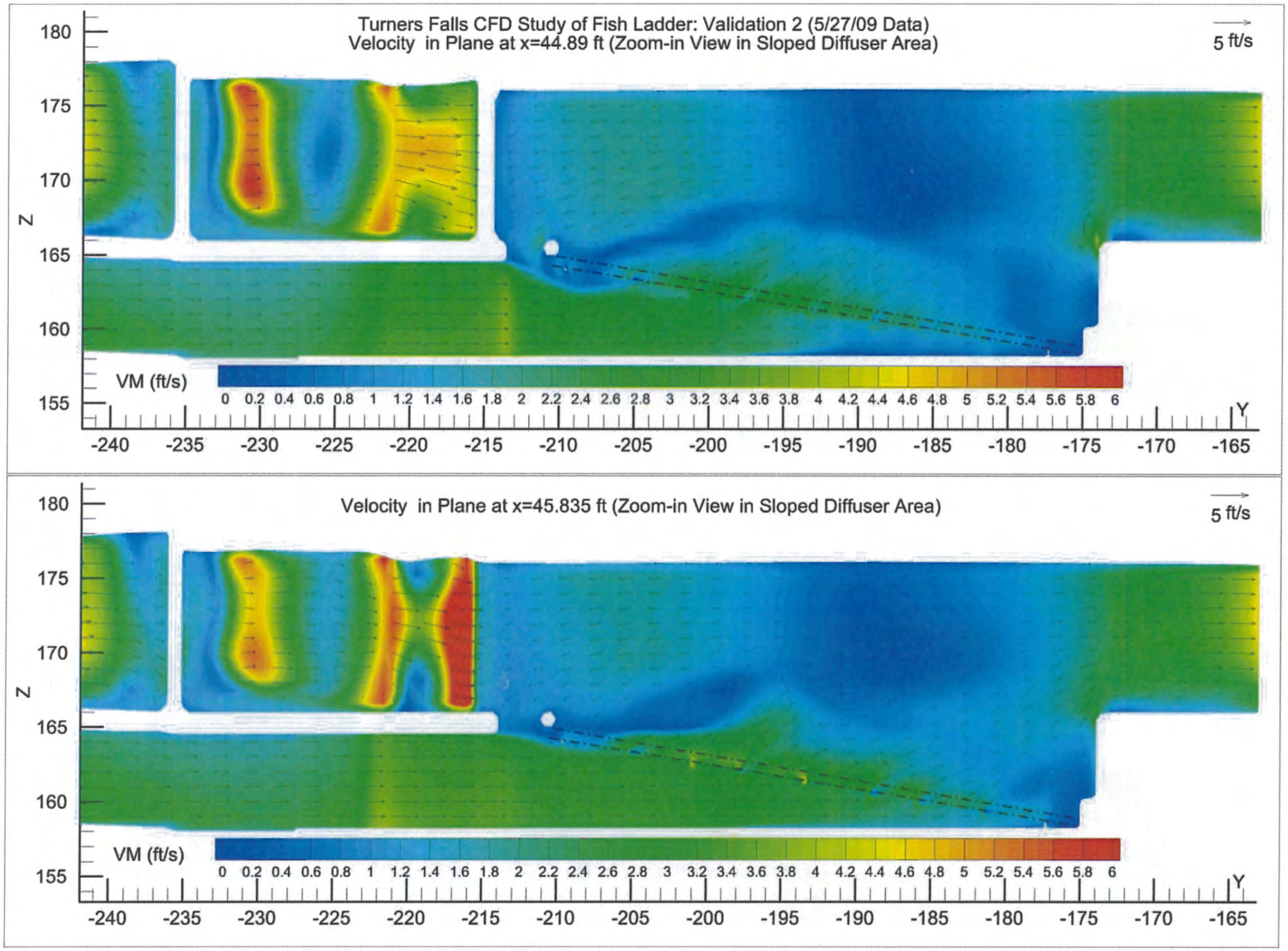
Turners Falls CFD Study of Fish Ladder: Validation 2 (5/27/09 Data)
Velocity in Plane at x=44.89 ft (Zoom-in View in Sloped Diffuser Area)
5 ft/s
Z
Y
VM (ft/s)
0 0.2 0.4 0.6 0.8 1 1.2 1.4 1.6 1.8 2 2.2 2.4 2.6 2.8 3 3.2 3.4 3.6 3.8 4 4.2 4.4 4.6 4.8 5 5.2 5.4 5.6 5.8 6
Velocity in Plane at x=45.835 ft (Zoom-in View in Sloped Diffuser Area)
5 ft/s
Z
Y
VM (ft/s)
0 0.2 0.4 0.6 0.8 1 1.2 1.4 1.6 1.8 2 2.2 2.4 2.6 2.8 3 3.2 3.4 3.6 3.8 4 4.2 4.4 4.6 4.8 5 5.2 5.4 5.6 5.8 6

Figure 23 Validation Case 2: Velocity in Vertical Planes in the Left Channel of Sloped Diffuser

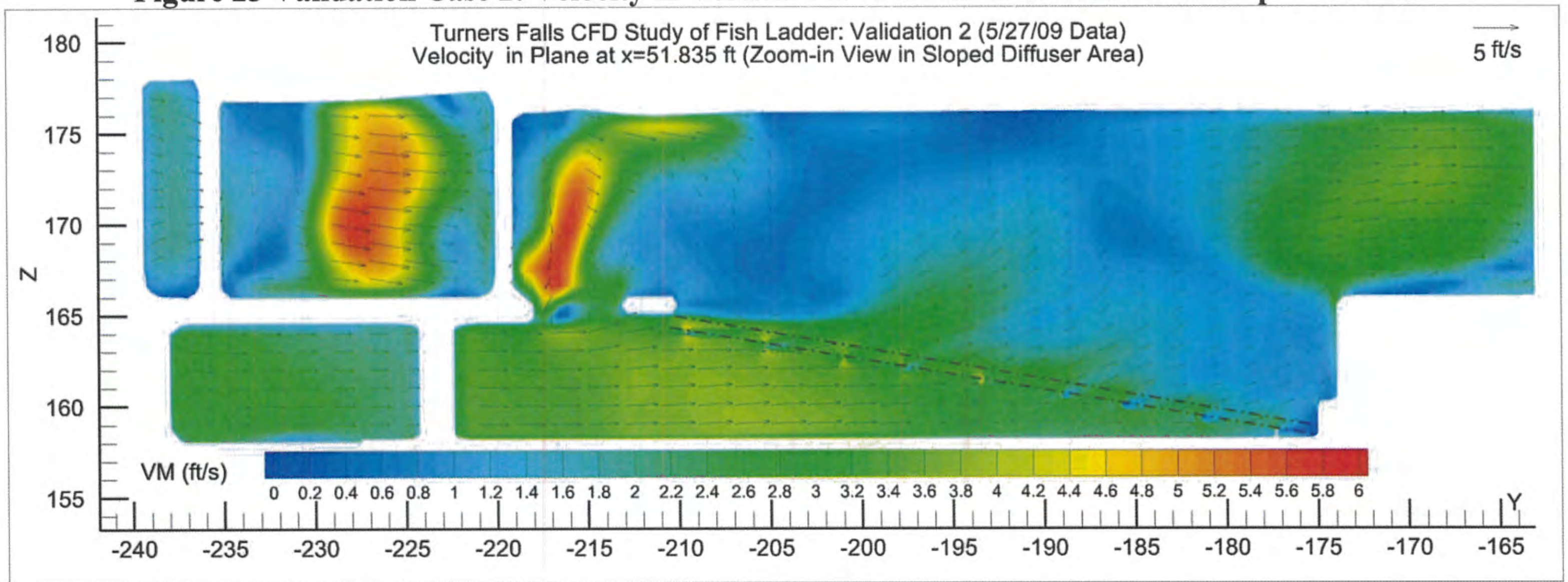

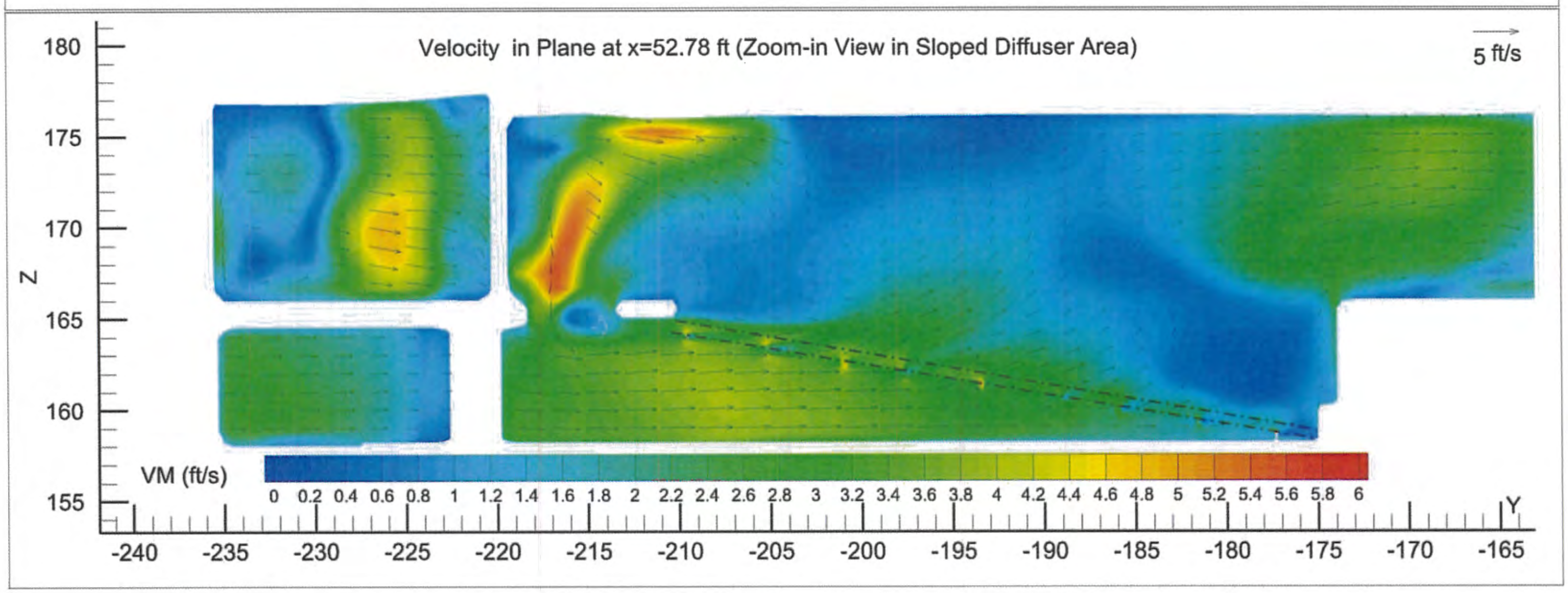

Figure 24 Validation Case 2: Velocity in Vertical Planes in the Middle Channel of Sloped Diffuser

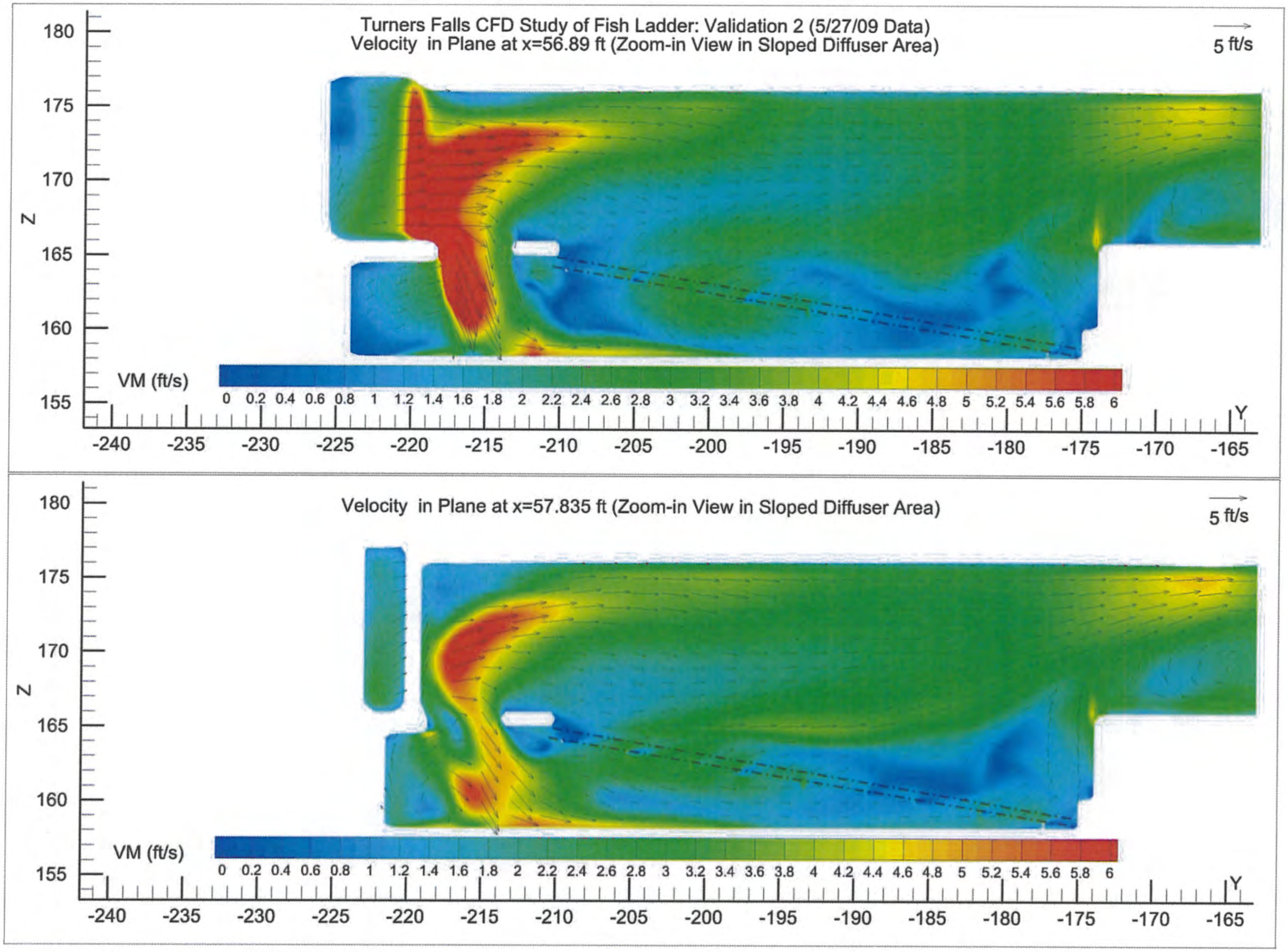

Figure 25 Validation Case 2: Velocity in Vertical Planes in the Right Channel of Sloped Diffuser

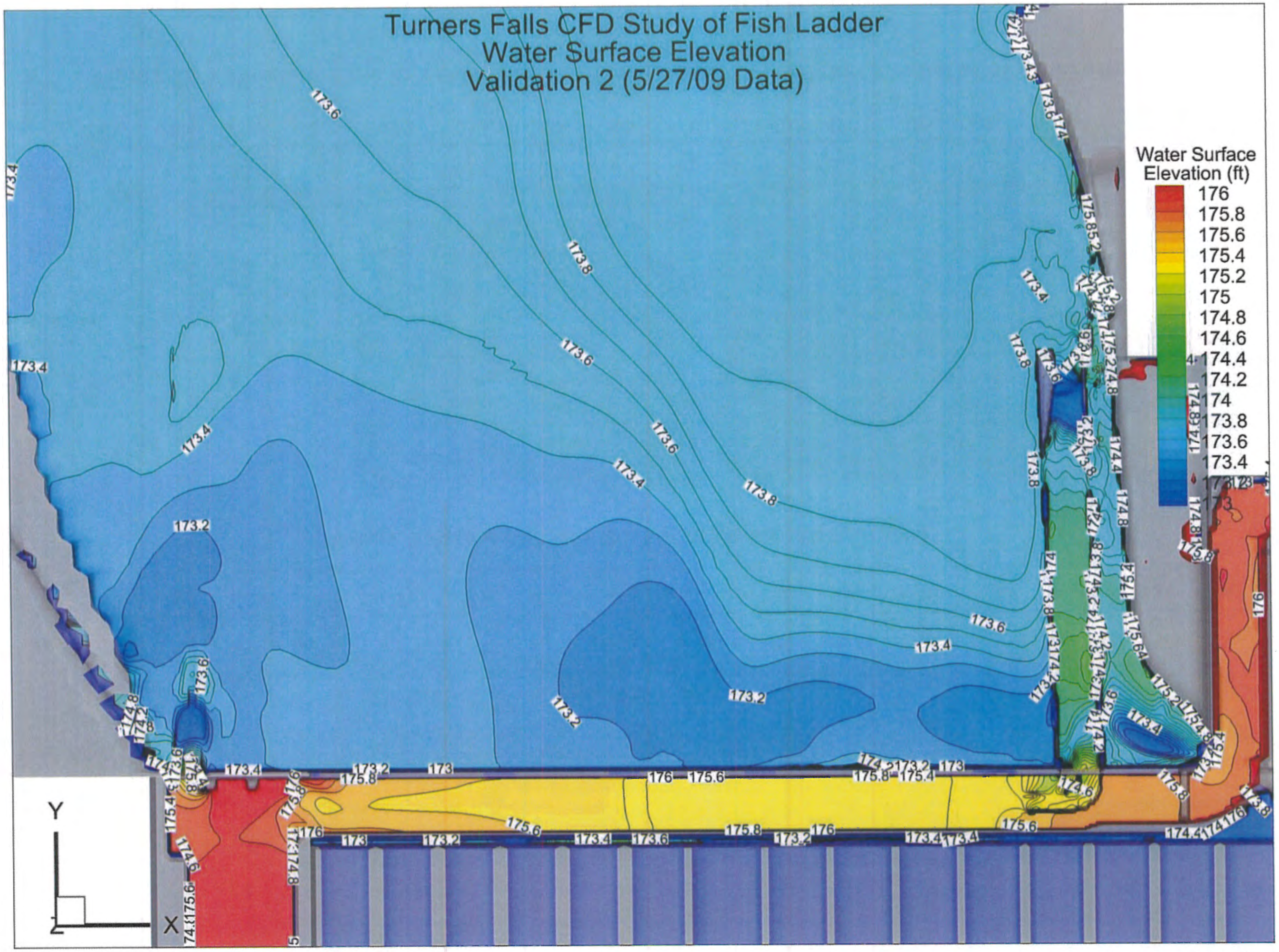

Figure 26 Validation Case 2: Water Surface Elevation in the Vicinity of Old and New Entrances in the Canal

Figure 27 Validation Case 2: Water Surface Elevation in the Vicinity of Old Entrance and Measurement Points Locations

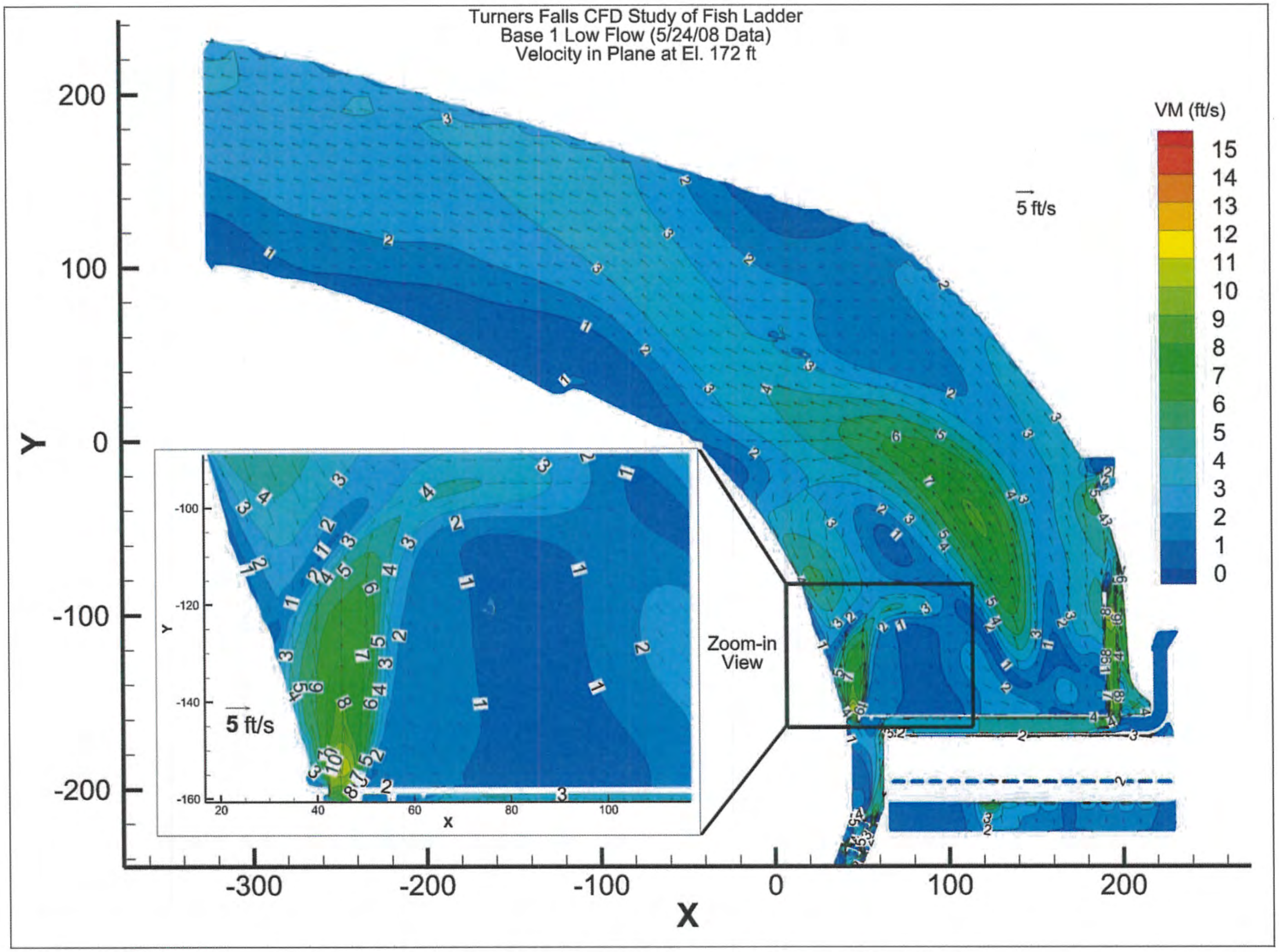

Figure 28 Base 1 Low Flow: Velocity in Plane at El. 172 ft

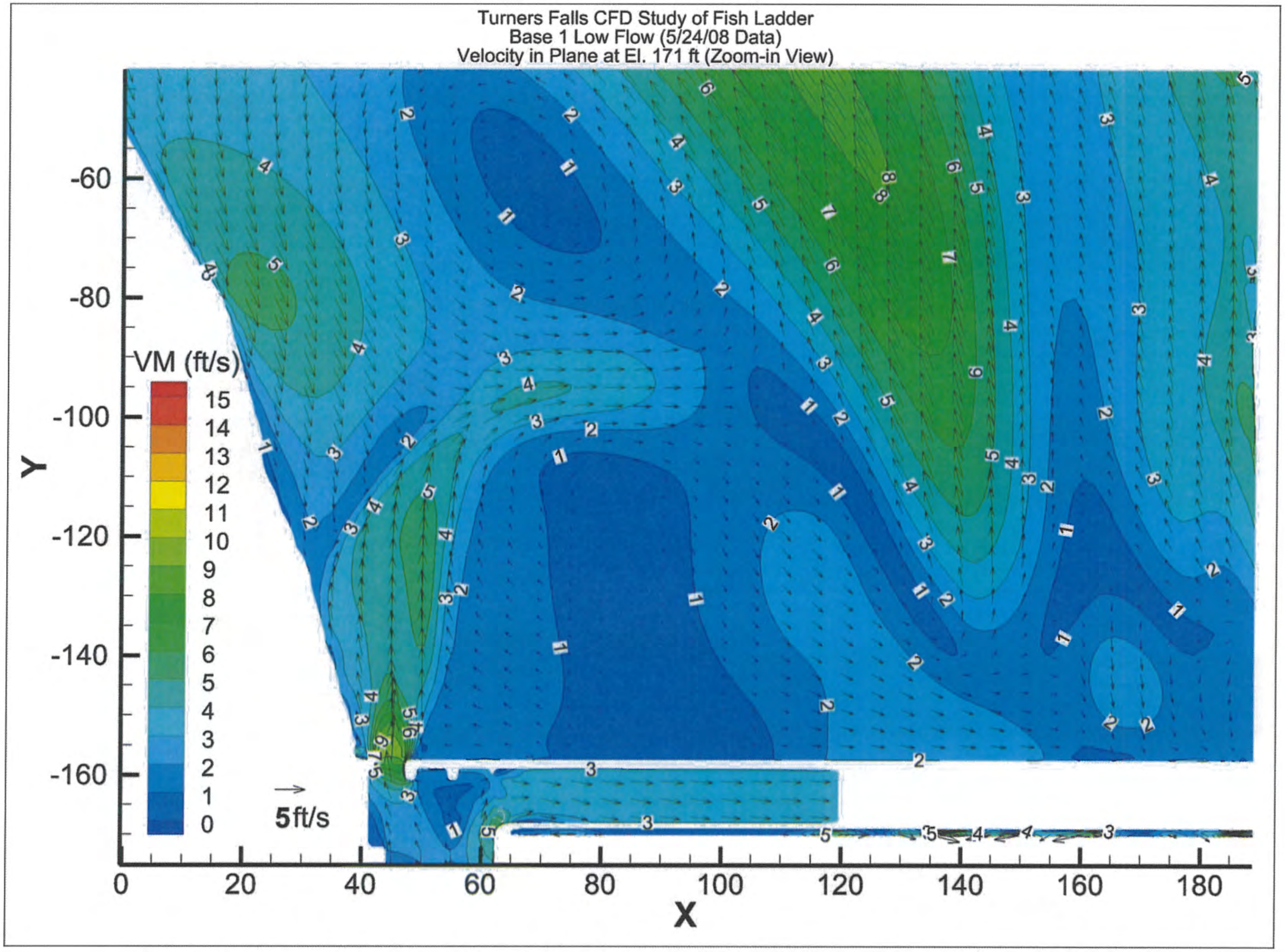

Figure 29 Base 1 Low Flow: Velocity in the Vicinity of Old Entrance in Plane at El. 172 ft

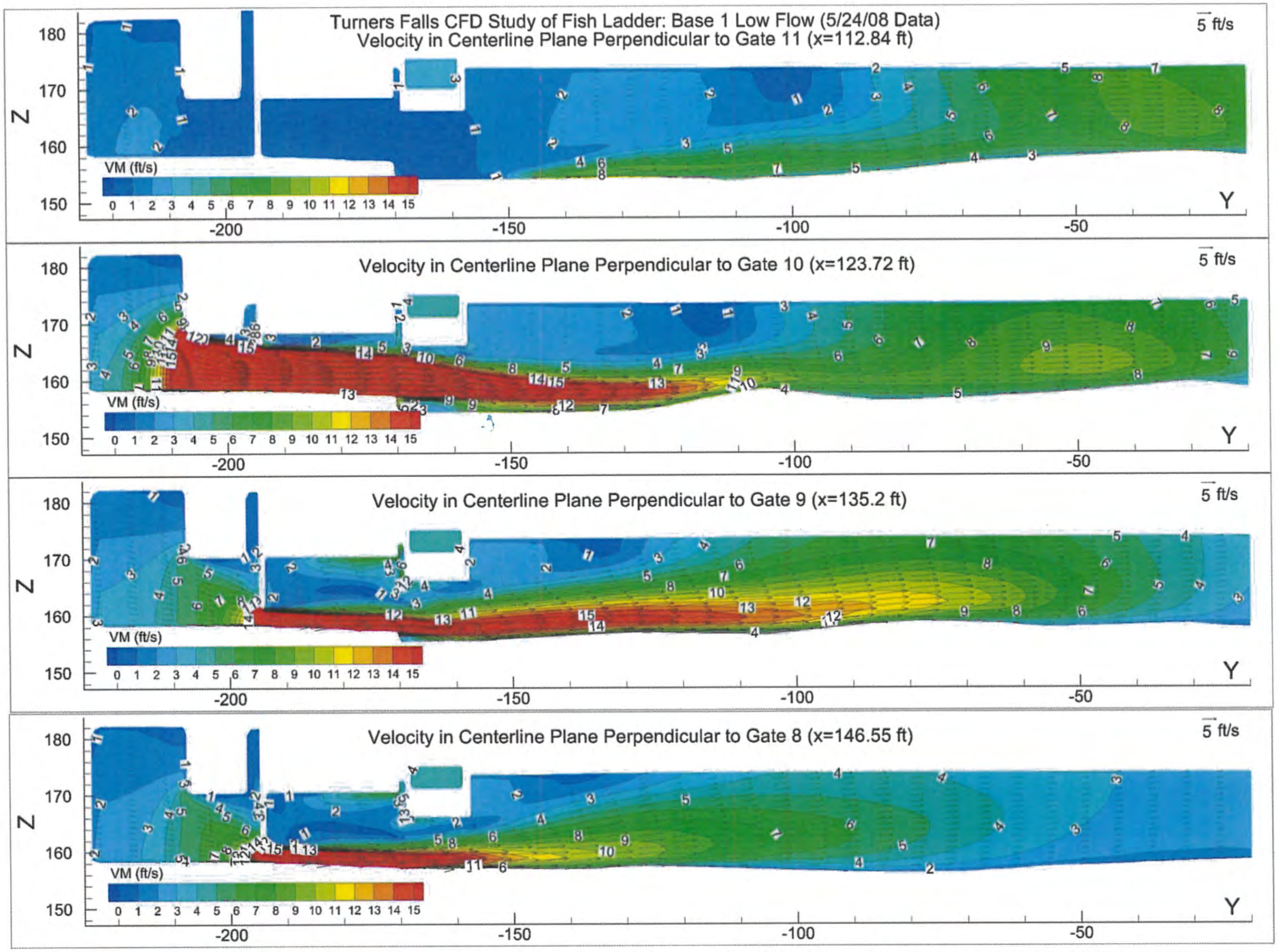

Figure 30 Base 1 Low Flow: Velocity in Centerline Planes of Gates 8 through 11

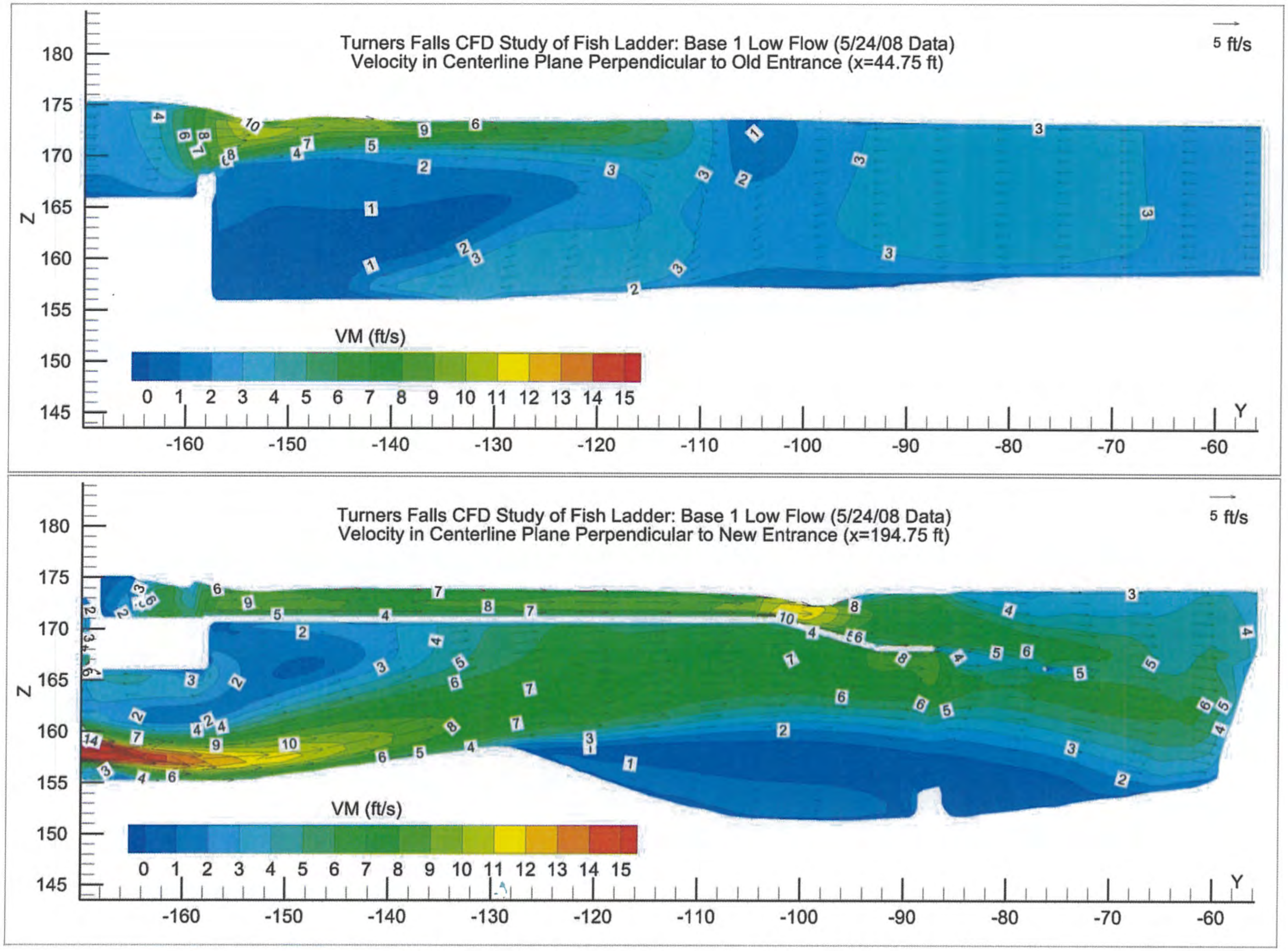

Figure 31 Base 1 Low Flow: Velocity in Centerline Planes of Old and New Entrance

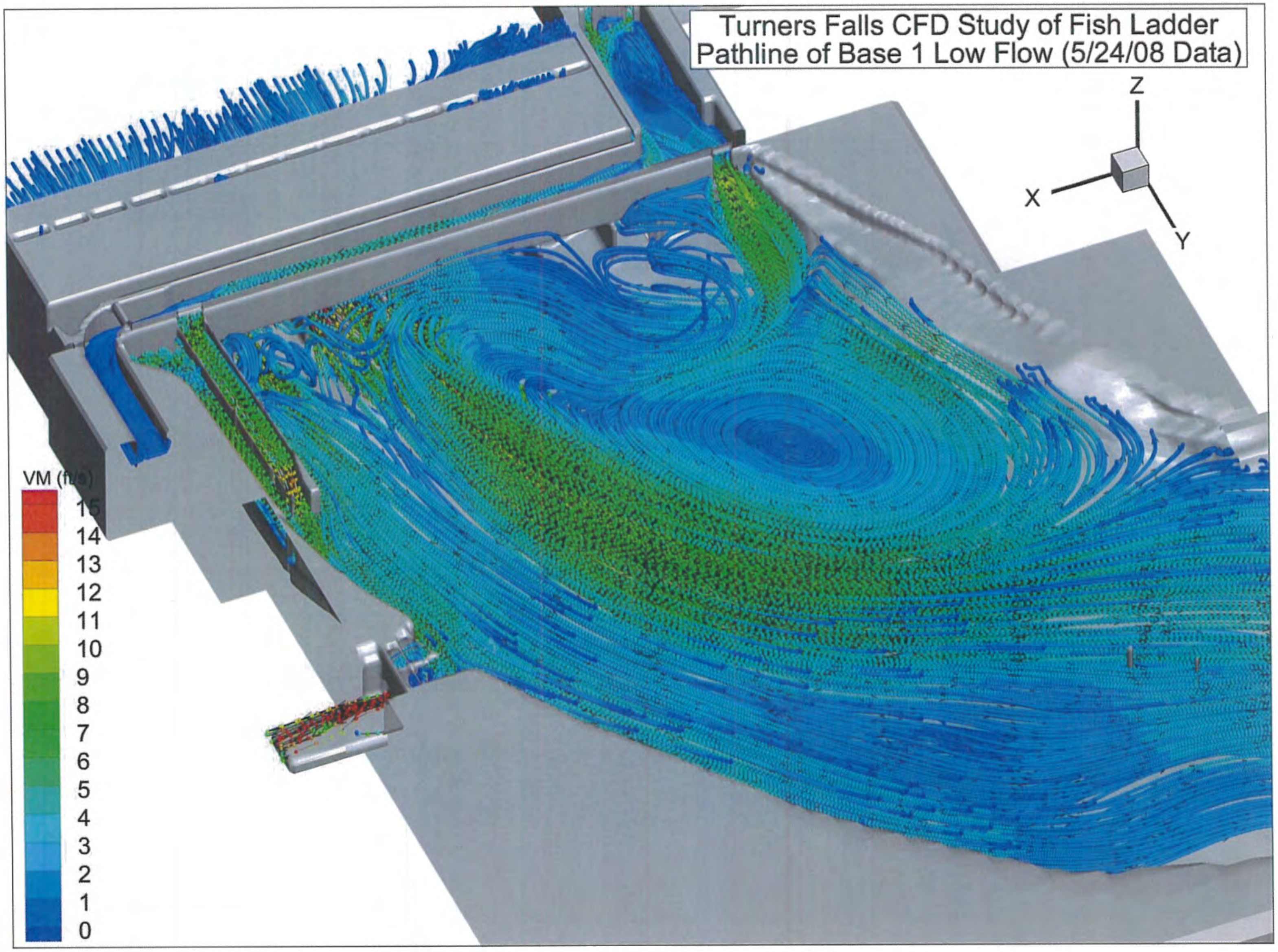

Figure 32 Base 1 Low Flow: 3D Pathlines

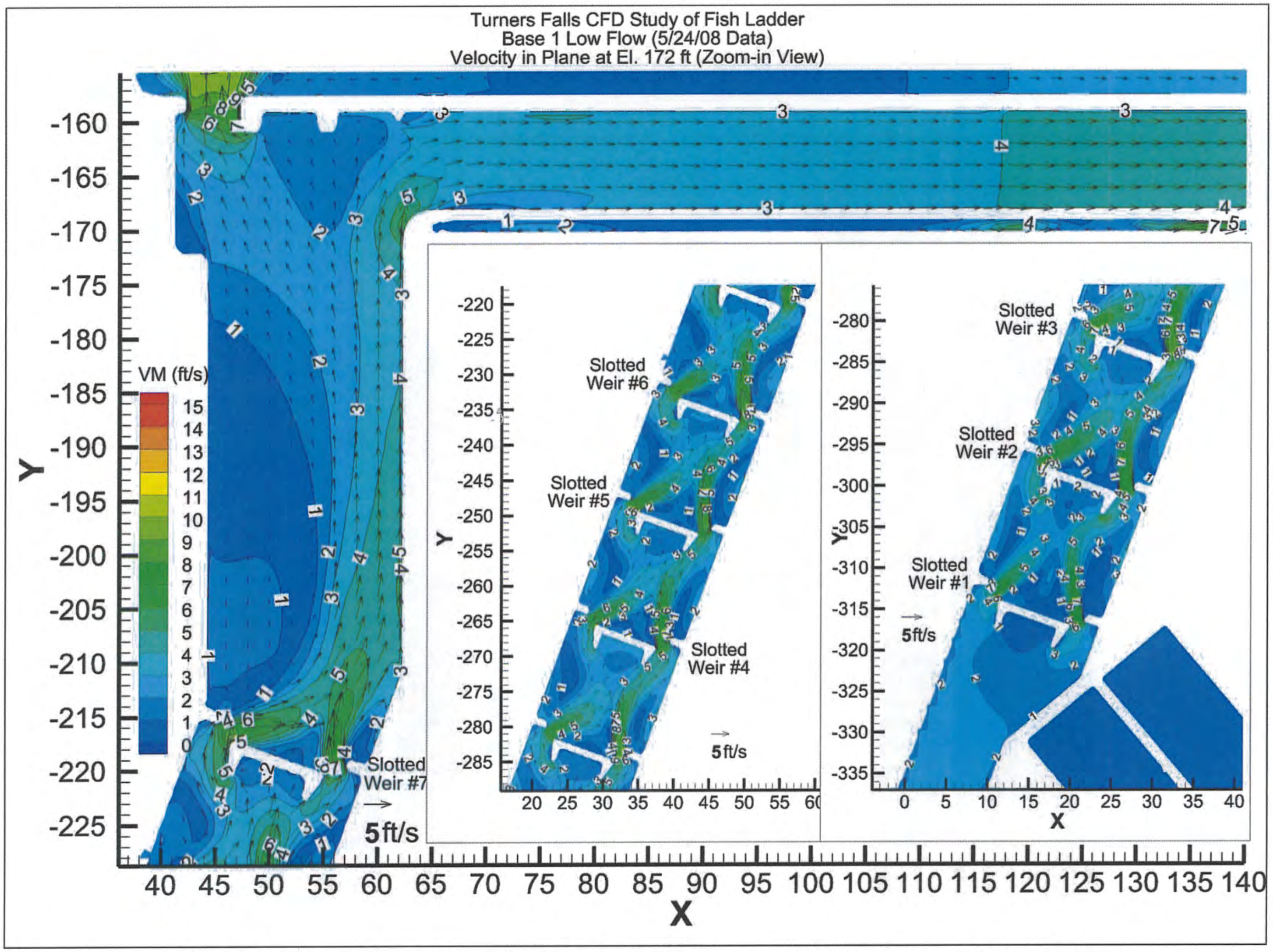

Figure 33 Base 1 Low Flow: Velocity in the Gallery and Slotted Weirs at El. 172 ft

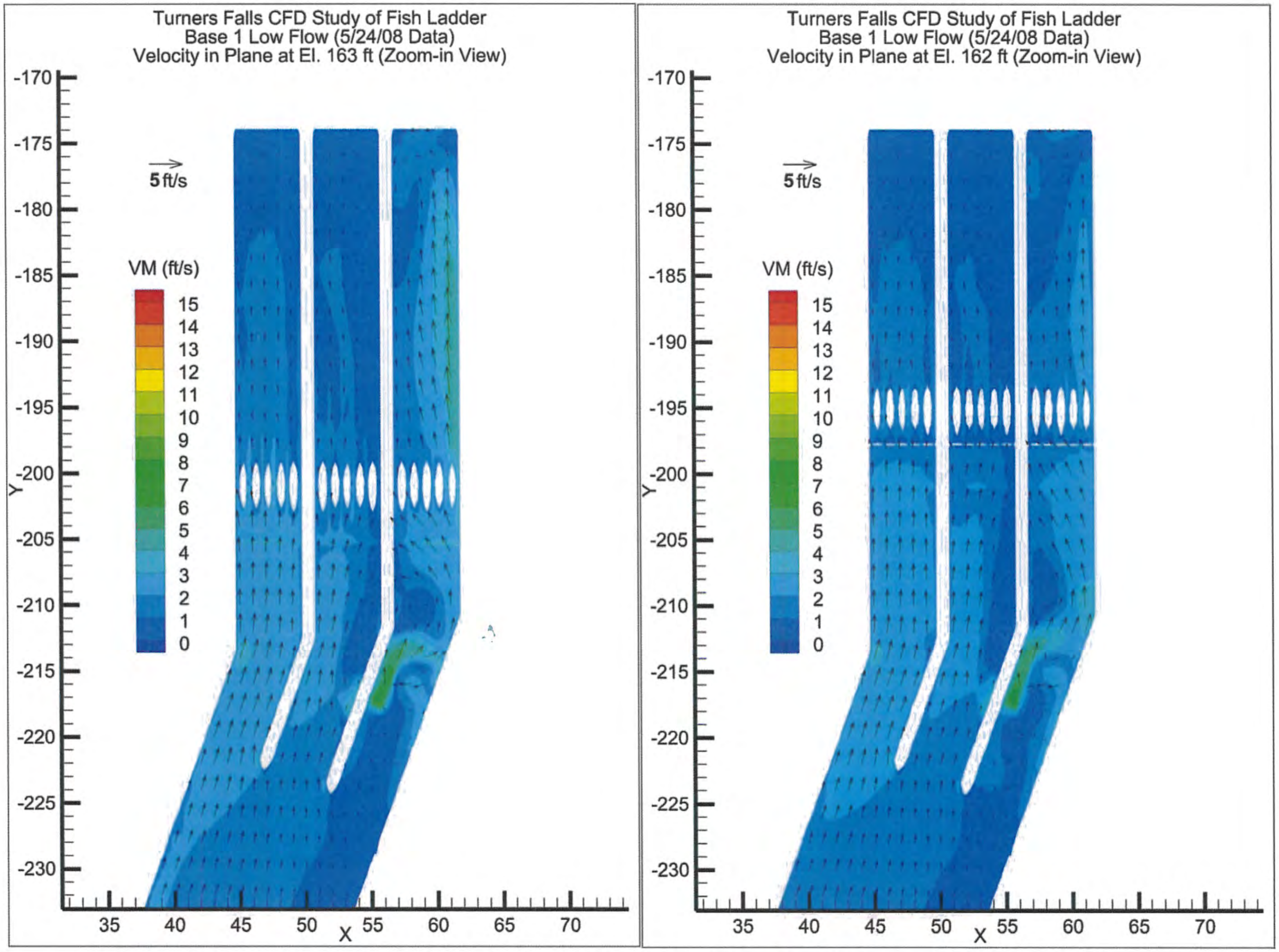

Figure 34 Base 1 Low Flow: Velocity in the Upstream Attraction Tunnel at El. 163 and El. 162 ft

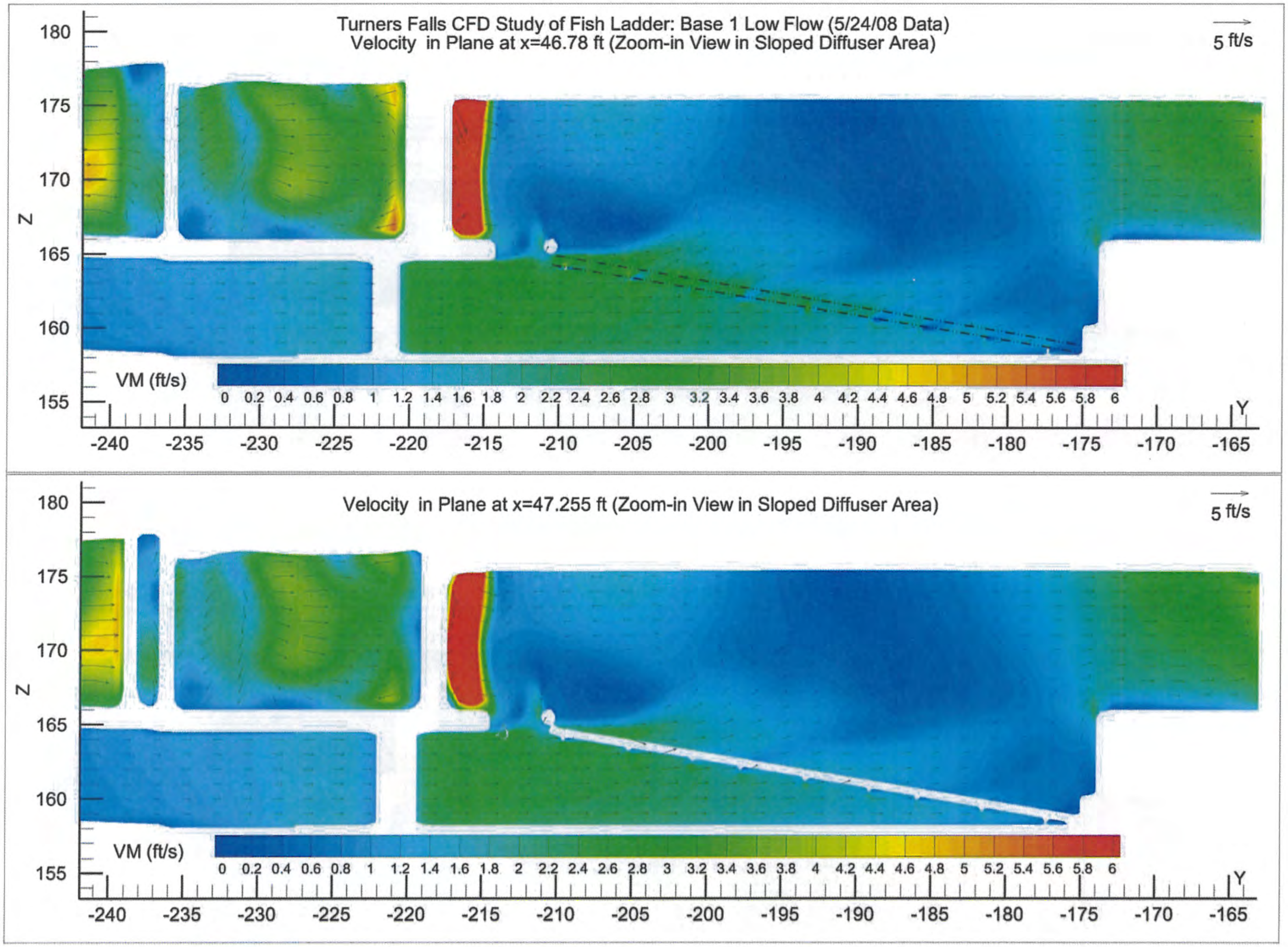

Figure 35 Base 1 Low Flow: Velocity in Vertical Planes of the Left Channel of Sloped Diffuser

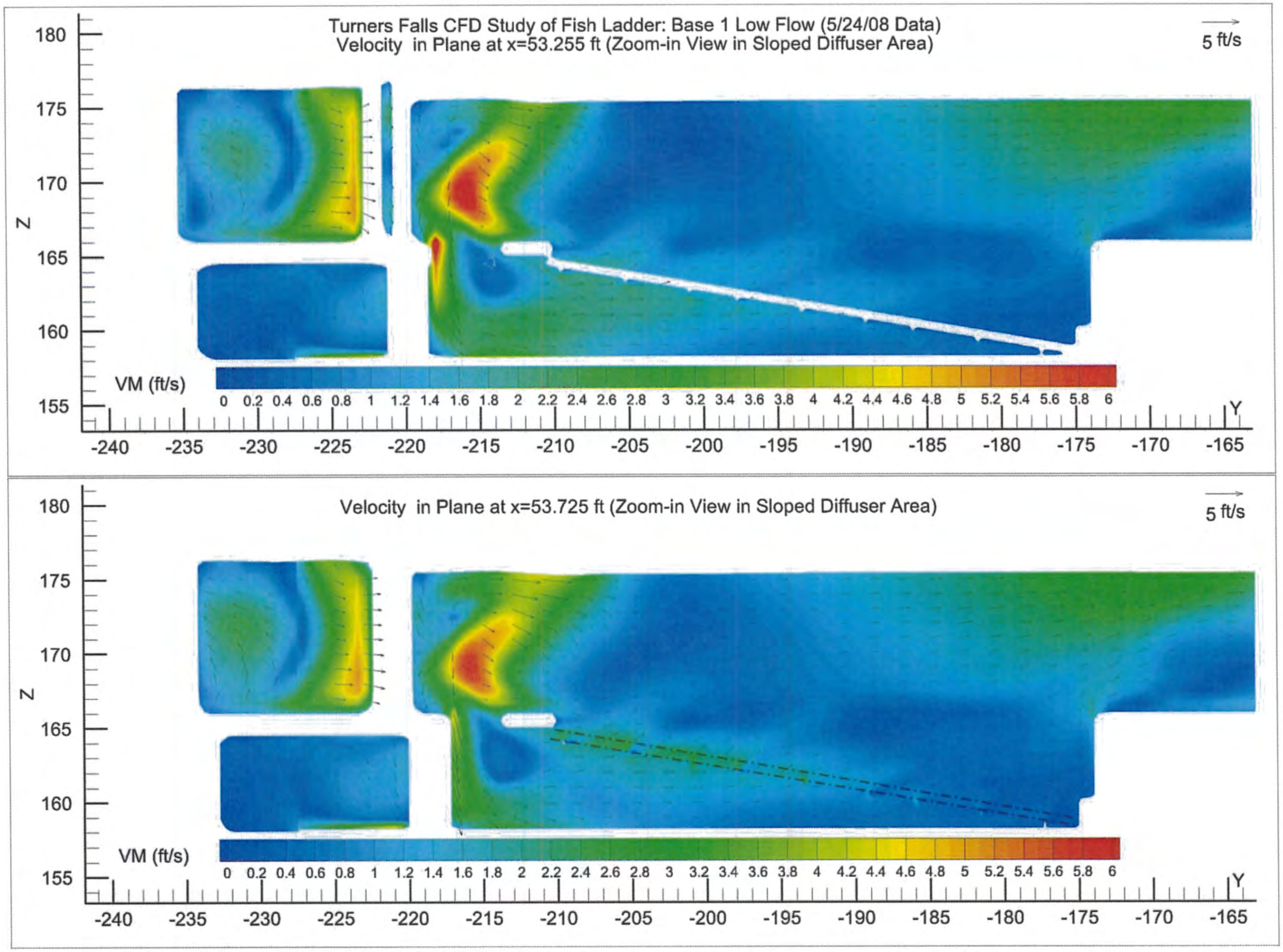

Figure 36 Base 1 Low Flow: Velocity in Vertical Planes of the Middle Channel of Sloped Diffuser

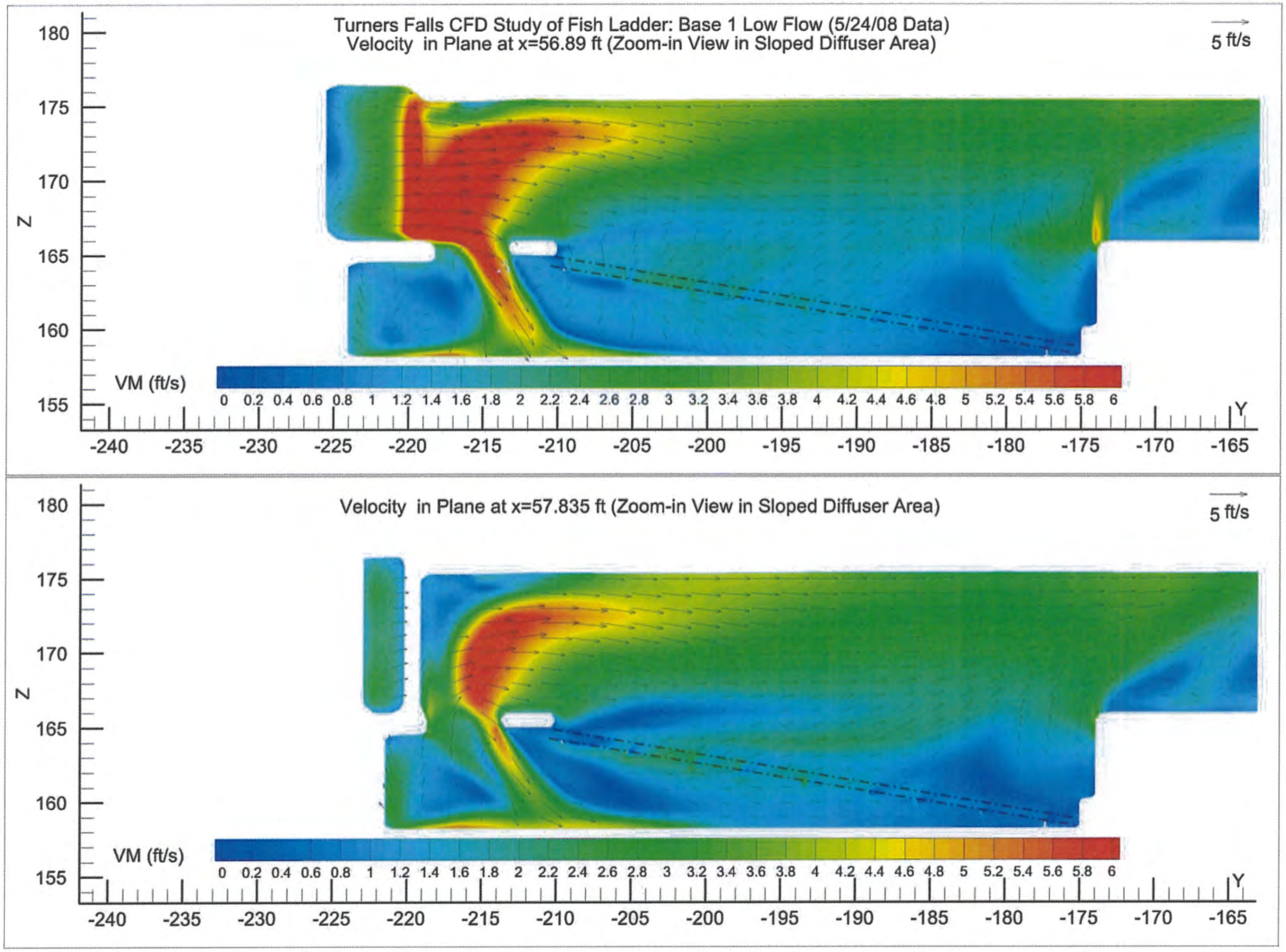

Figure 37 Base 1 Low Flow: Velocity in Vertical Planes in the Right Channel of Sloped Diffuser

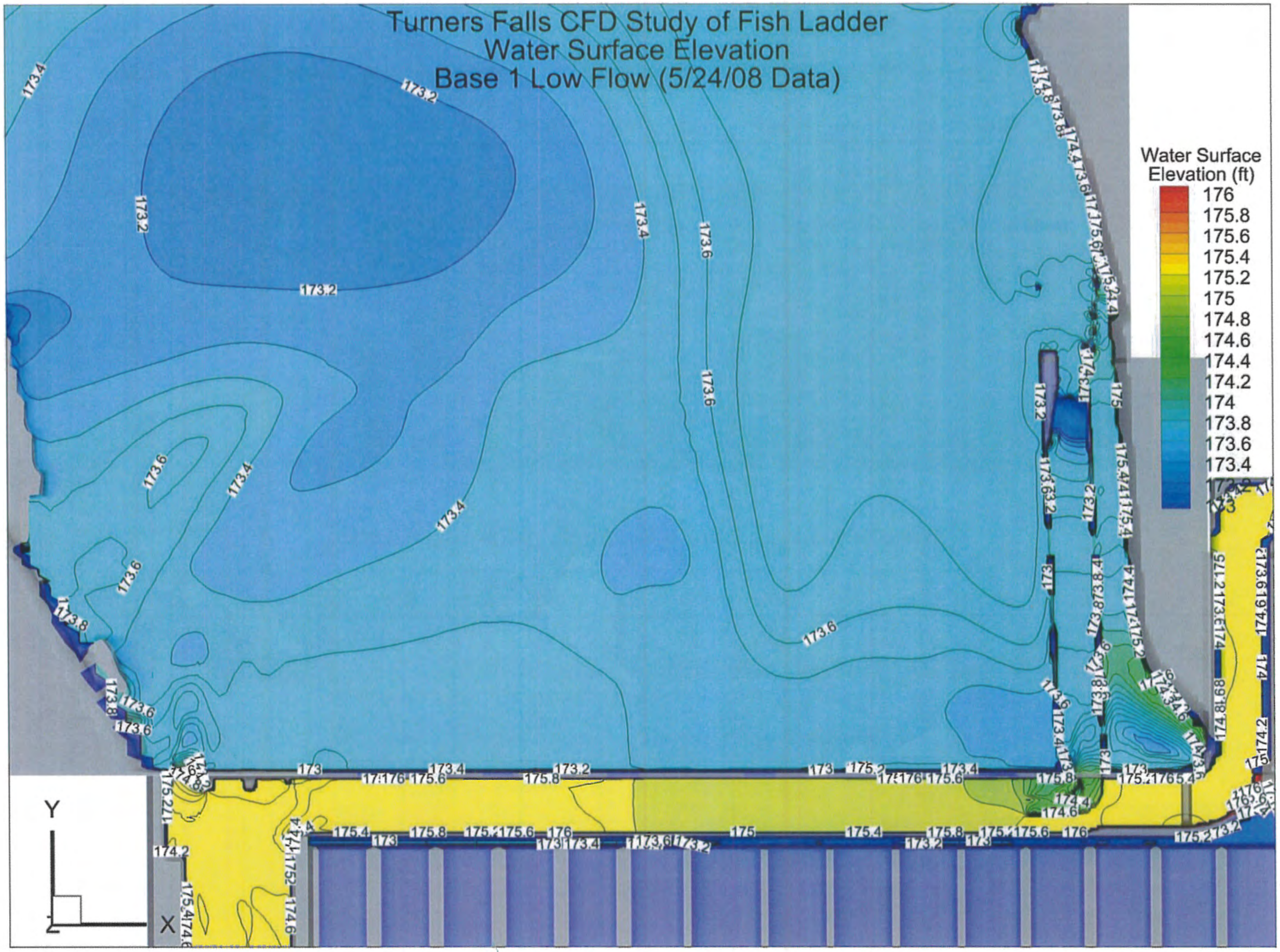

Figure 38 Base 1 Low Flow: Water Surface Elevation in the Vicinity of Old and New Entrances in the Canal

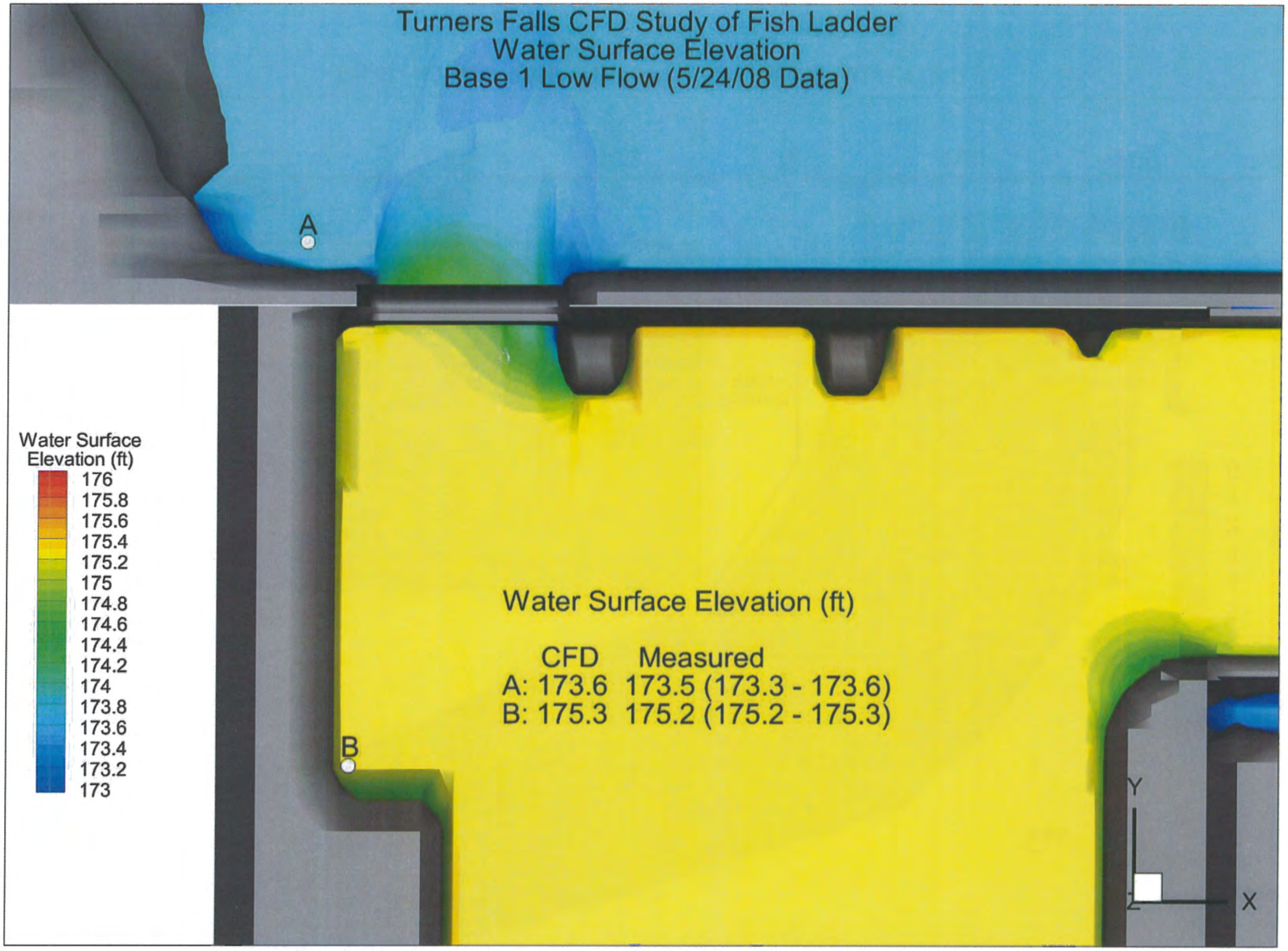

Figure 39 Base 1 Low Flow: Water Surface Elevation in the Vicinity of Old Entrance and Measurement Points Locations

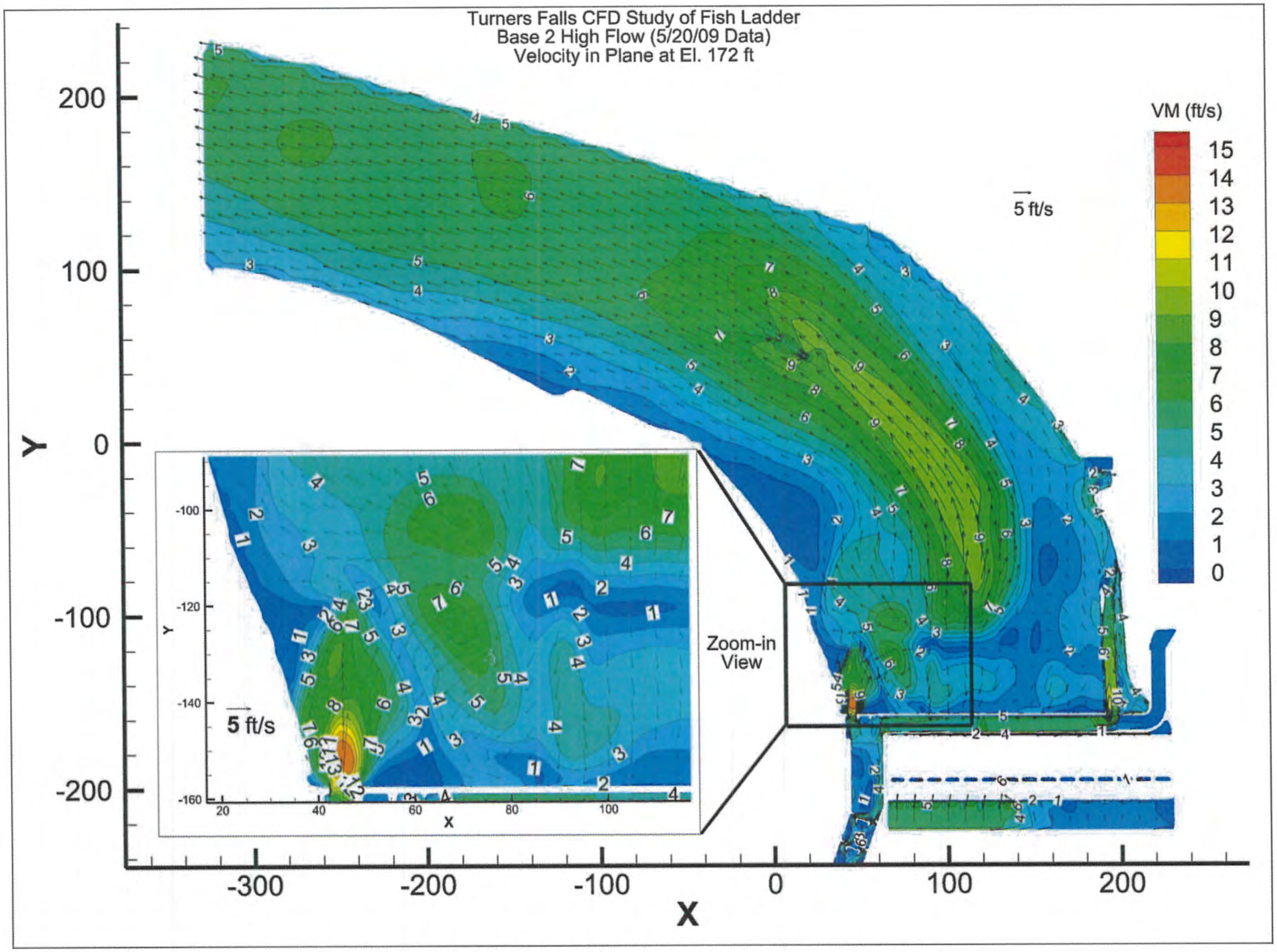

Figure 40 Base 2 High Flow: Velocity at Elevation 172 ft

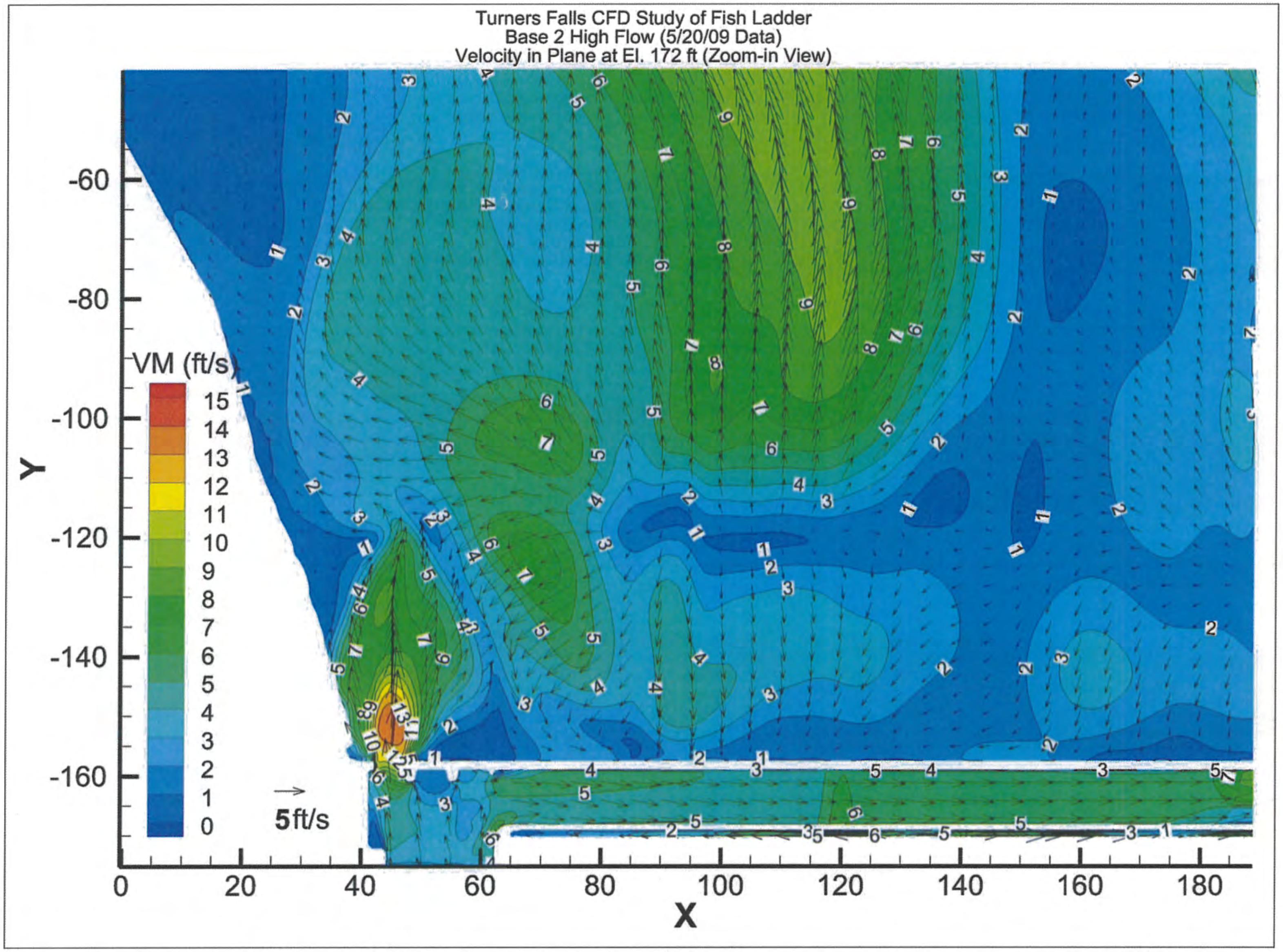

Figure 41 Base 2 High Flow: Velocity in the Vicinity of Old Entrance in the Canal at Elevation 172 ft

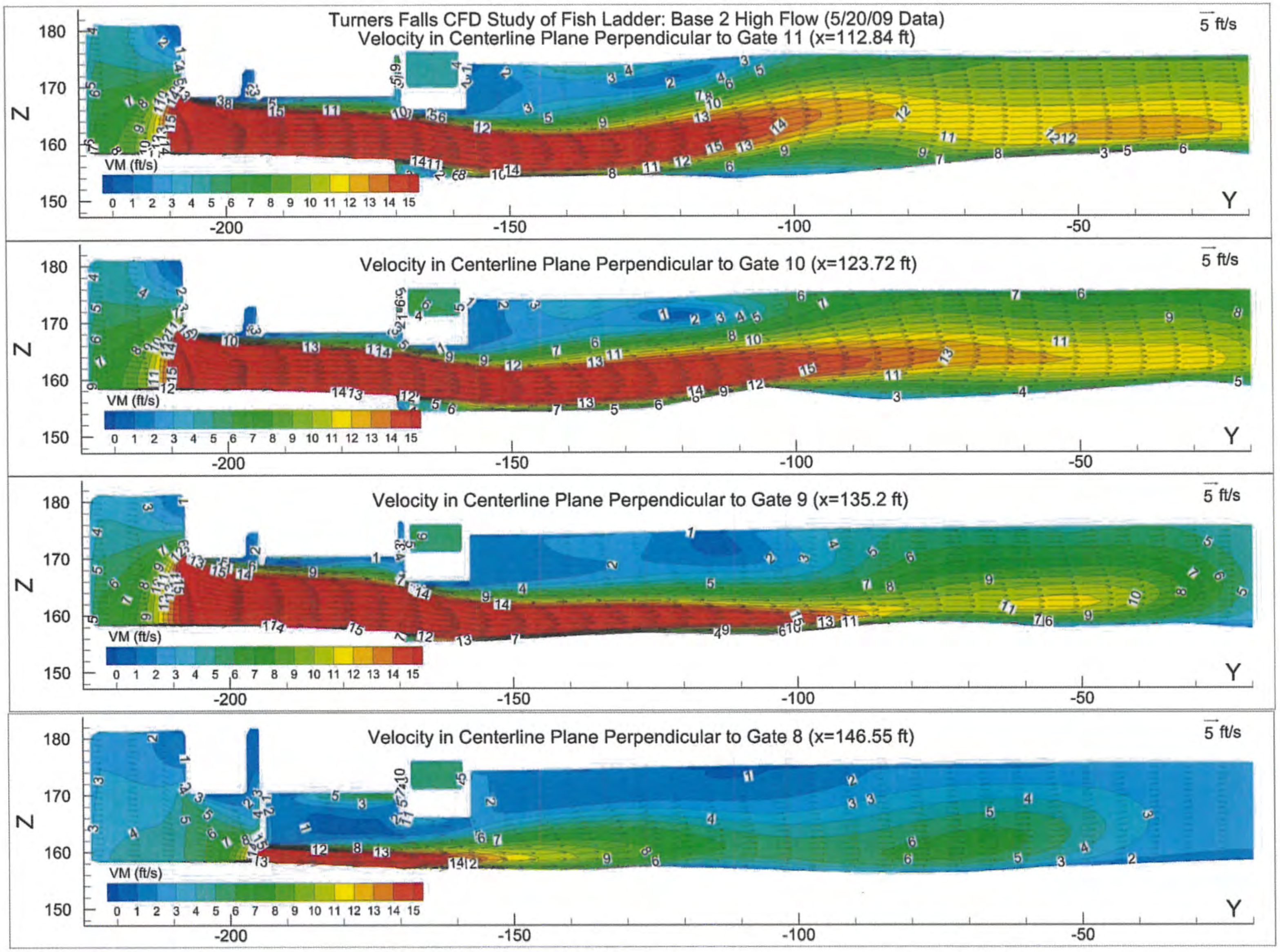

Figure 42 Base 2 High Flow: Velocity in Centerline Planes of Gates 8 through 11

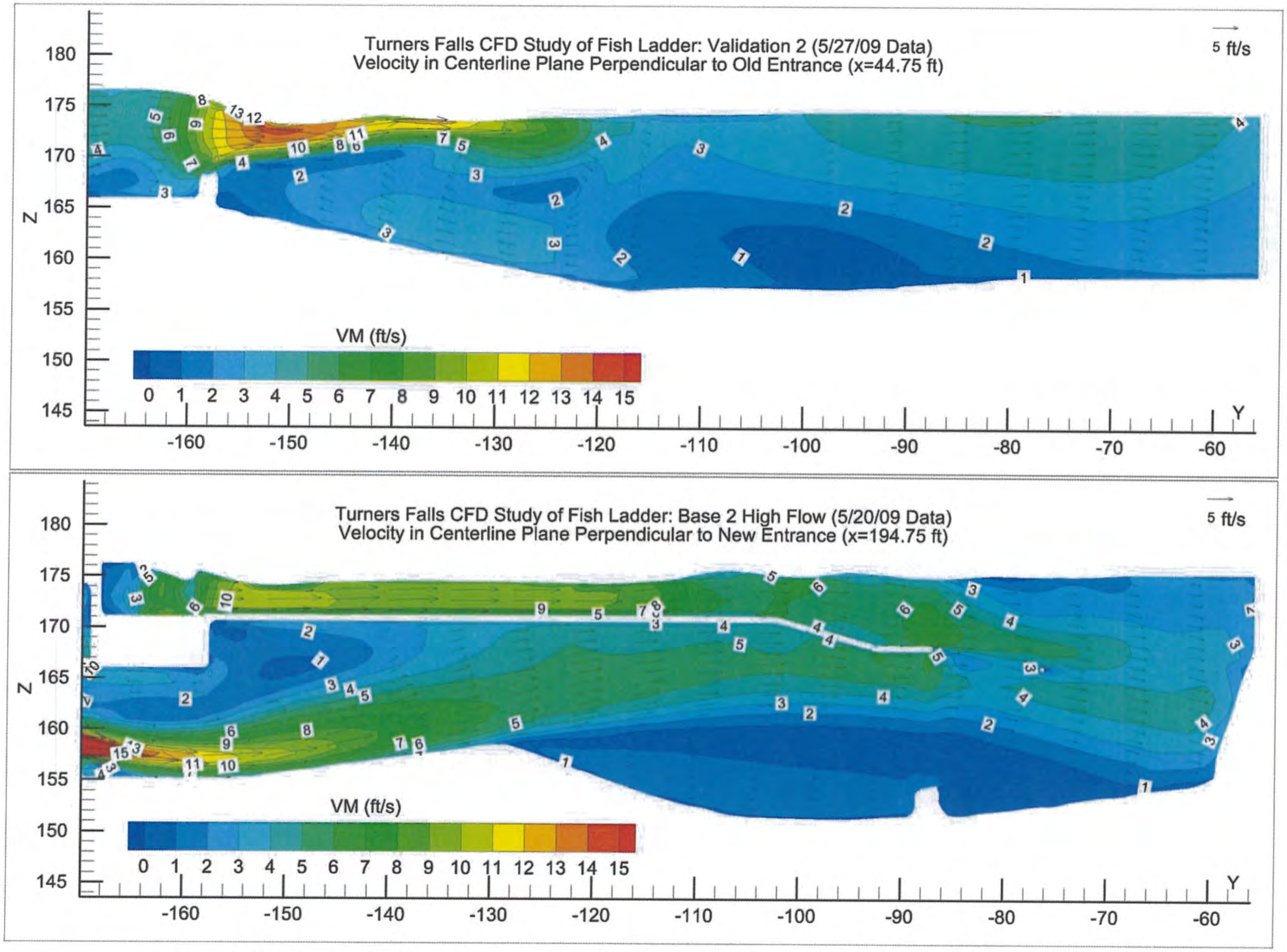

Figure 43 Base 2 High Flow: Velocity in the Centerline Planes of Old and New Entrances

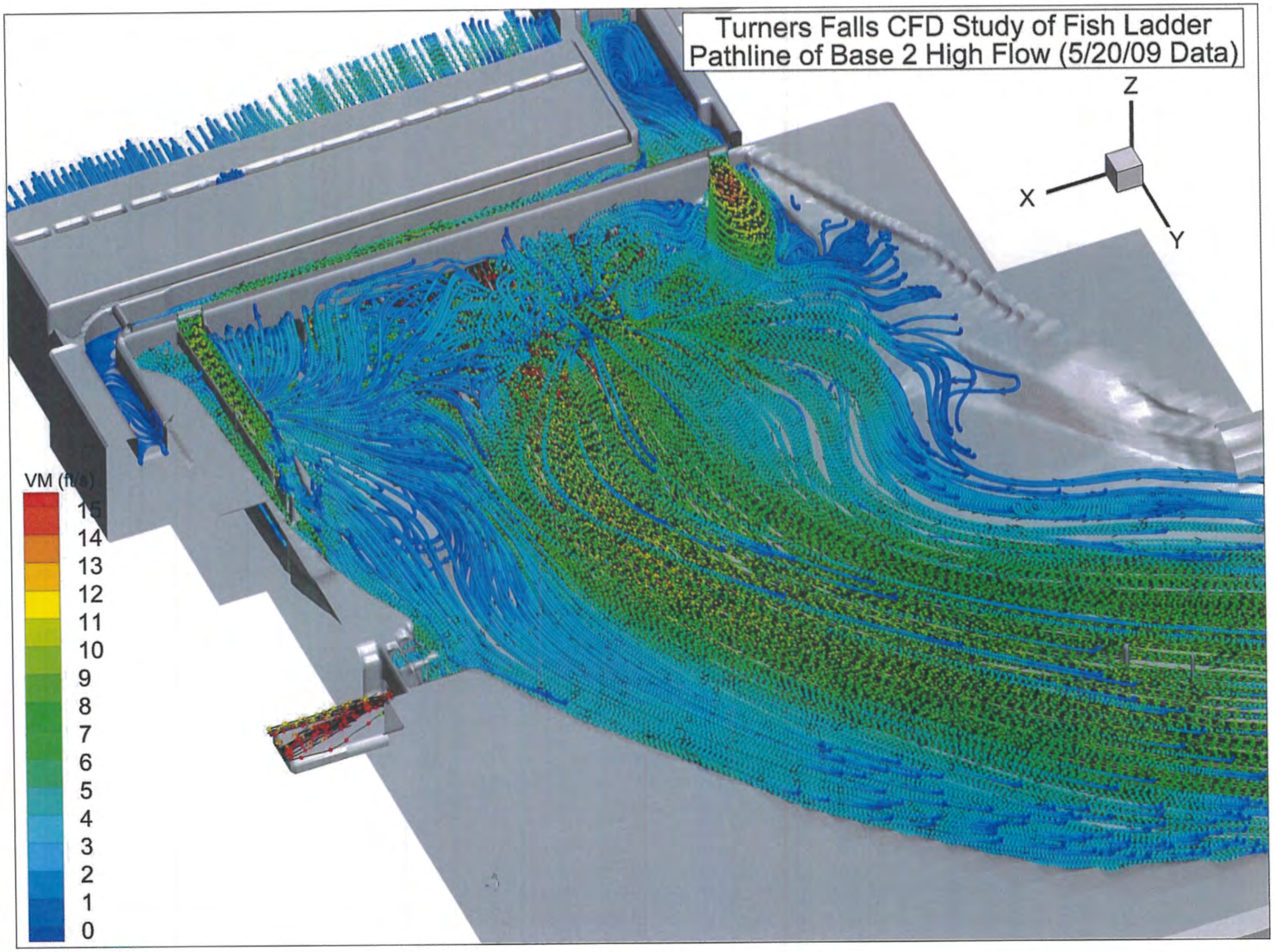

Figure 44 Base 2 High Flow: 3D Pathlines

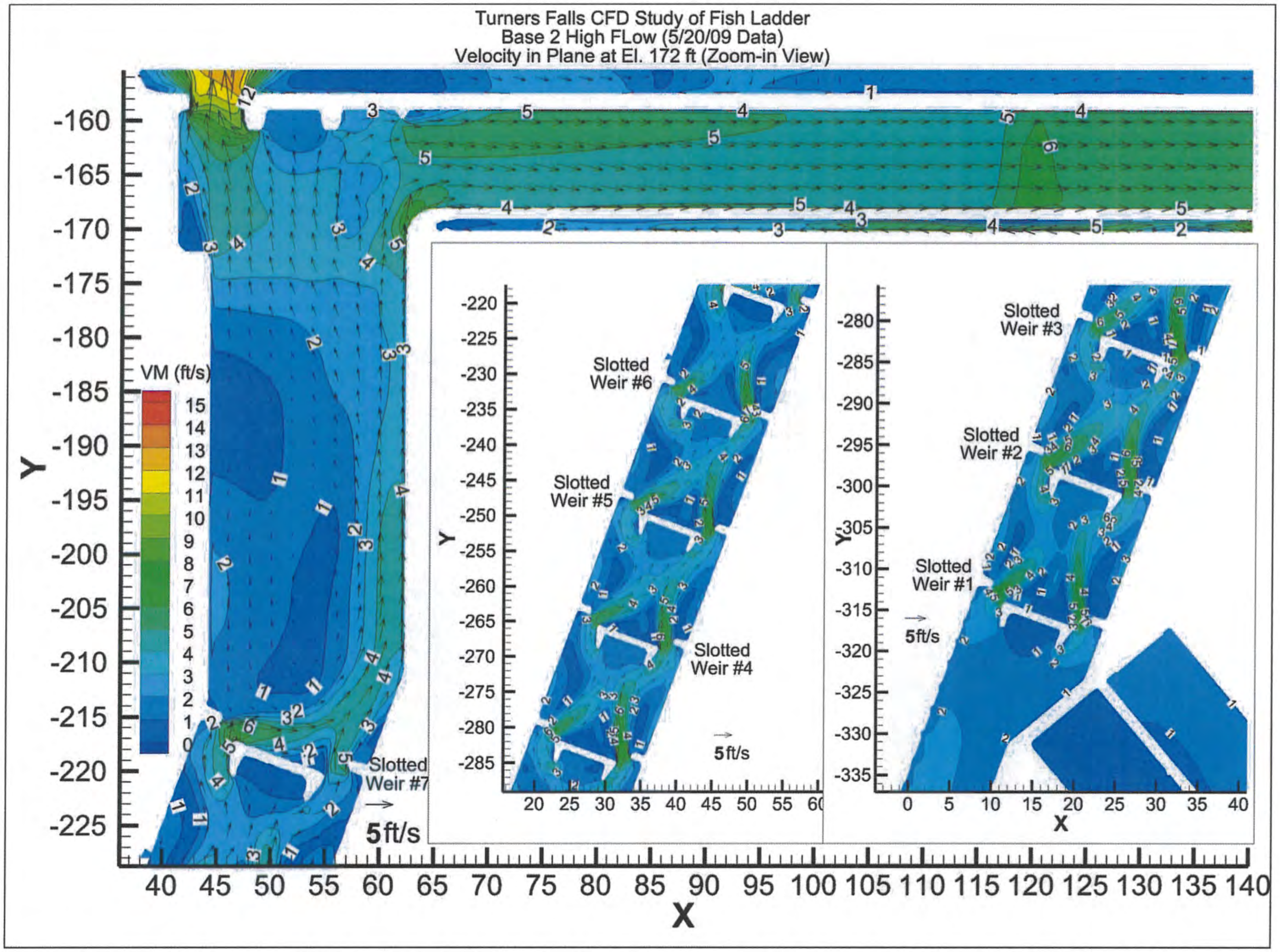

Figure 45 Base 2 High Flow: Velocity in the Upstream Slotted Weir and Gallery at Elevation 172 ft

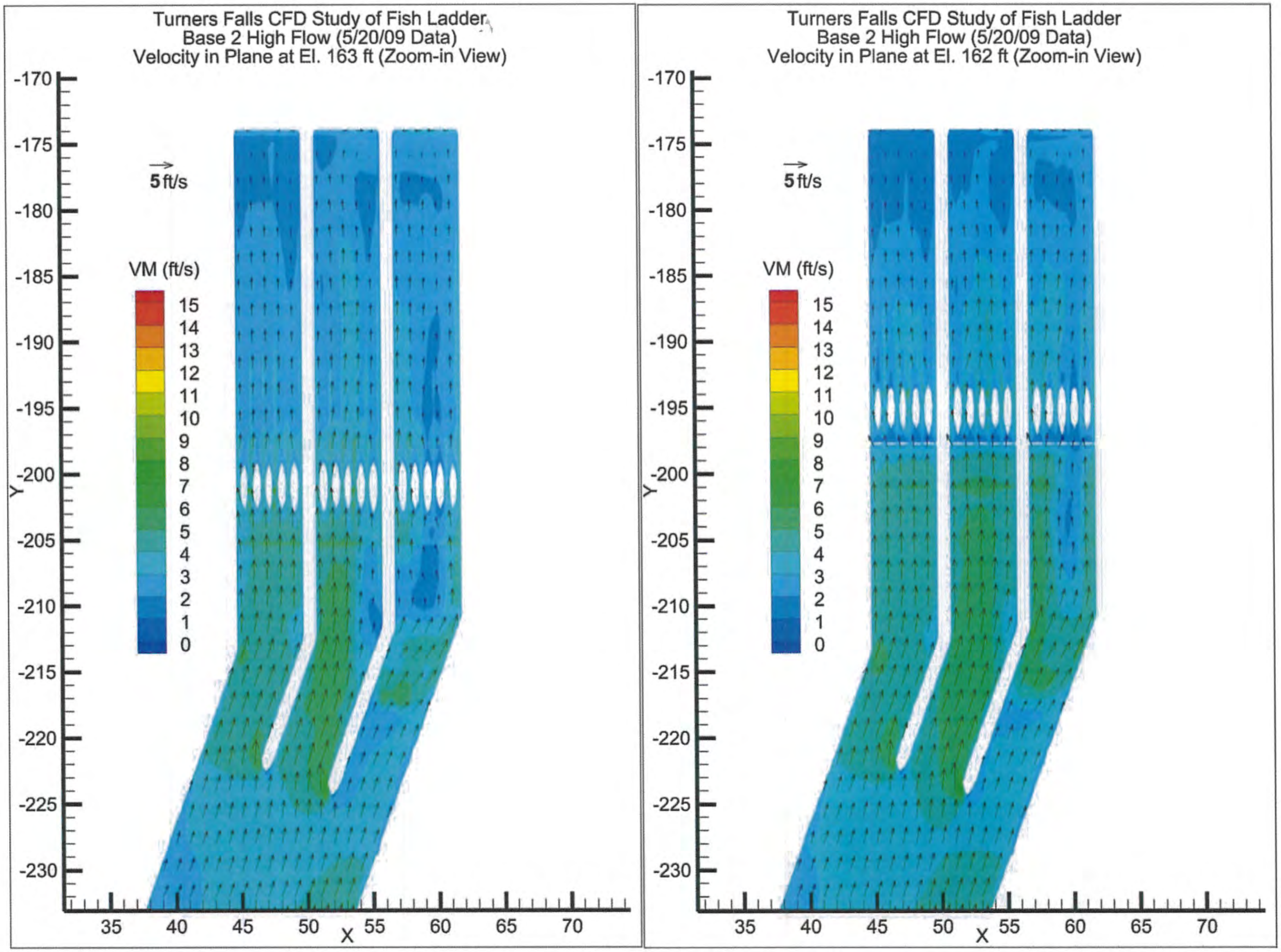

Figure 46 Base 2 High Flow: Velocity in the Upstream Attraction Channel at El. 163 ft and El. 162 ft

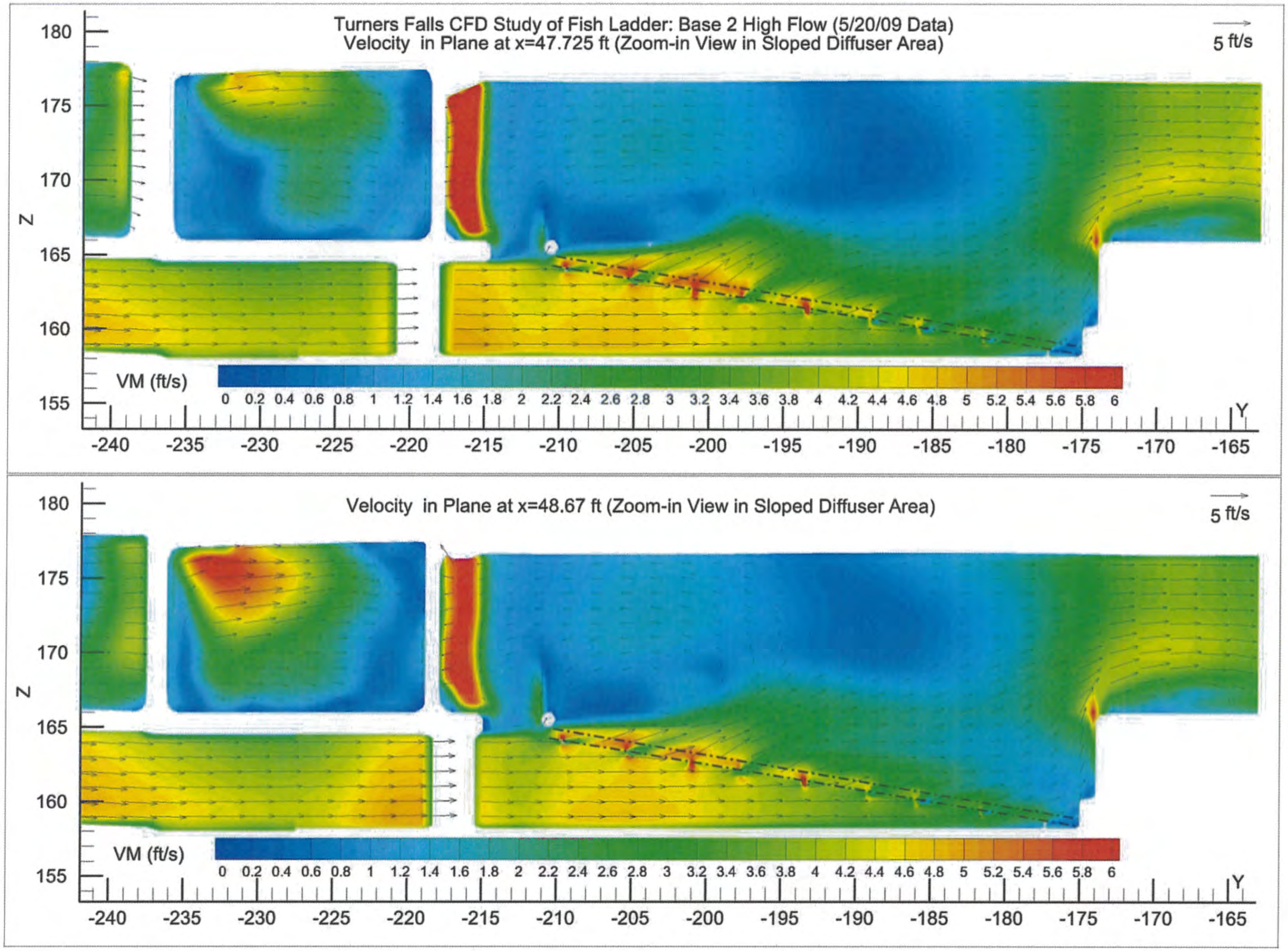

Figure 47 Base 2 High Flow: Velocity in Vertical Planes in the Left Channel of Sloped Diffuser

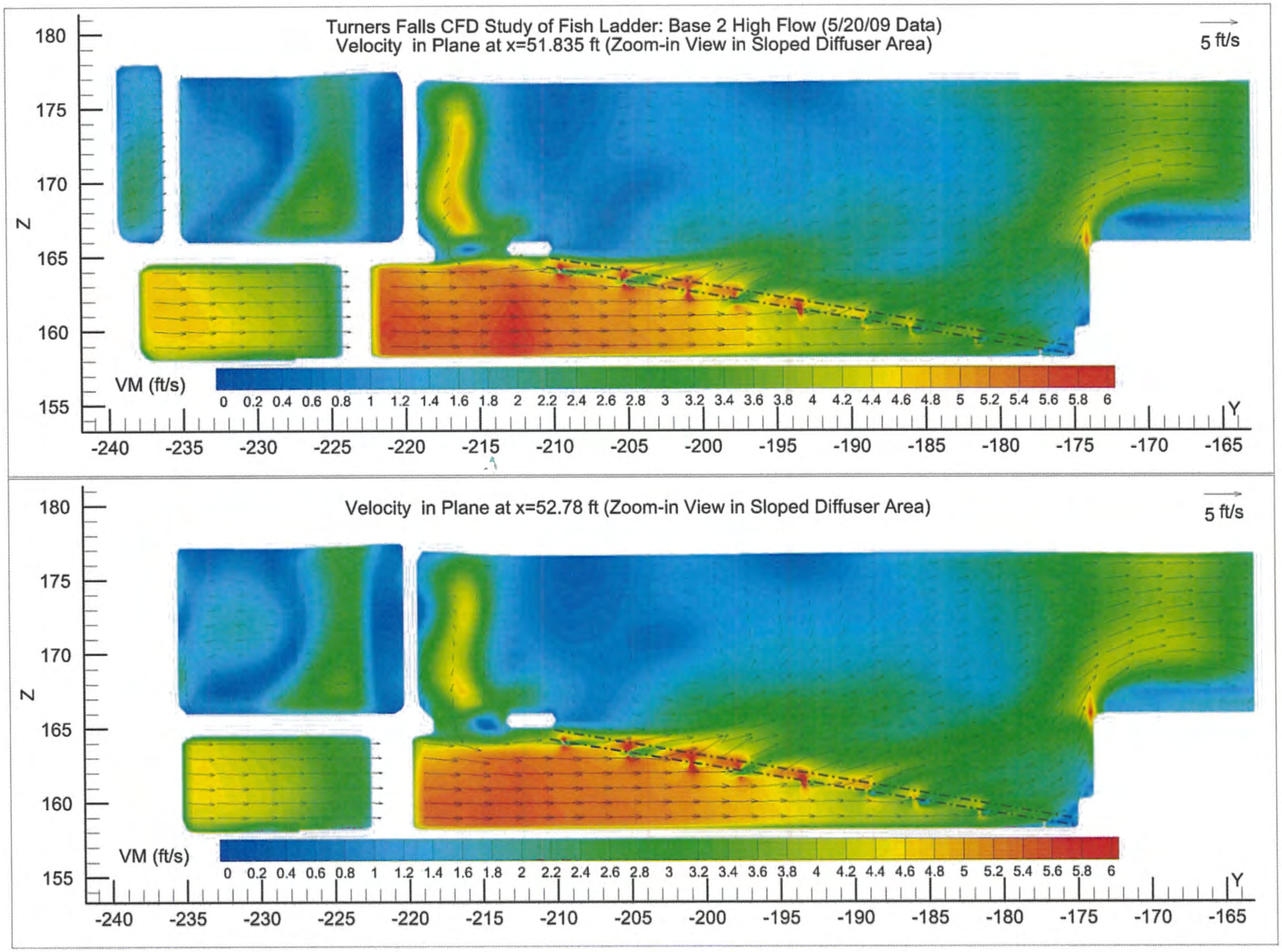

Figure 48 Base 2 High Flow: Velocity in Vertical Planes in the Middle Channel of Sloped Diffuser

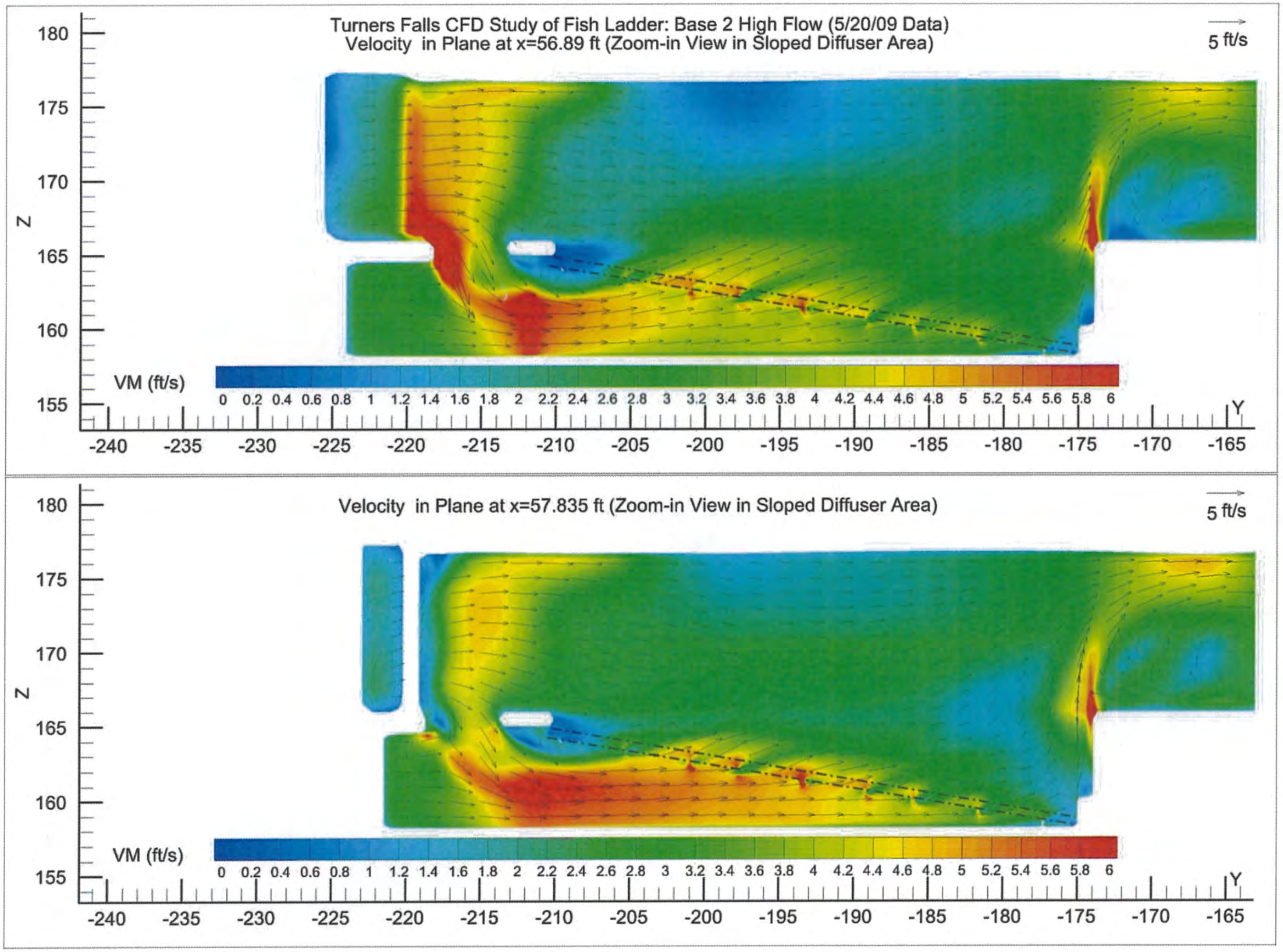

Figure 49 Base 2 High Flow: Velocity in Vertical Planes in the Right Channel of Sloped Diffuser

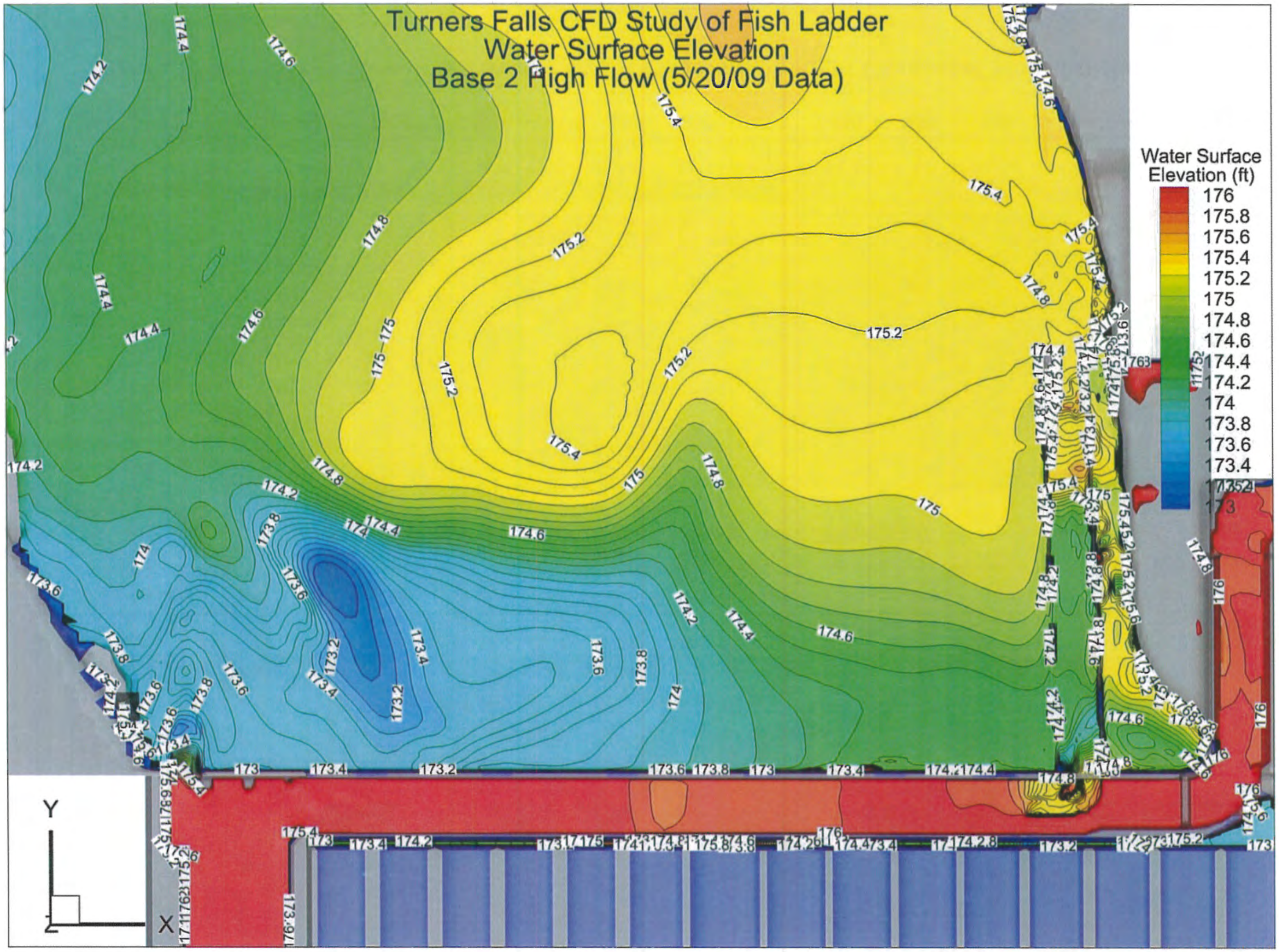

Figure 50 Base 2 High Flow: Water Surface Elevations in the Vicinity of Old and New Entrances in the Canal

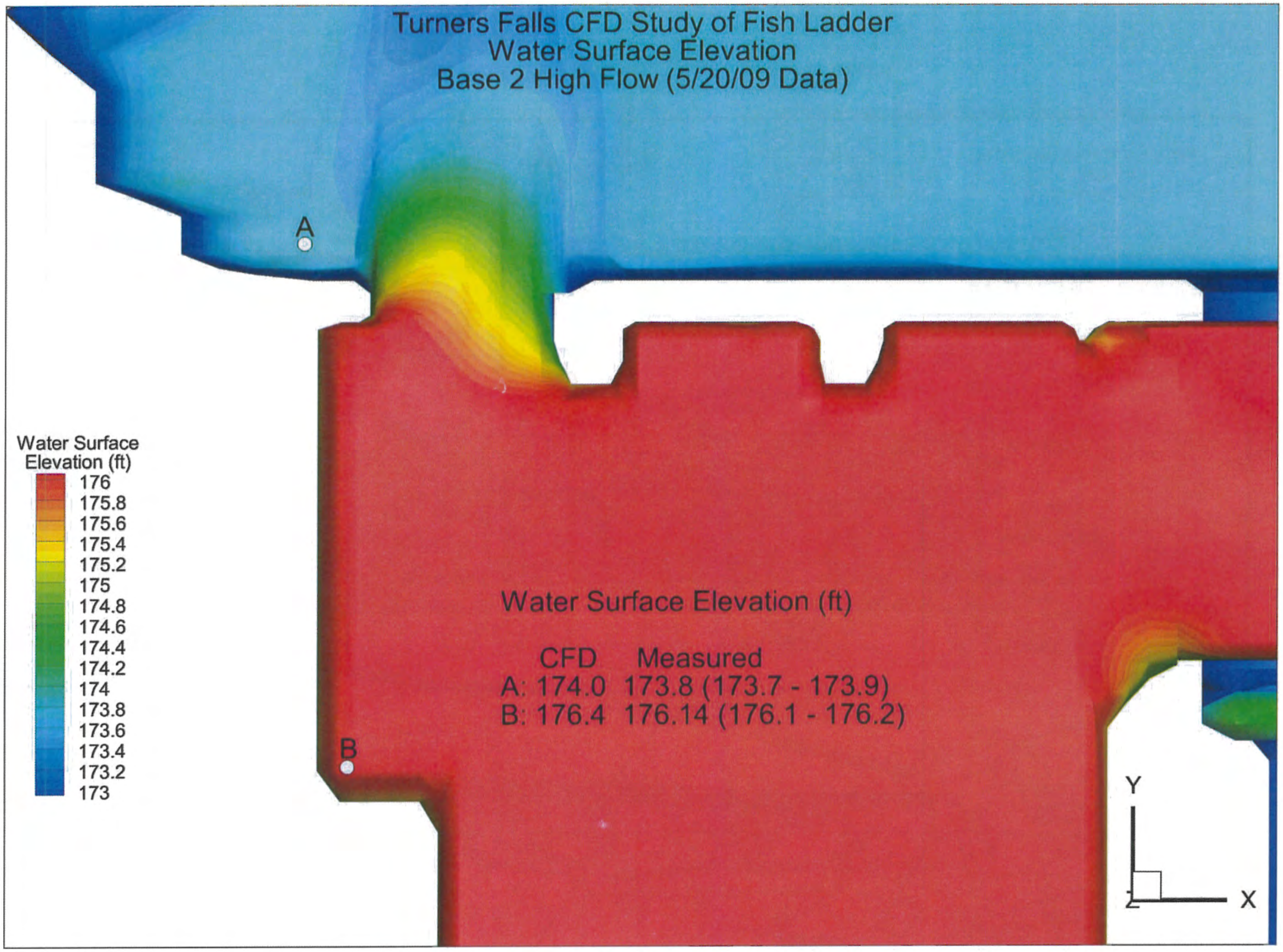

Figure 51 Base 2 High Flow: Water Surface Elevations in the Vicinity of Old Entrance and Measurement Points Locations

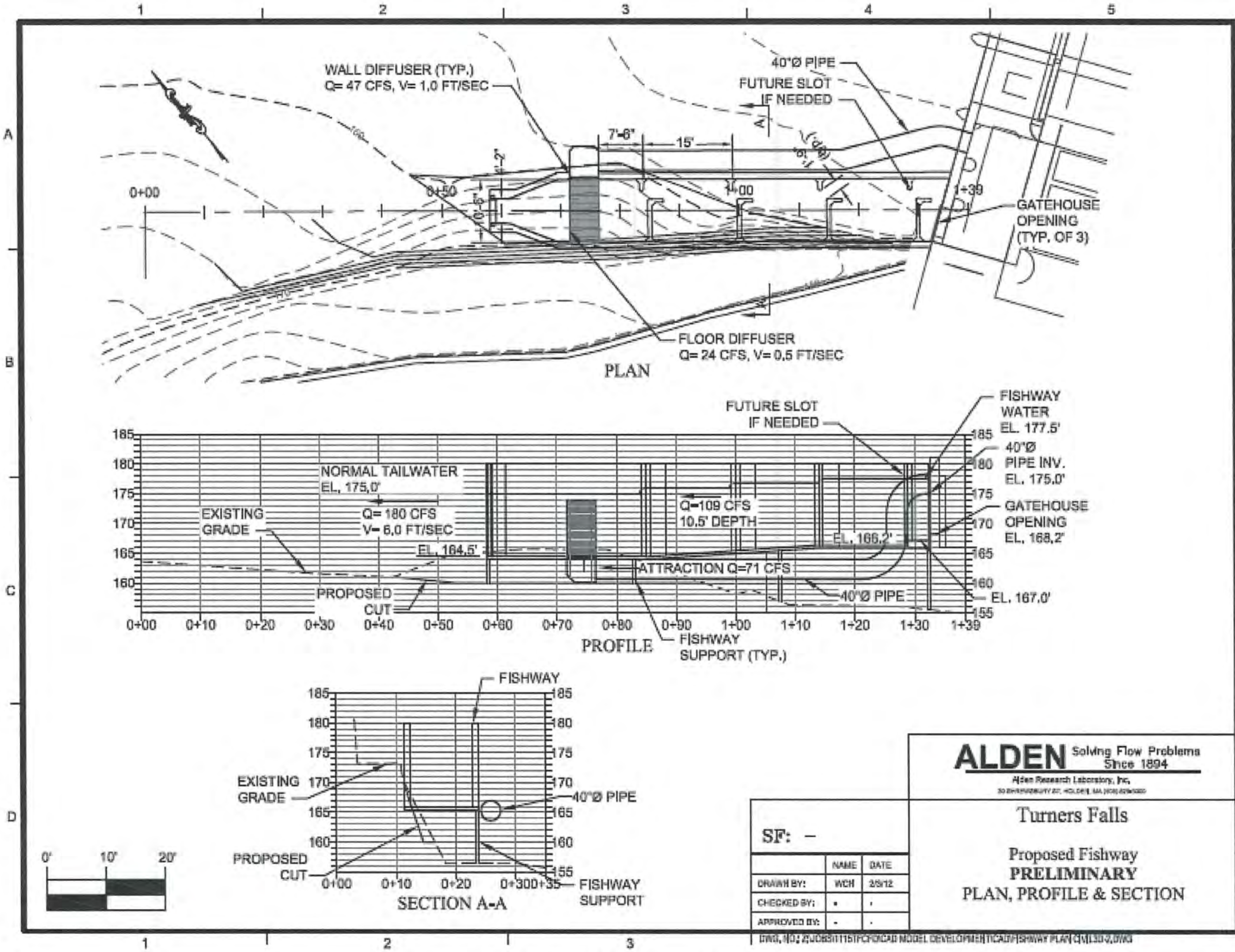

Figure 52 Plan and Vertical Views of Mod 0

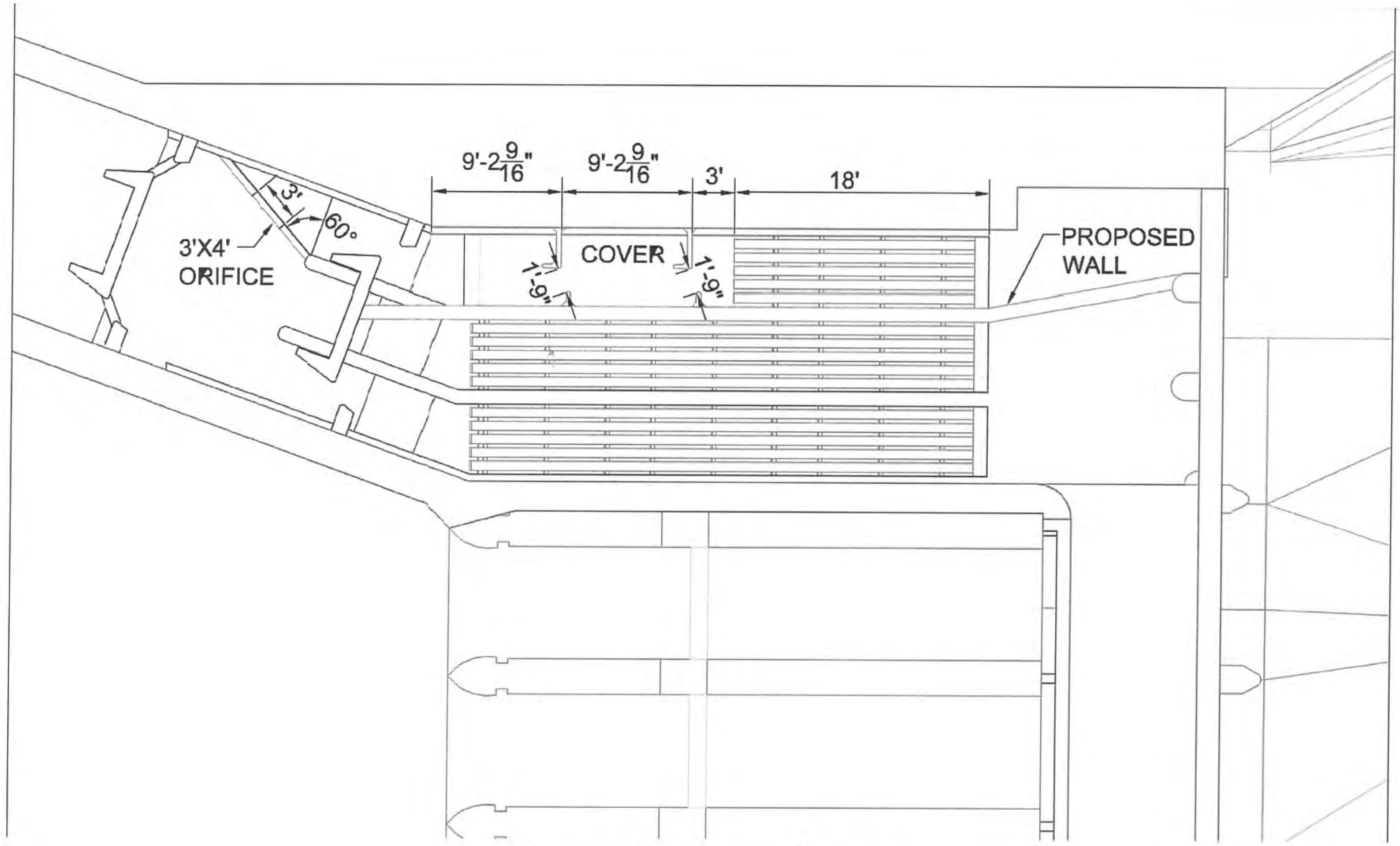

Figure 53 Description of Mod 1

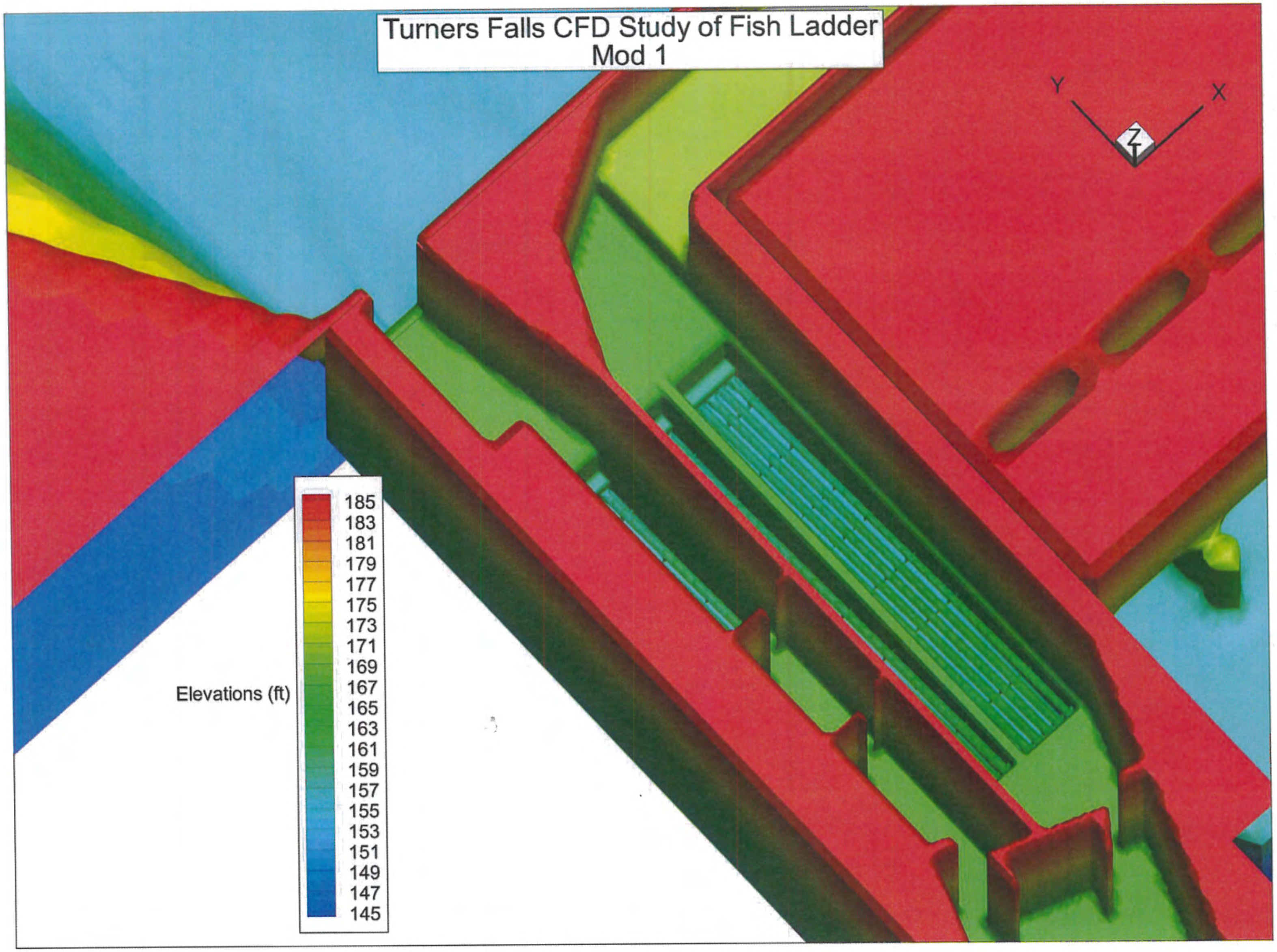

Figure 54 3D View of Mod 1 Concept

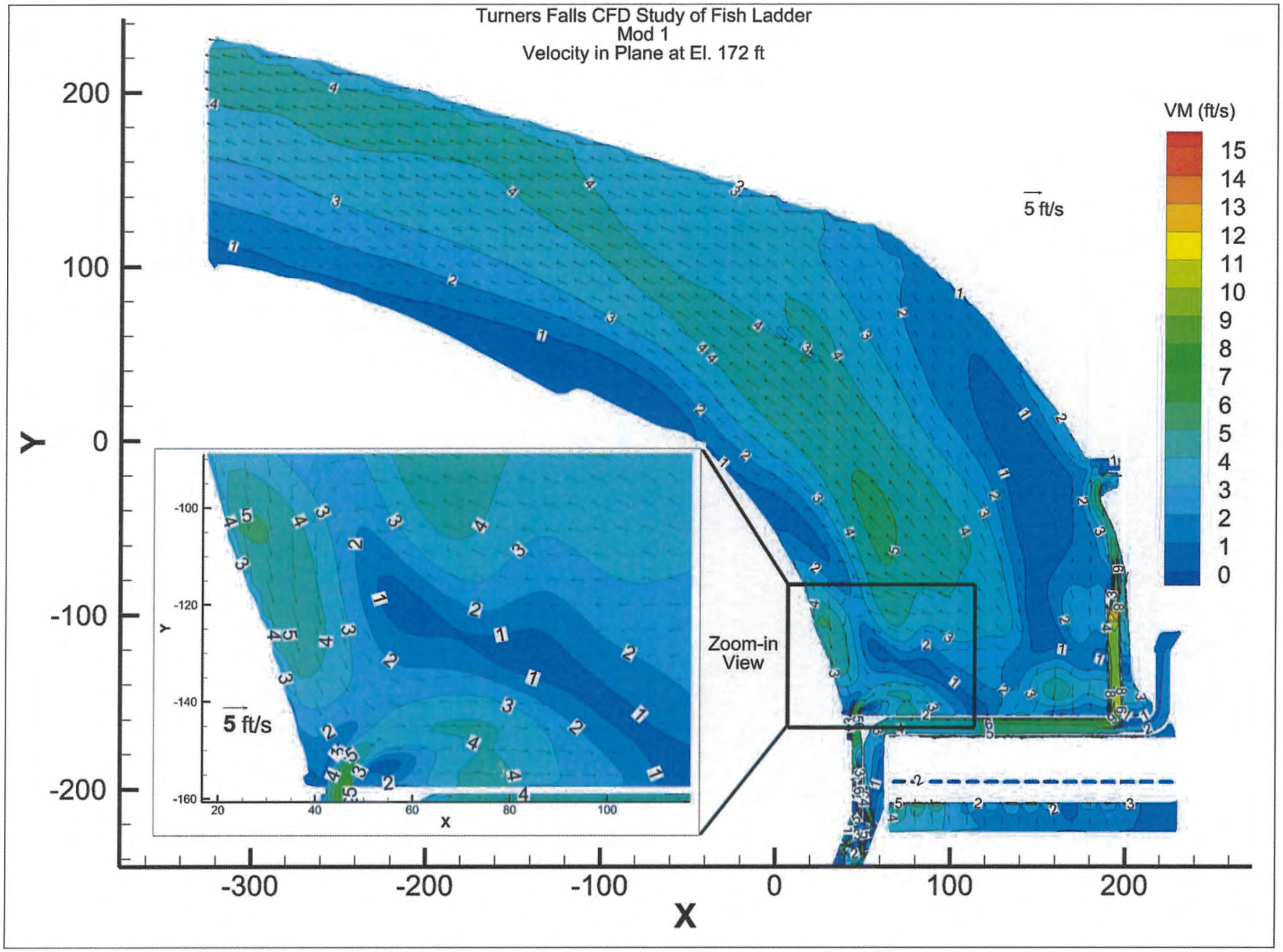

Figure 55 Mod 1: Velocity in Plane at El. 172 ft

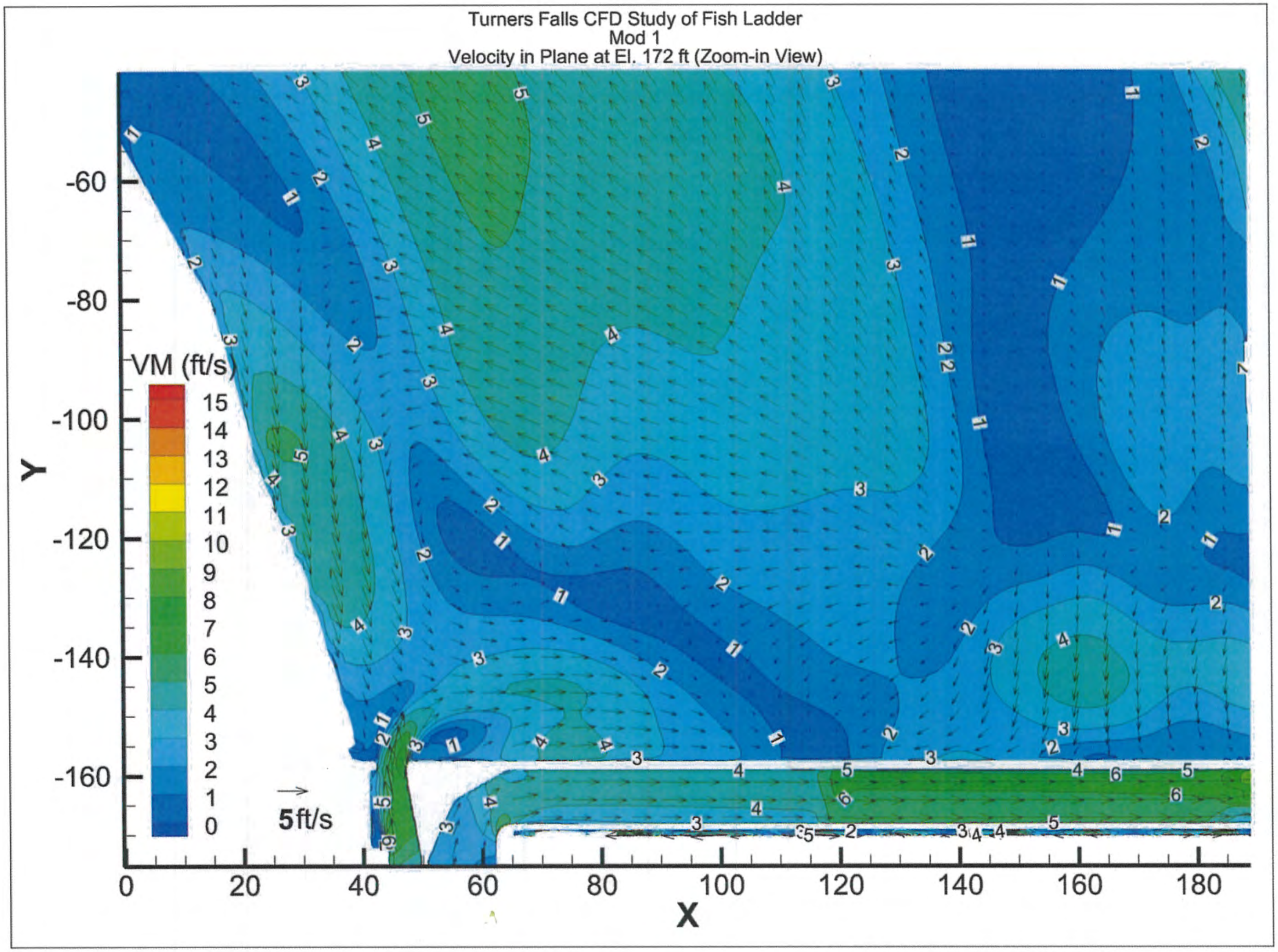

Figure 56 Mod 1: Velocity in the Vicinity of Old Entrance in the Canal at El. 172 ft

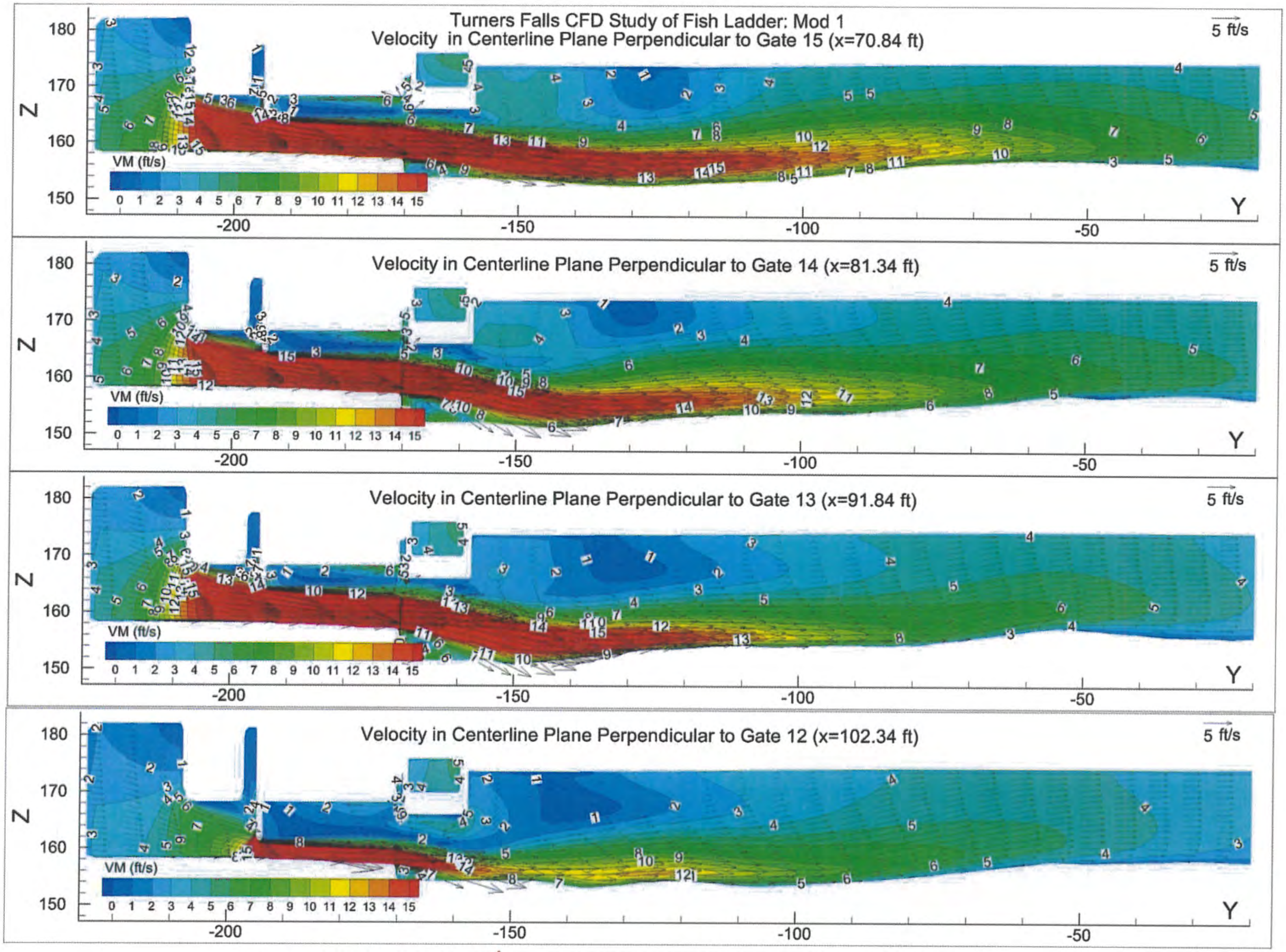

Figure 57 Mod 1: Velocity in Centerline Planes of Gates 12 through 15

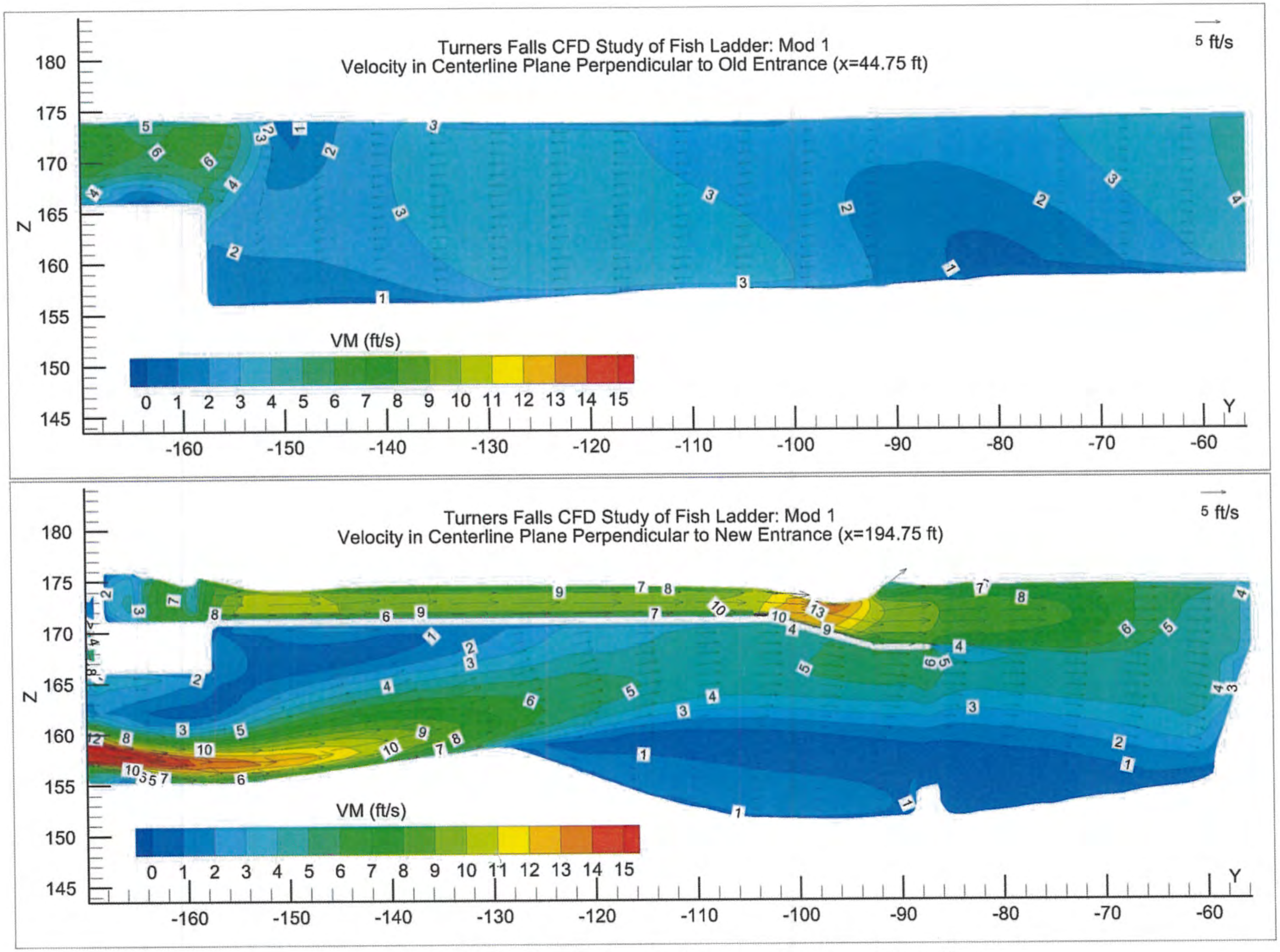

Figure 58 Mod 1: Velocity in Centerline Planes of Old and New Entrances

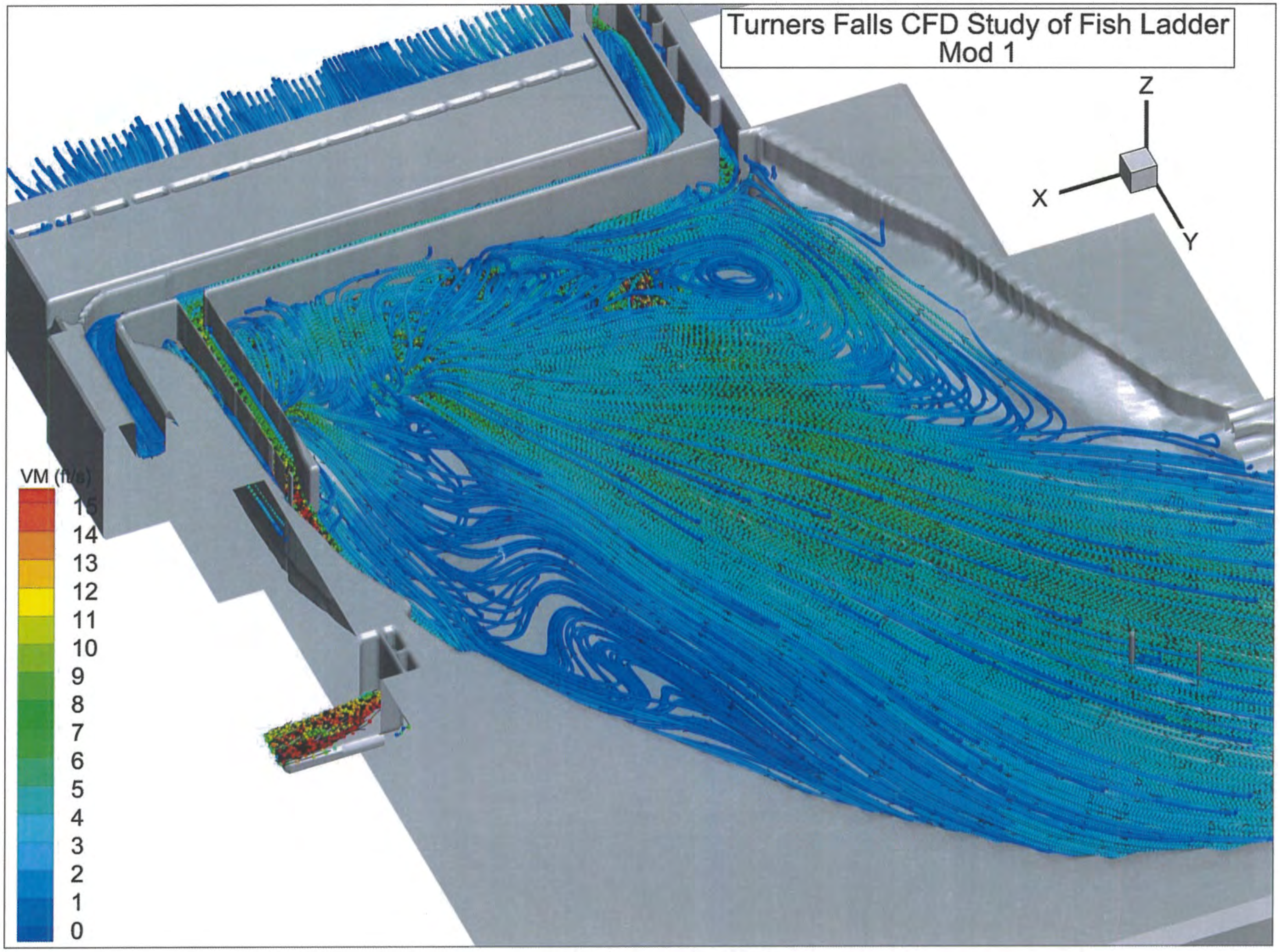

Figure 59 Mod 1: 3D Pathlines

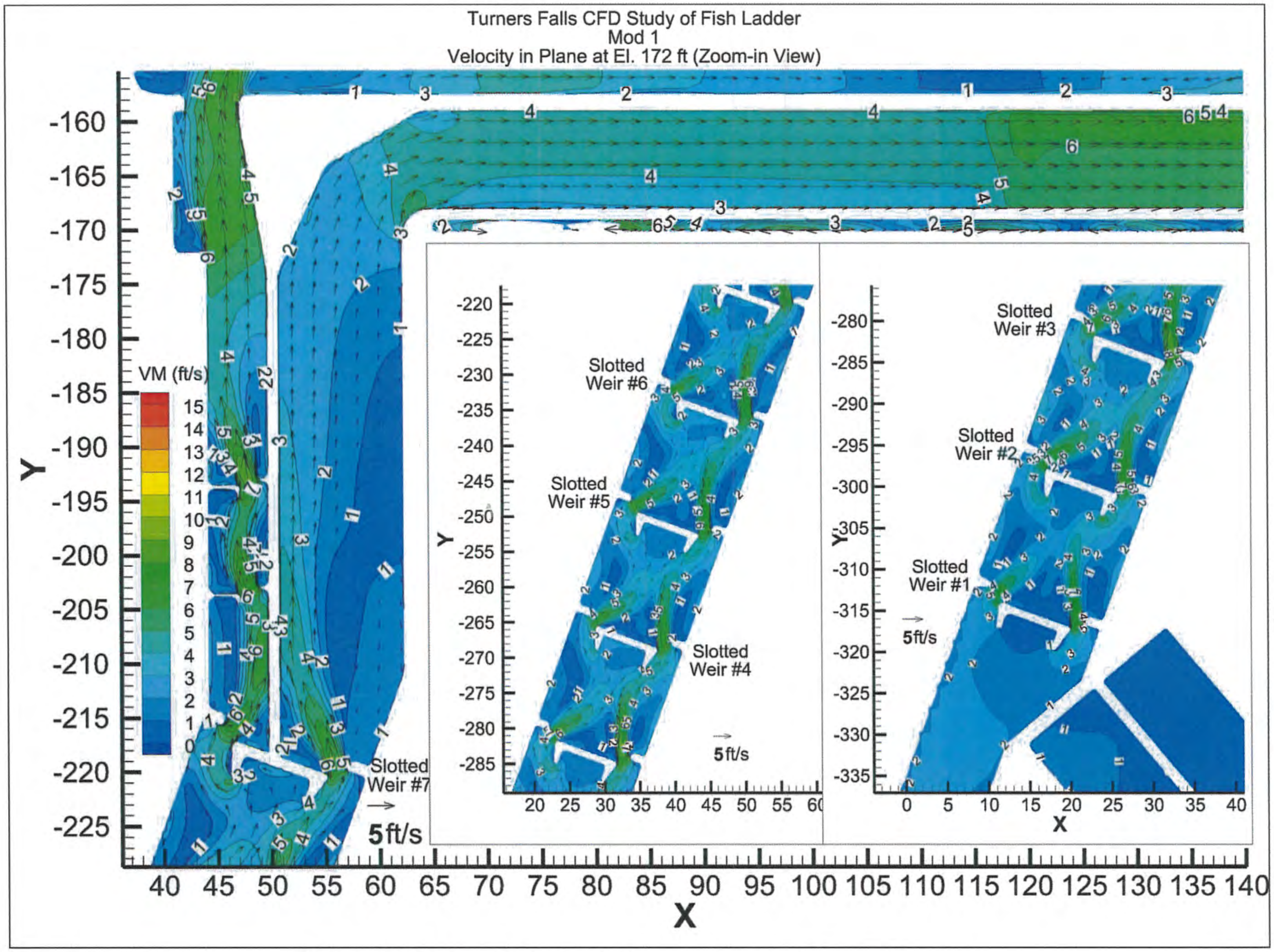

Figure 60 Mod 1: Velocity in Upstream Fish Way at El. 172 ft

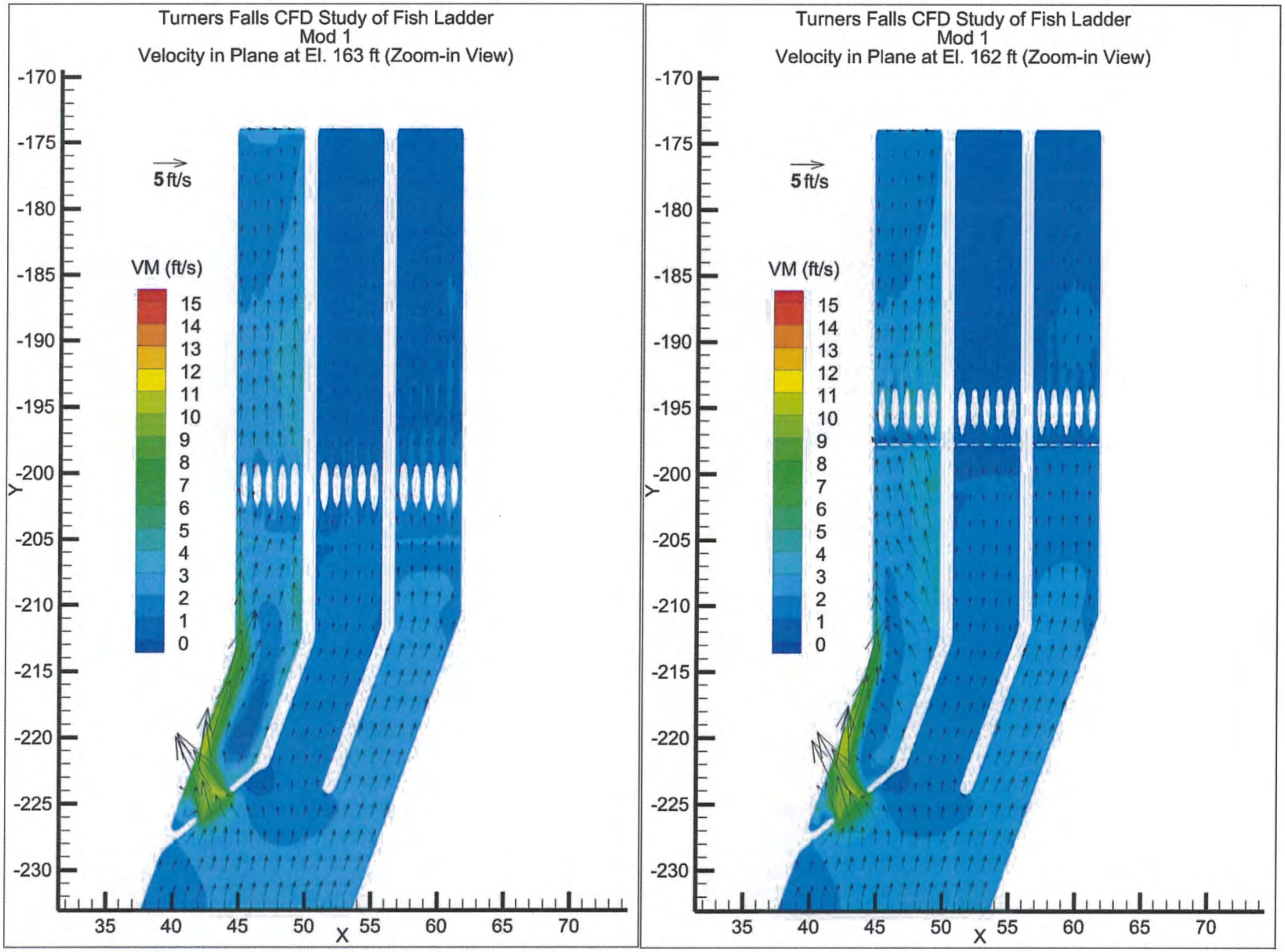

Figure 61 Mod 1: Velocity in Attraction Flow Channel at El. 163 and El. 162 ft

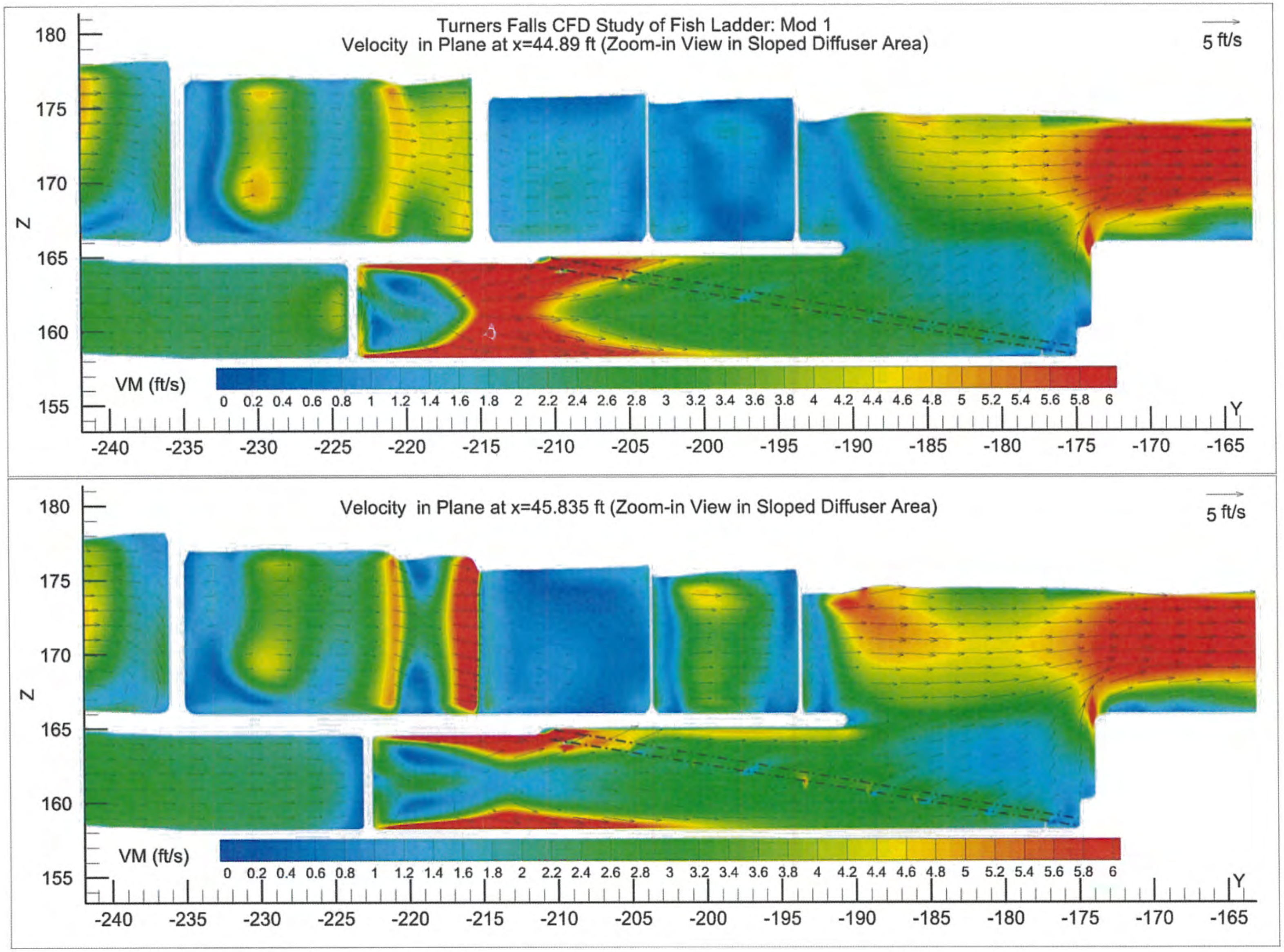

Figure 62 Mod 1: Velocity in Vertical Planes in the Left Sloped Diffuser Channel

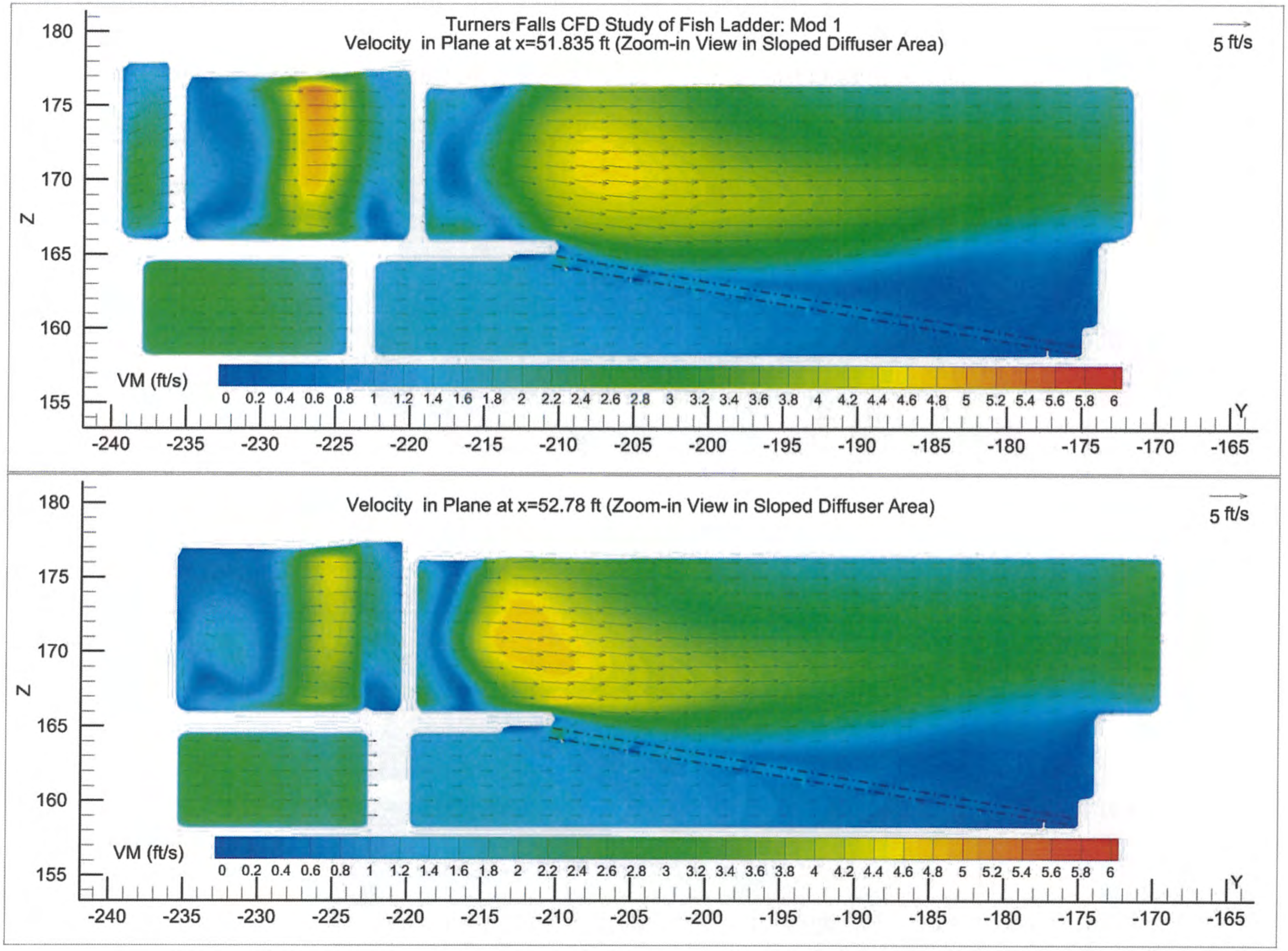

Figure 63 Mod 1: Velocity in Vertical Planes in the Middle Sloped Diffuser Channel

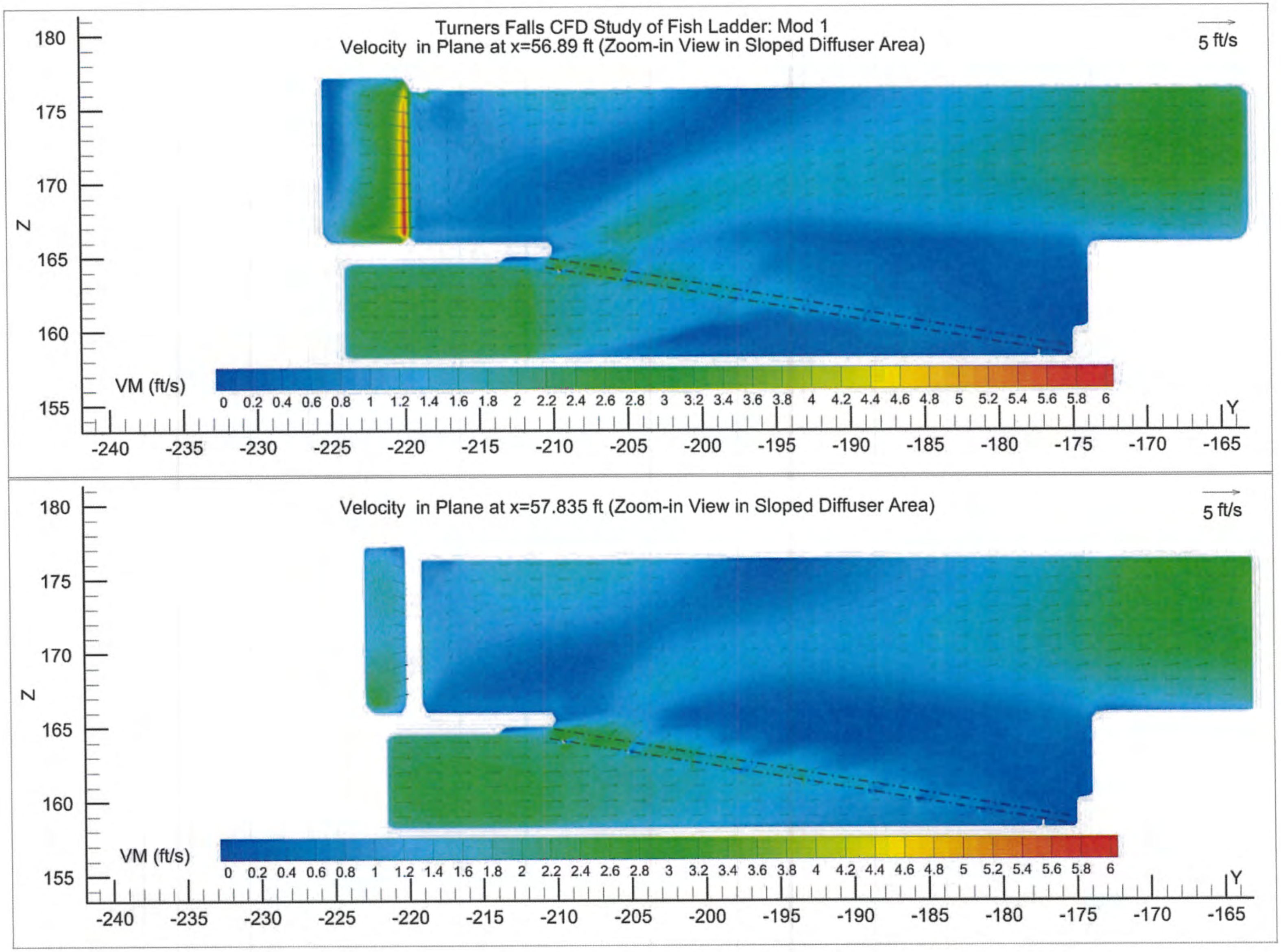

Figure 64 Mod 1: Velocity in Vertical Planes in the Right Sloped Diffuser Channel

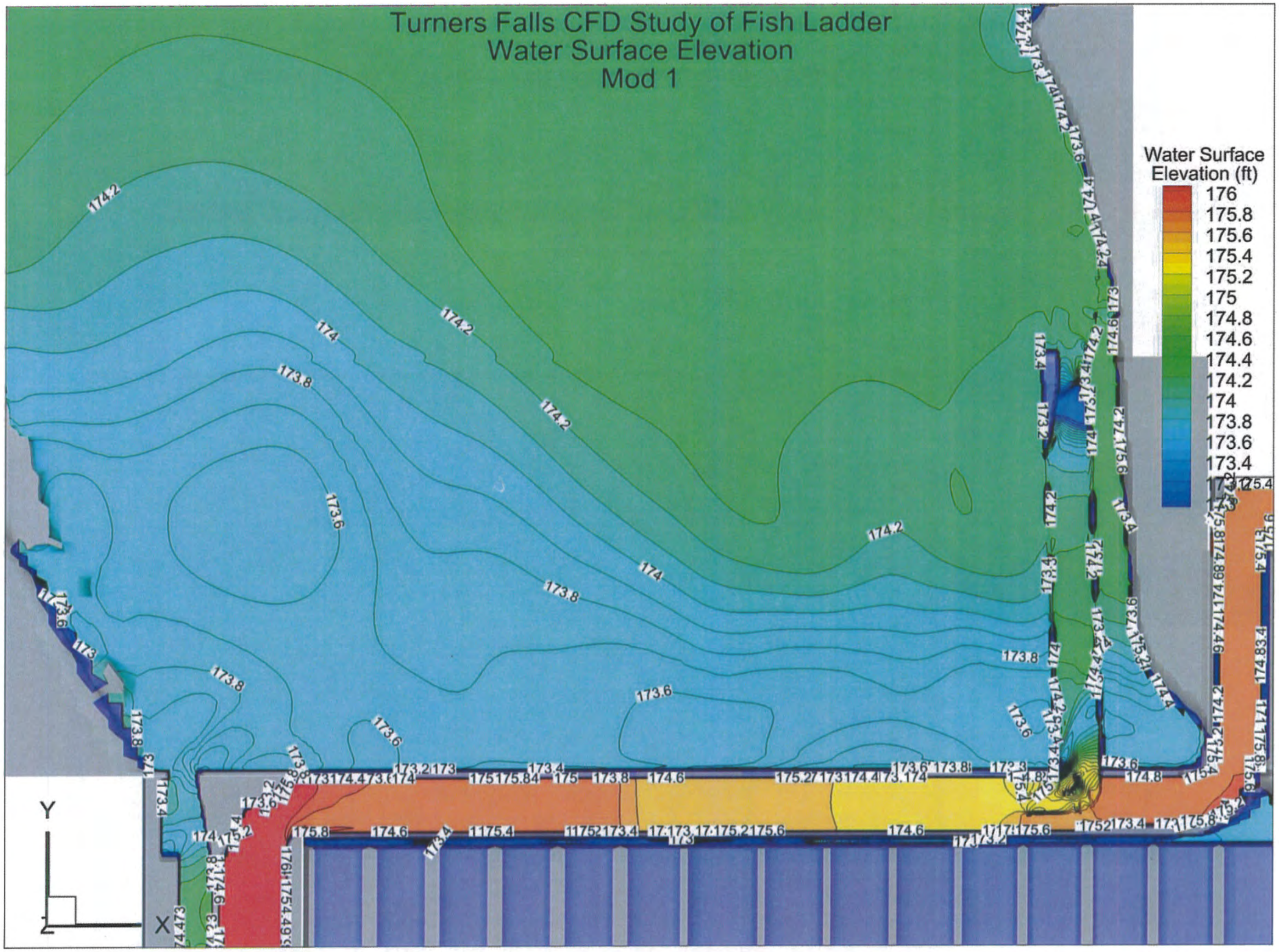

Figure 65 Mod 1: Water Surface Elevation in the Vicinity of Old and New Entrances in the Canal

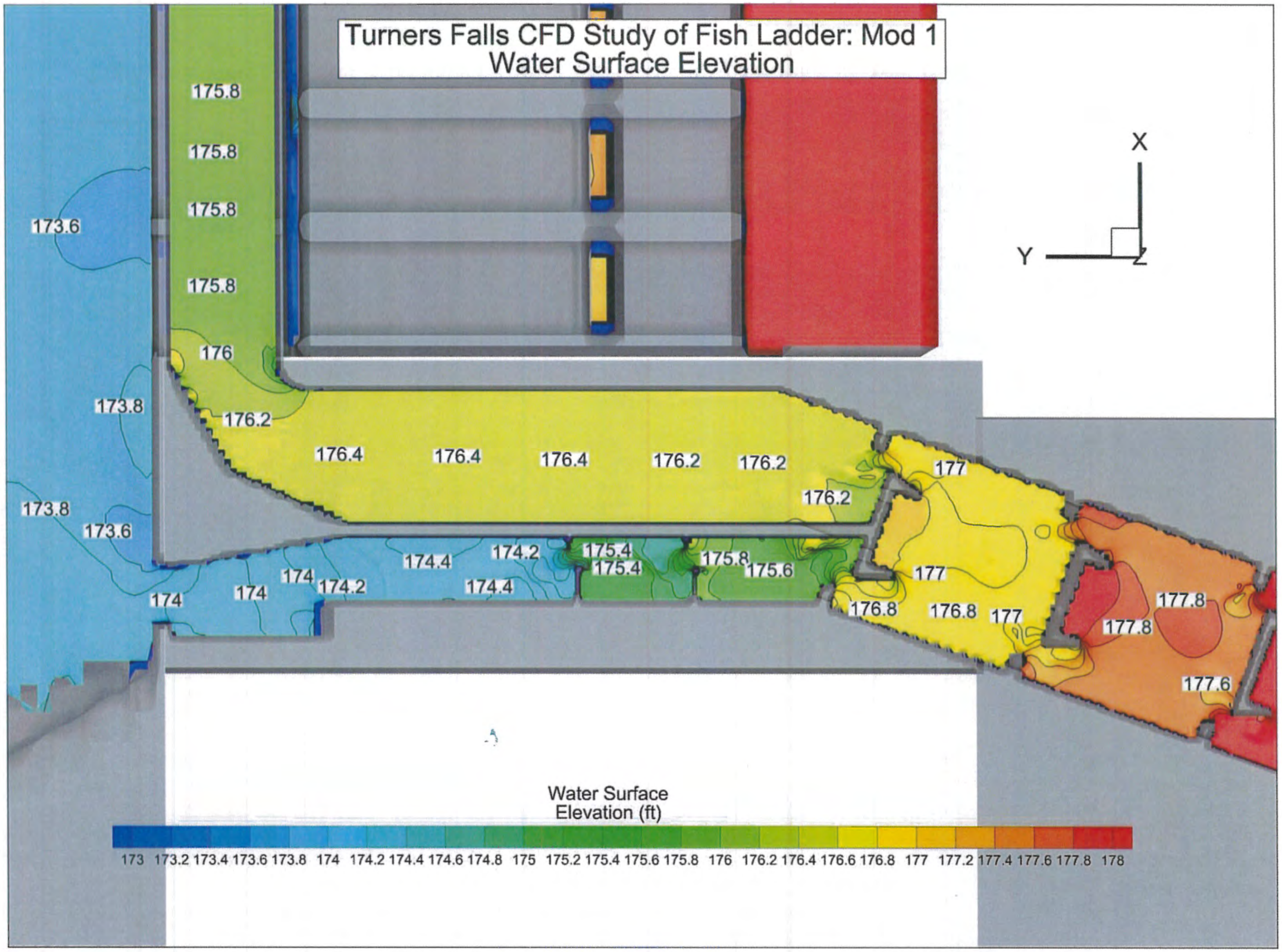

Figure 66 Mod 1: Water Surface Elevation in the Modified Area of Fish Way

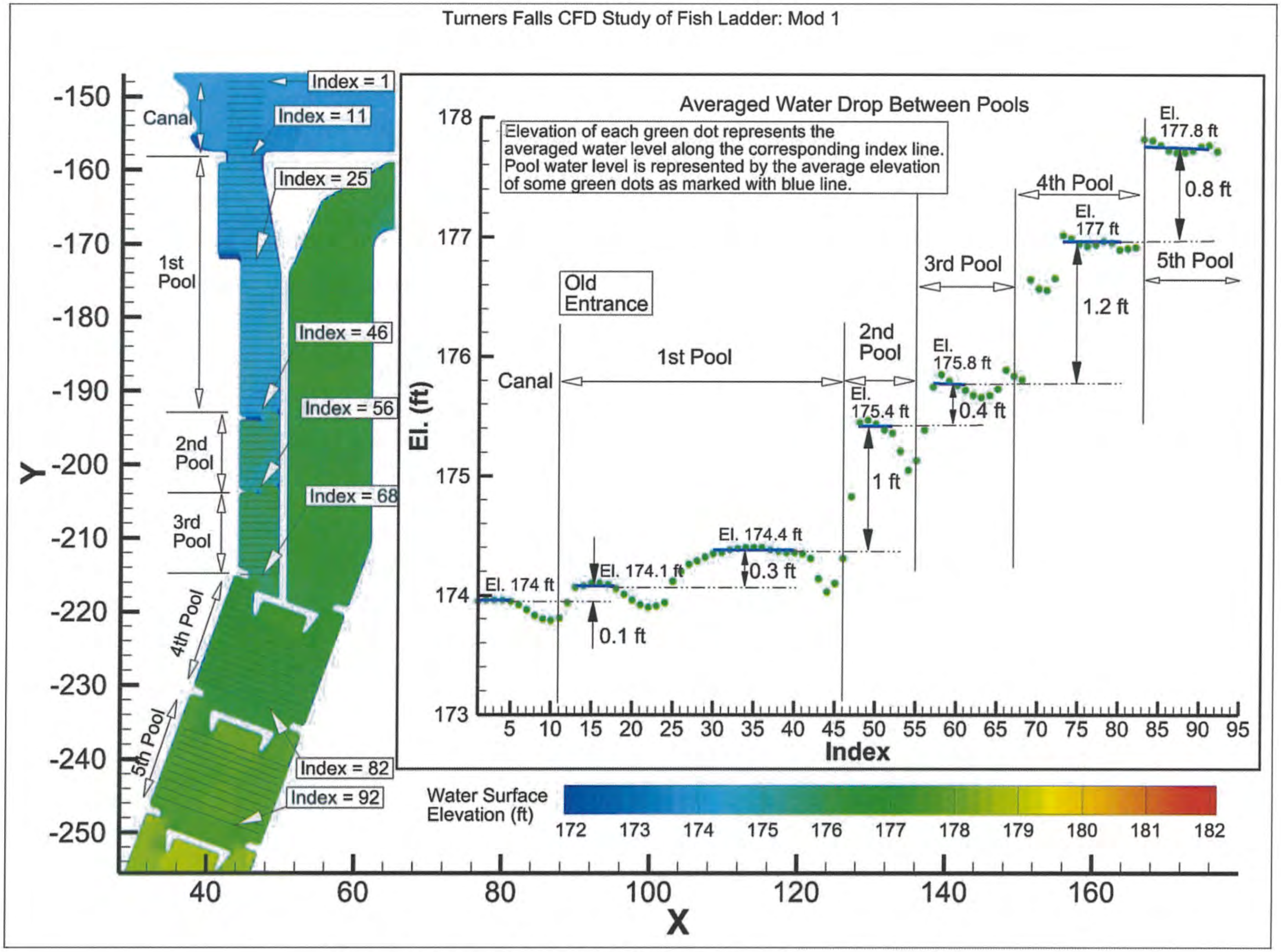

Figure 67 Mod 1: Averaged Water Drop between Pools

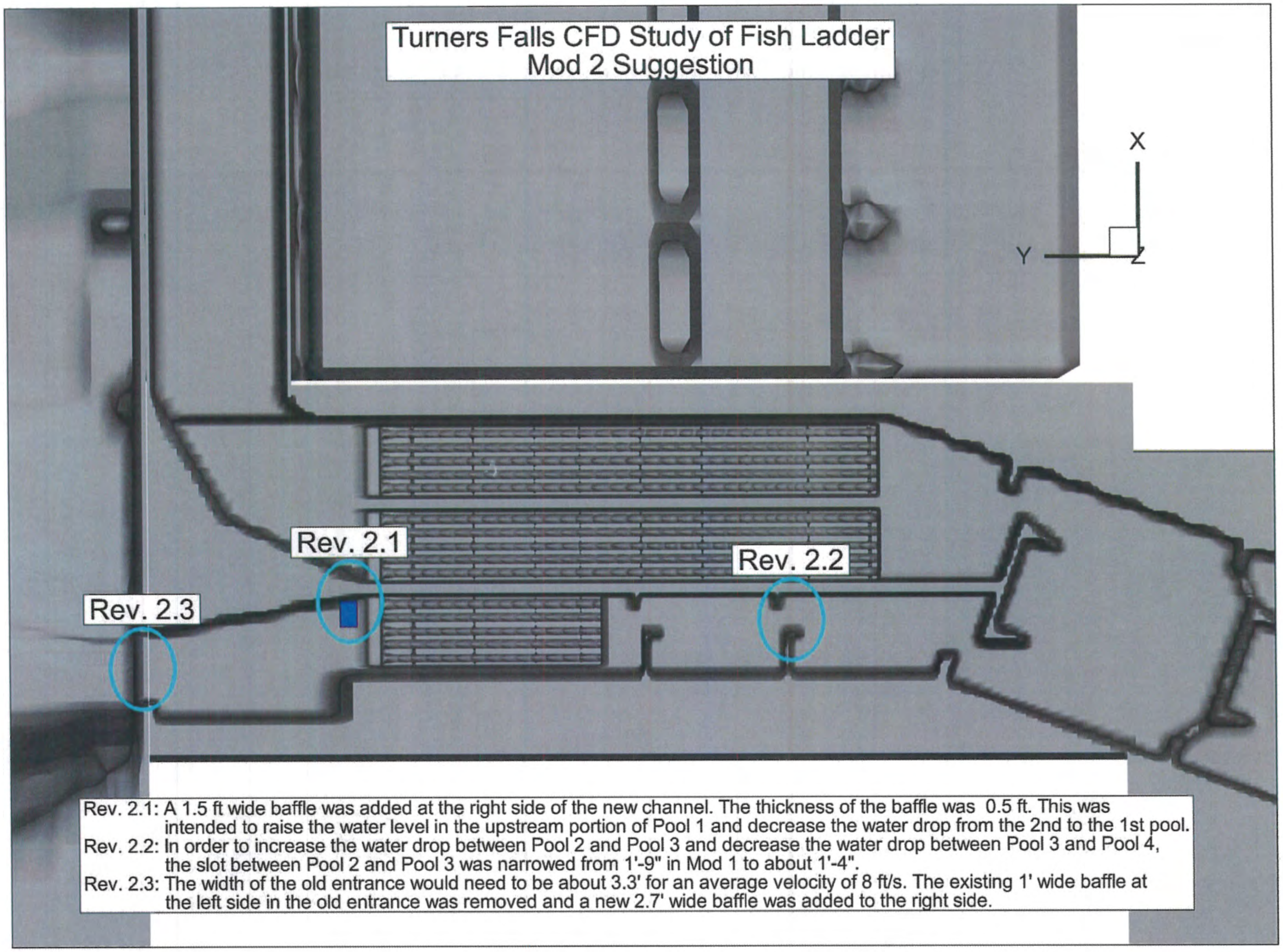

Figure 68 Schematic of Geometry Modification of Mod 2

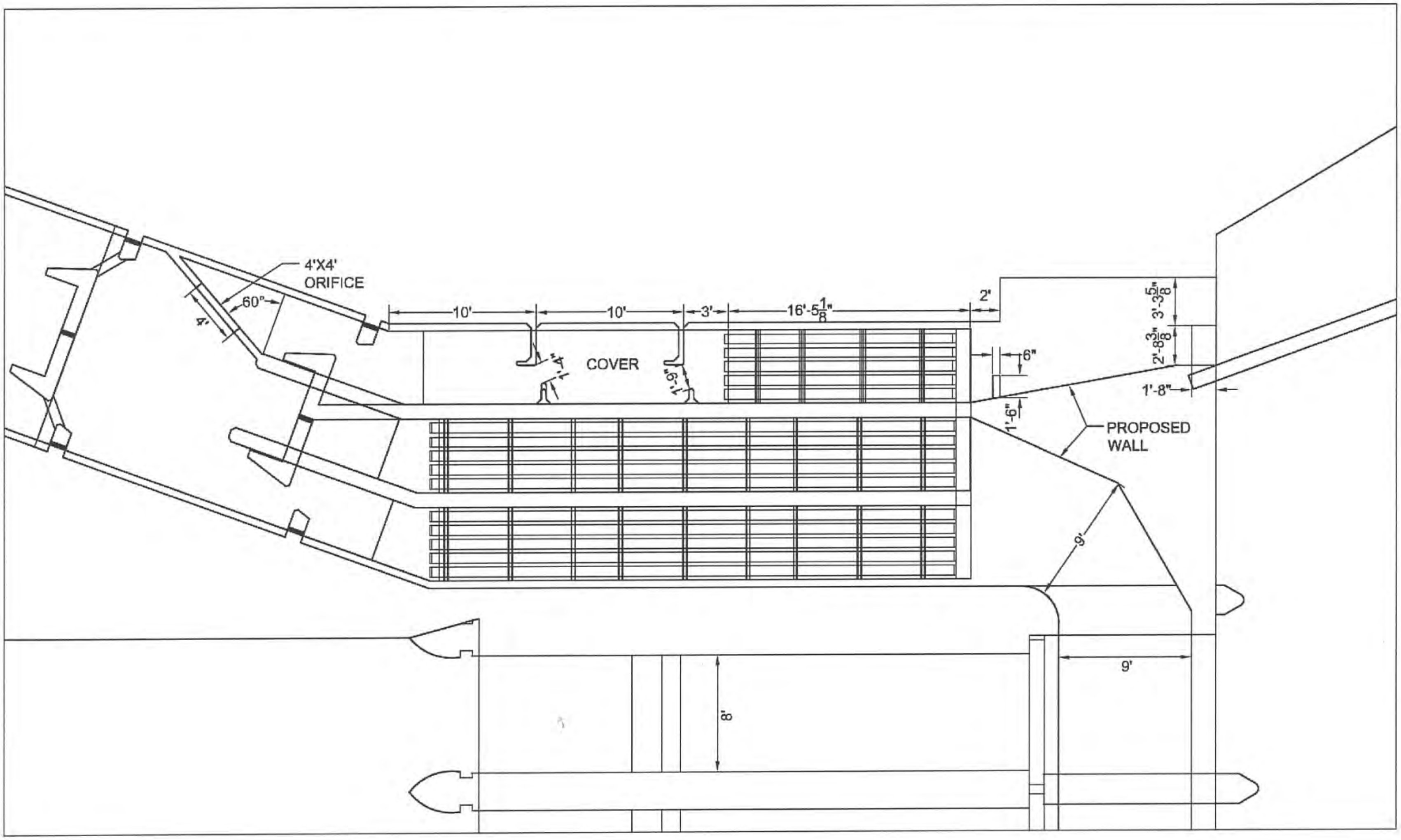

Figure 69 Plan View of Mod 2

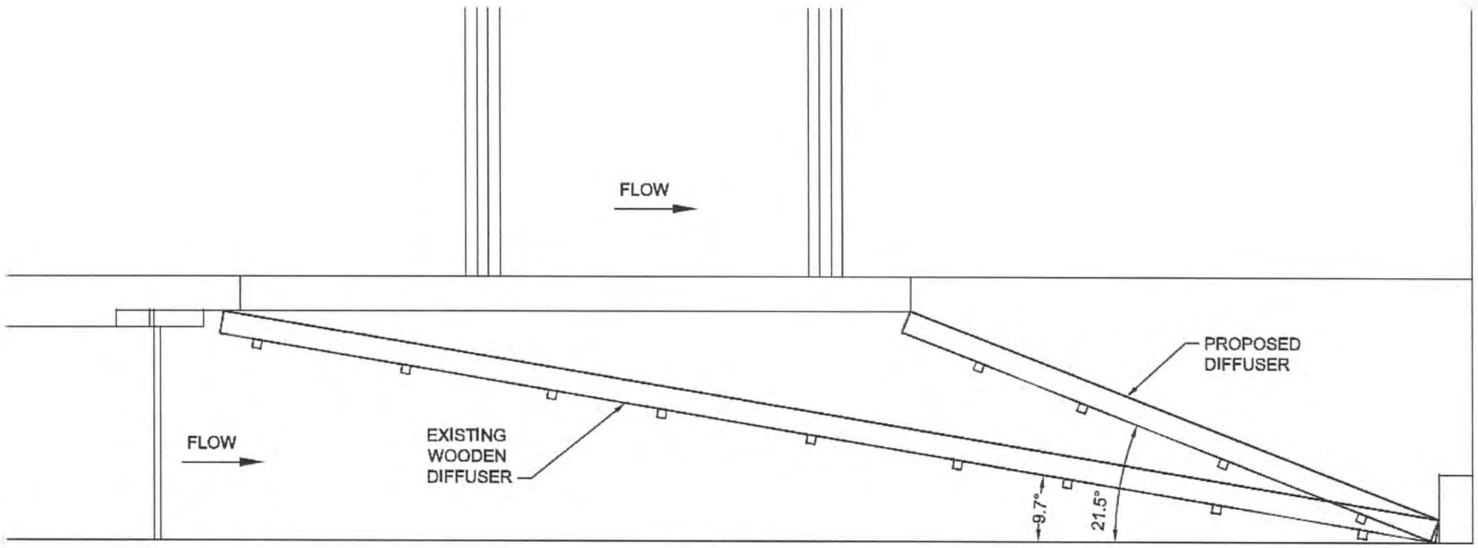

Figure 70 Schematic of Rev. 2.4 in Mod 2

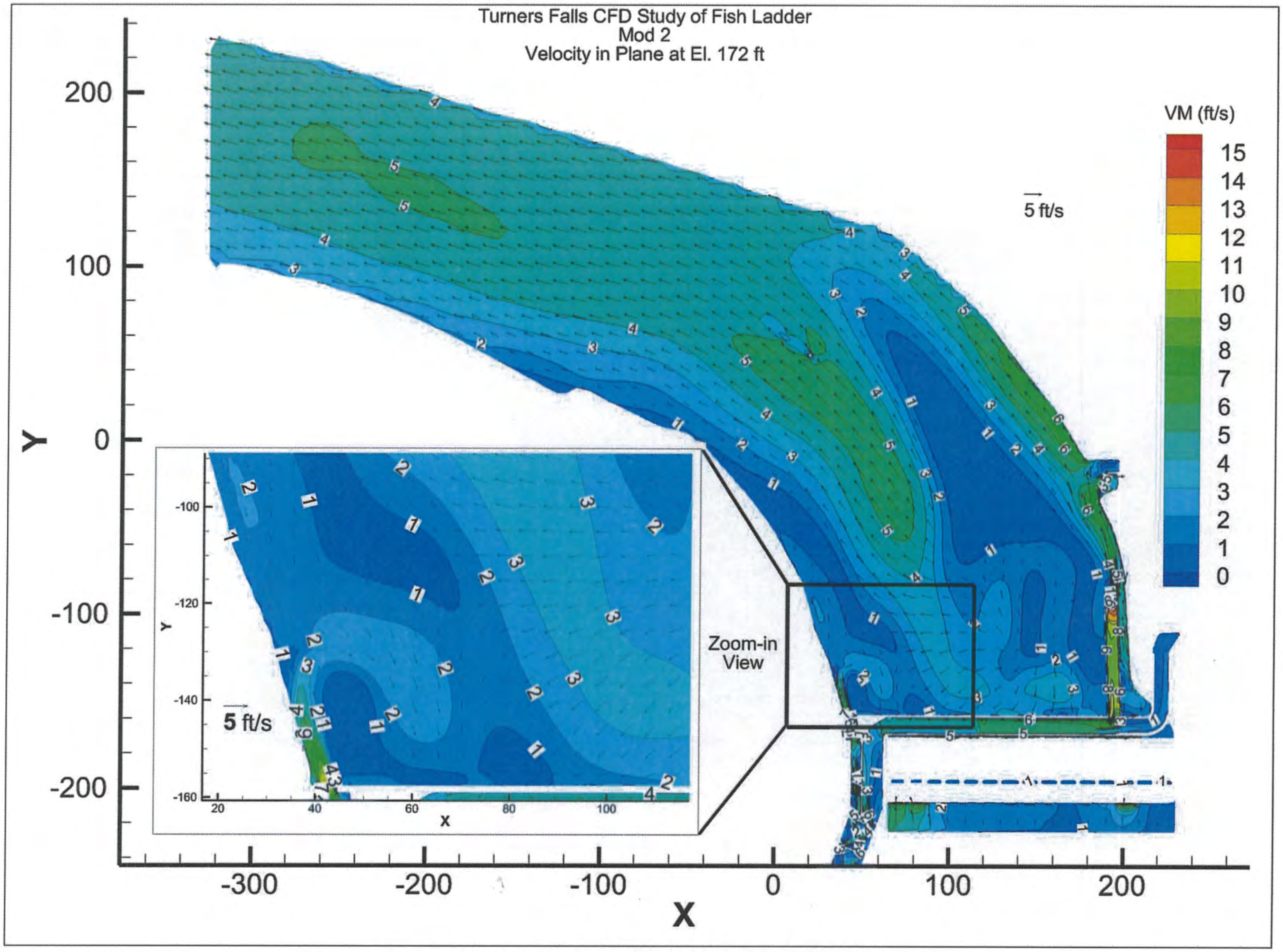

Figure 71 Mod 2: Velocity in Plane at El. 172 ft

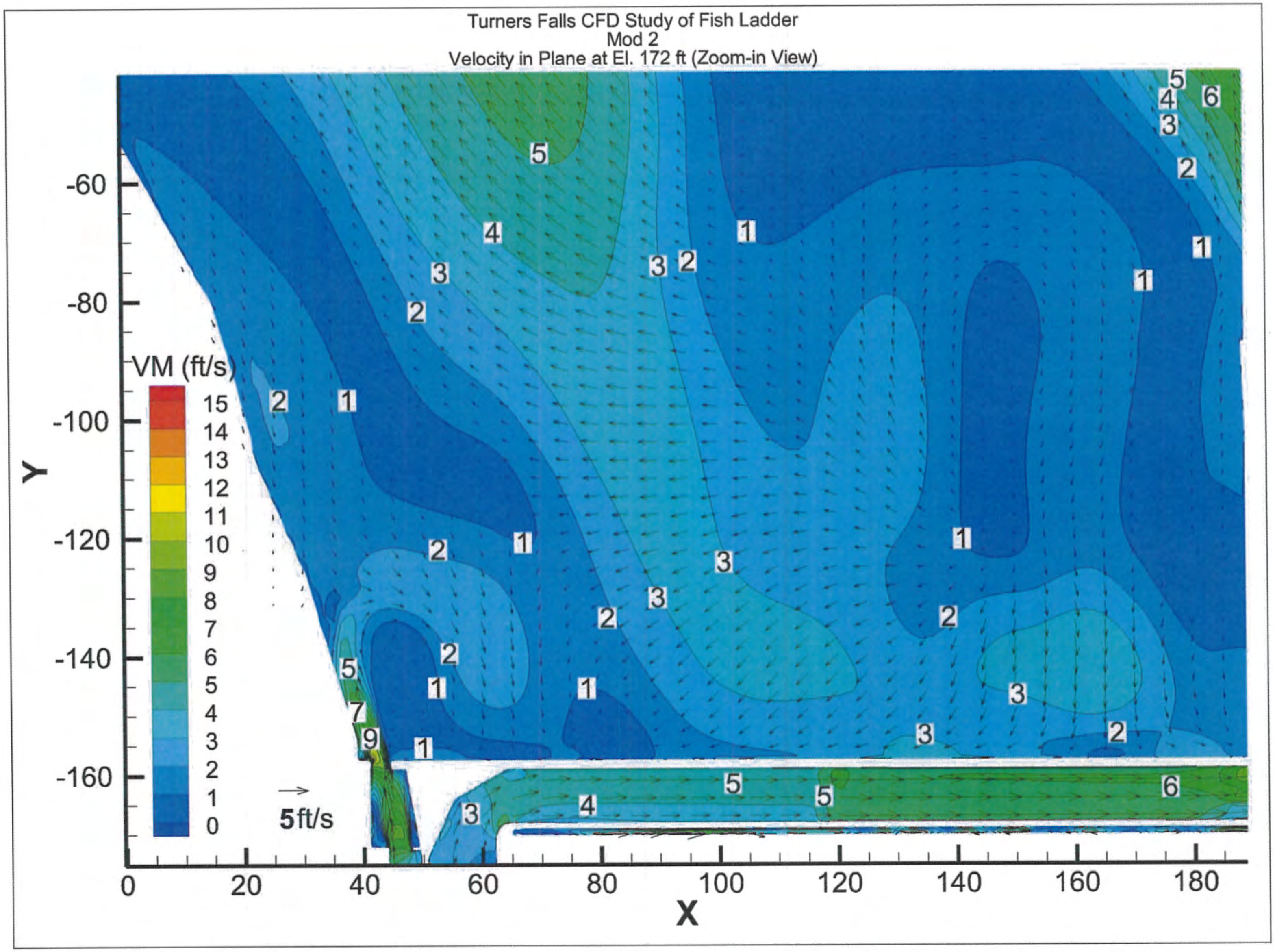

Figure 72 Mod 2: Velocity in the Vicinity of Old Entrance in the Canal in Plane at El. 172 ft

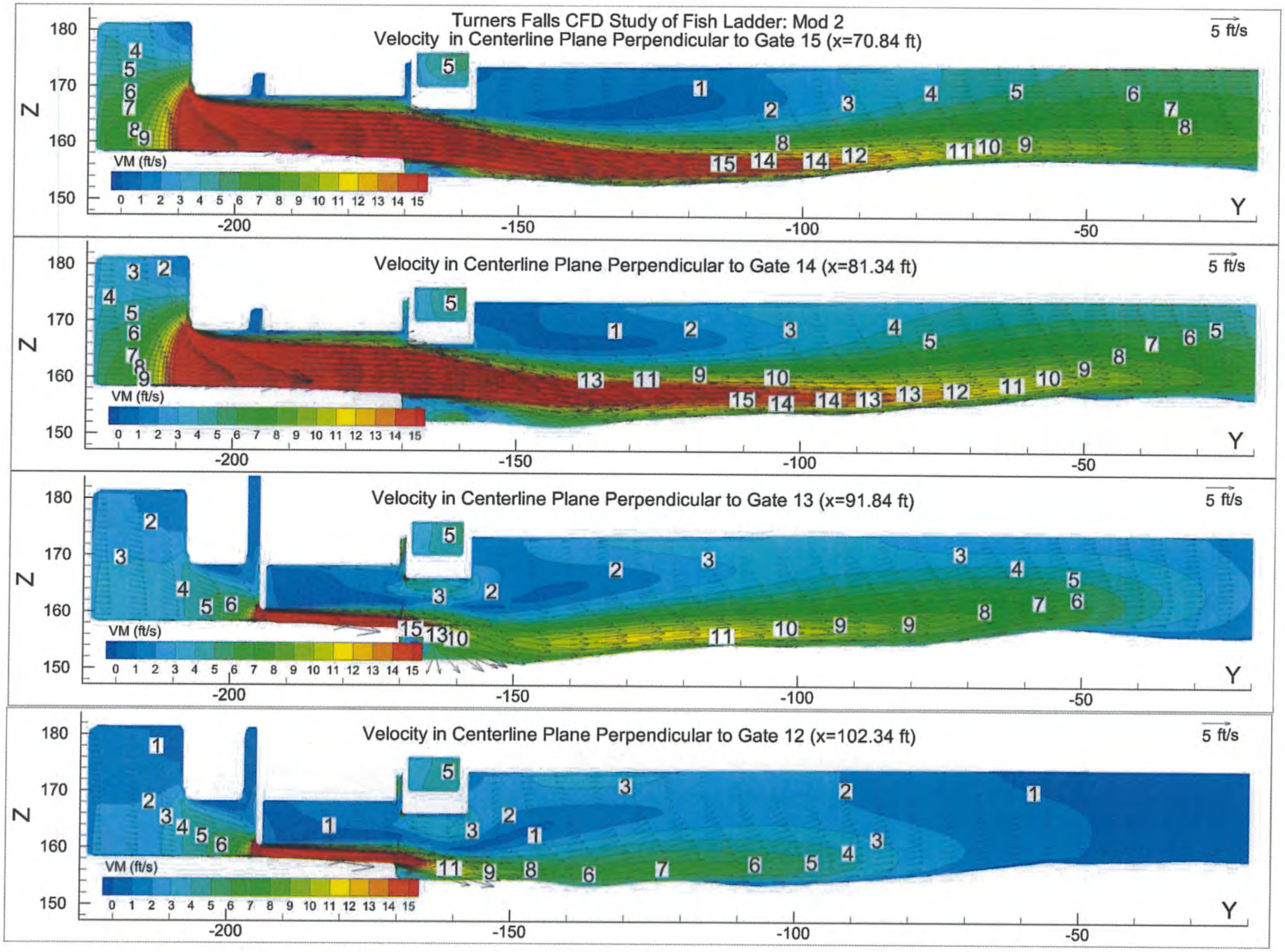

Figure 73 Mod 2: Velocity in Centerline Planes of Gates 12 through 15

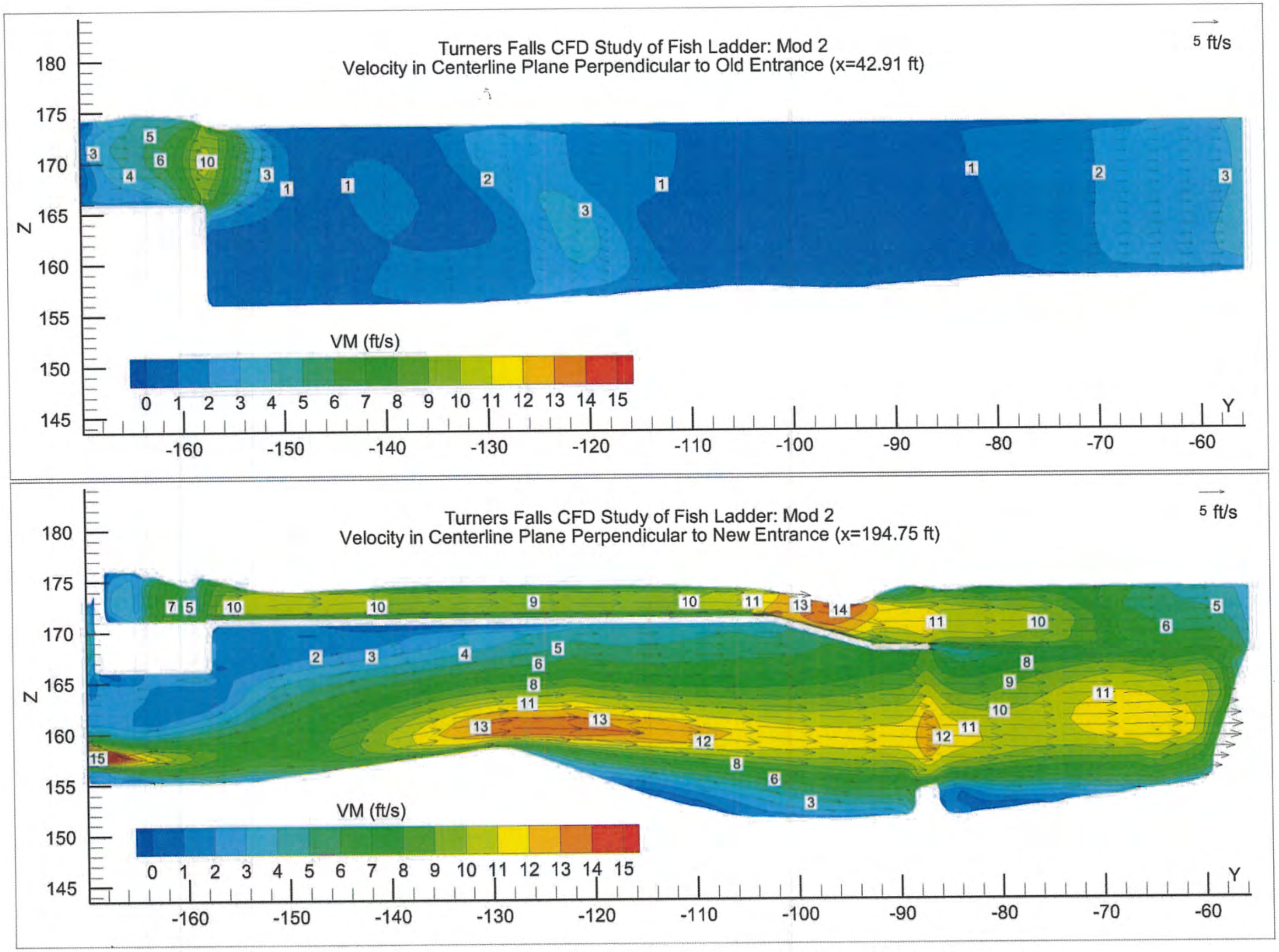

Figure 74 Mod 2: Velocity in Centerline Planes of Old and New Entrances

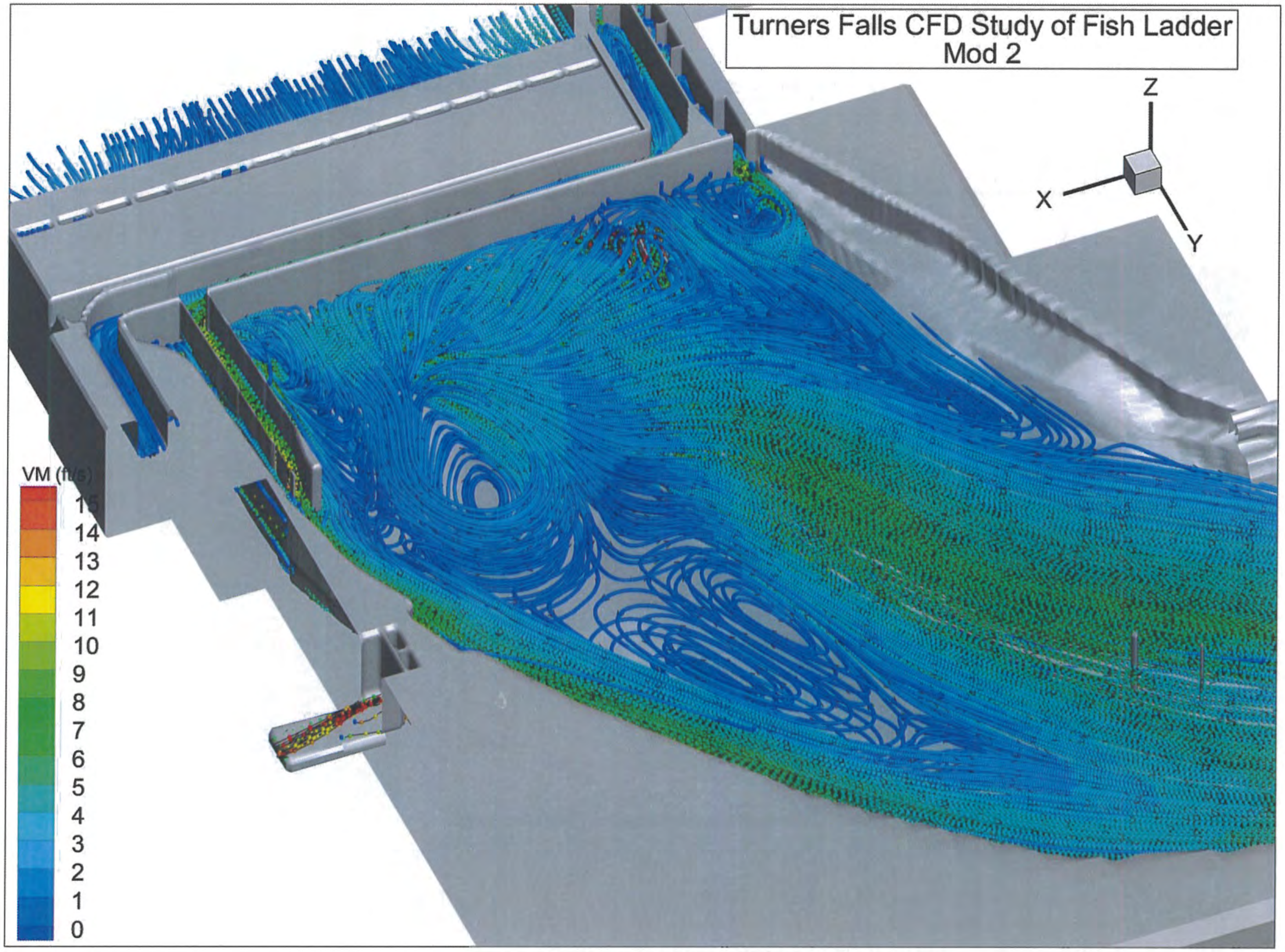

Figure 75 Mod 2: 3D Pathlines

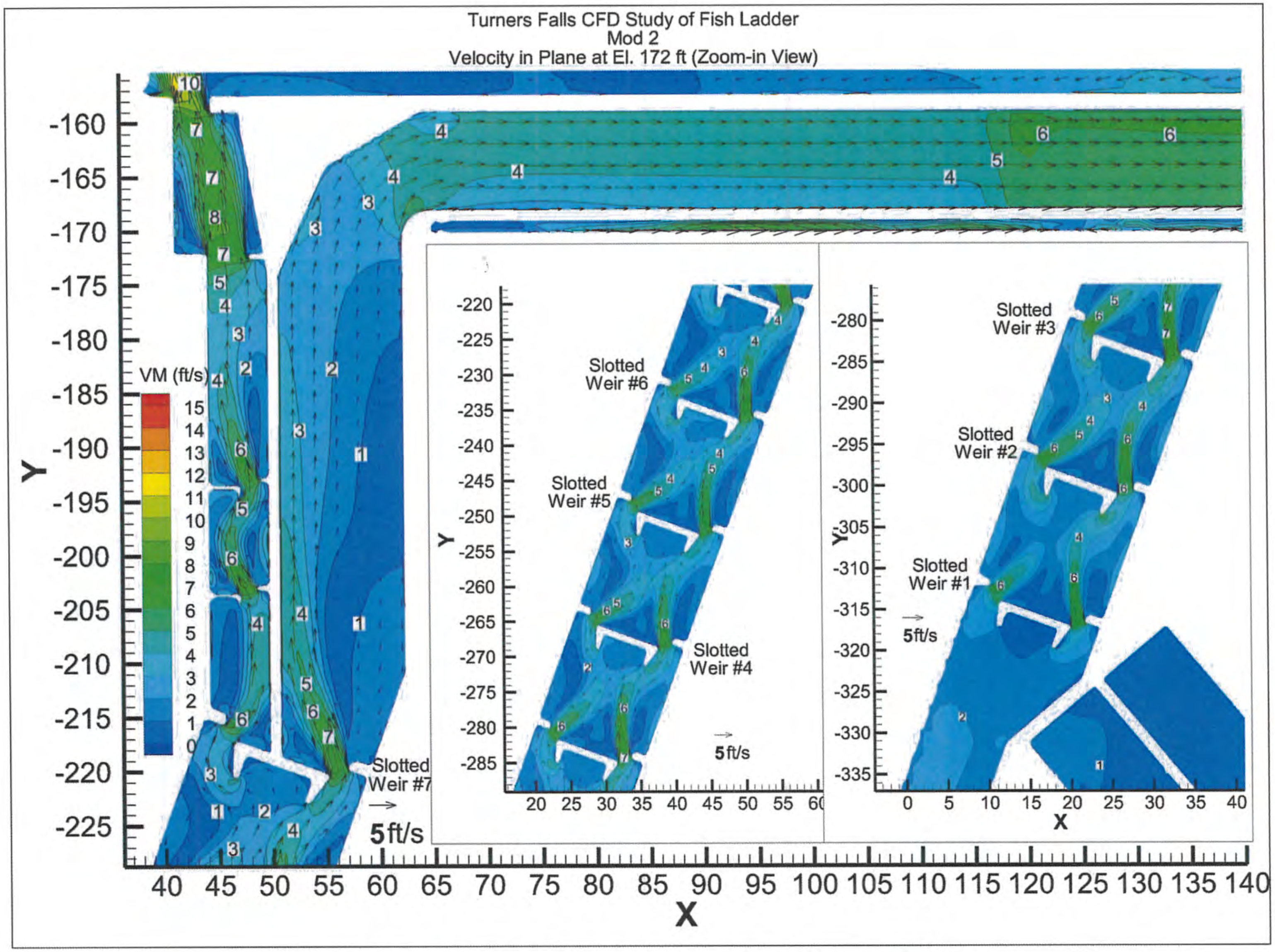

Figure 76 Mod 2: Velocity in Upstream Fish Way at El. 172 ft

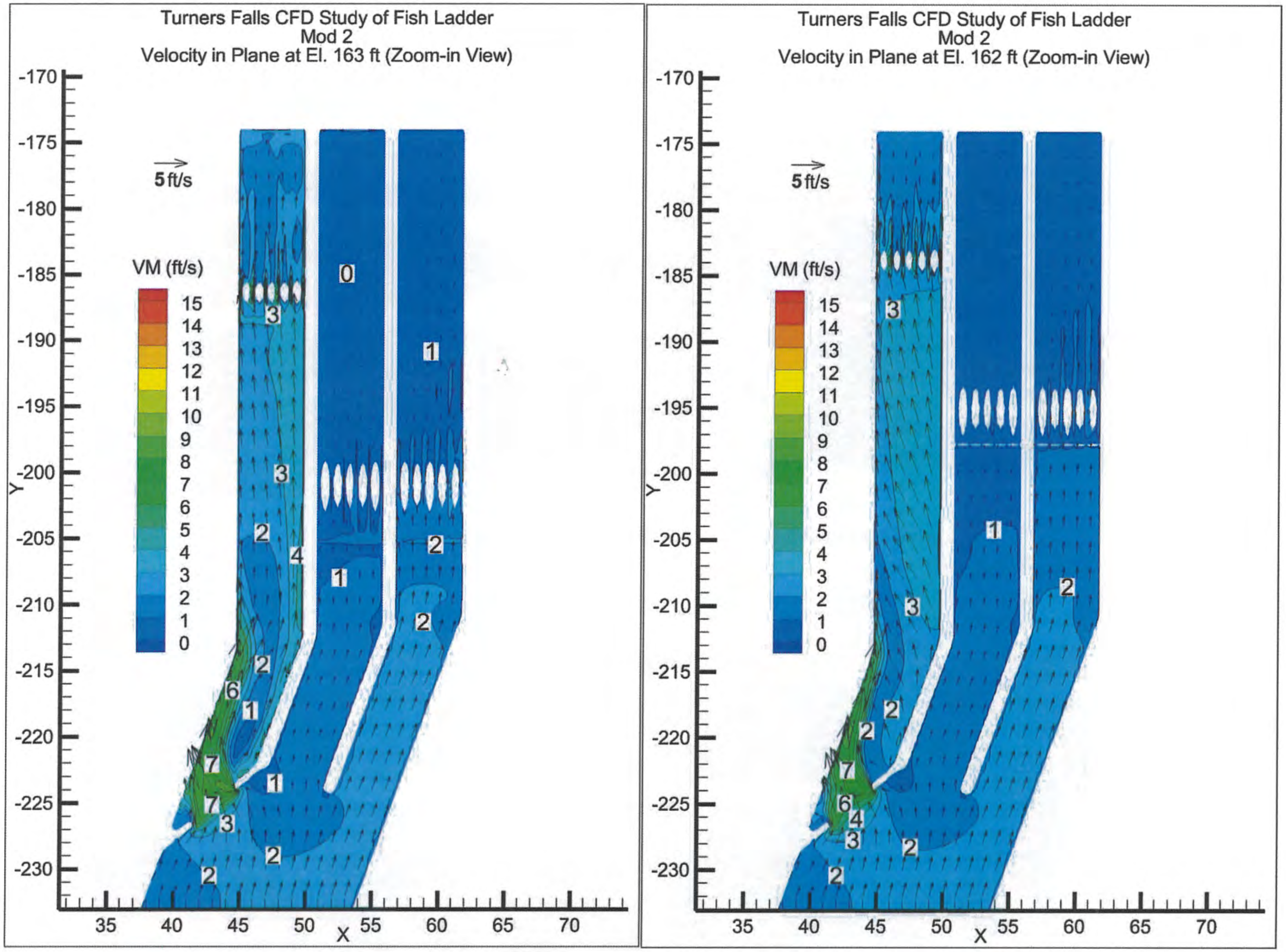

Figure 77 Mod 2: Velocity in Upstream Fishway at El. 163 ft and El. 162 ft

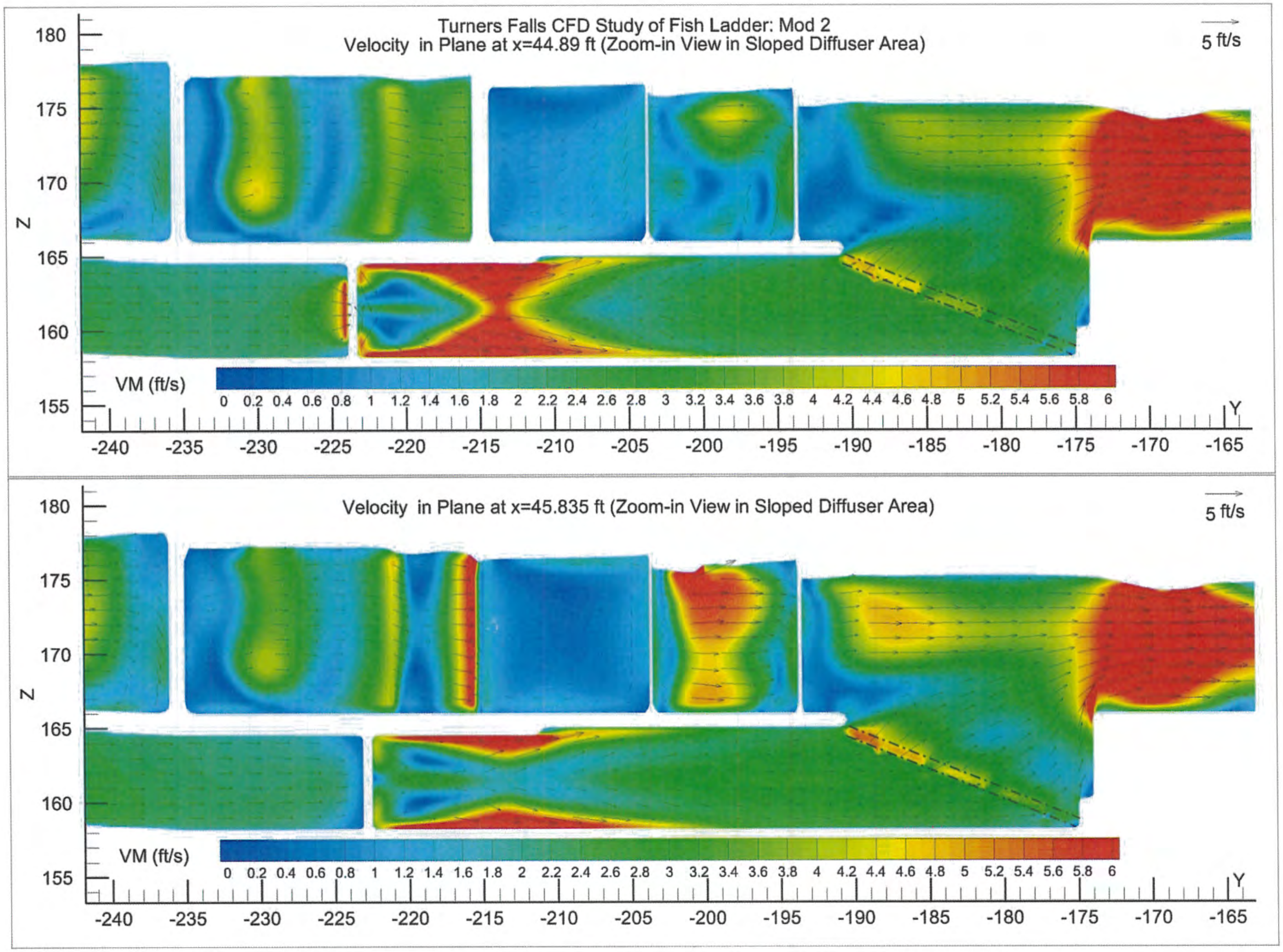

Figure 78 Mod 2: Velocity in Vertical Planes in the Left Sloped Diffuser Channel

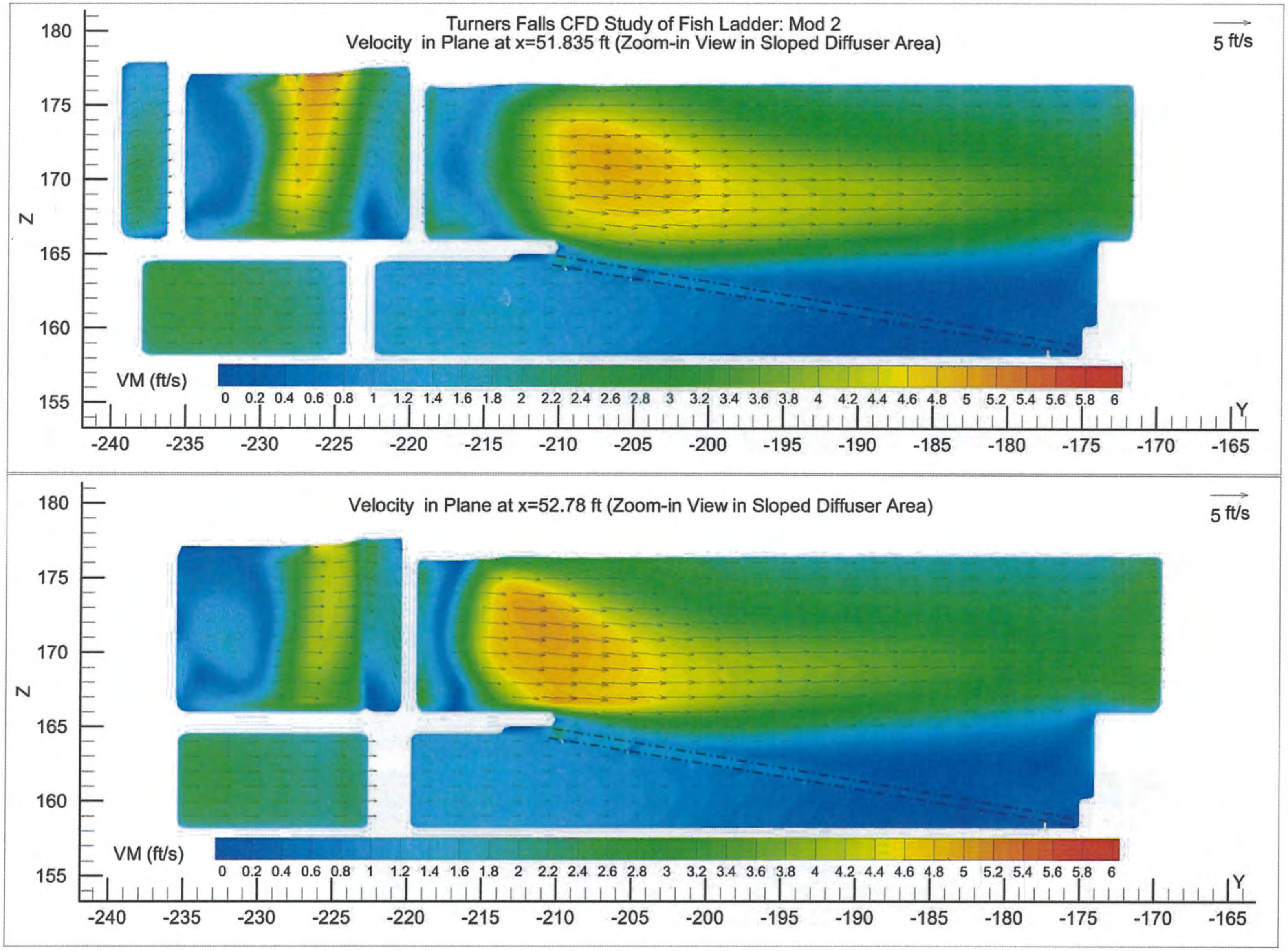
Turners Falls CFD Study of Fish Ladder: Mod 2
Velocity in Plane at x=51.835 ft (Zoom-in View in Sloped Diffuser Area)
5 ft/s
VM (ft/s)
Z
Y
Velocity in Plane at x=52.78 ft (Zoom-in View in Sloped Diffuser Area)
5 ft/s
VM (ft/s)
Z
Y

Figure 79 Mod 2: Velocity in Vertical Planes in the Right Sloped Diffuser Channel

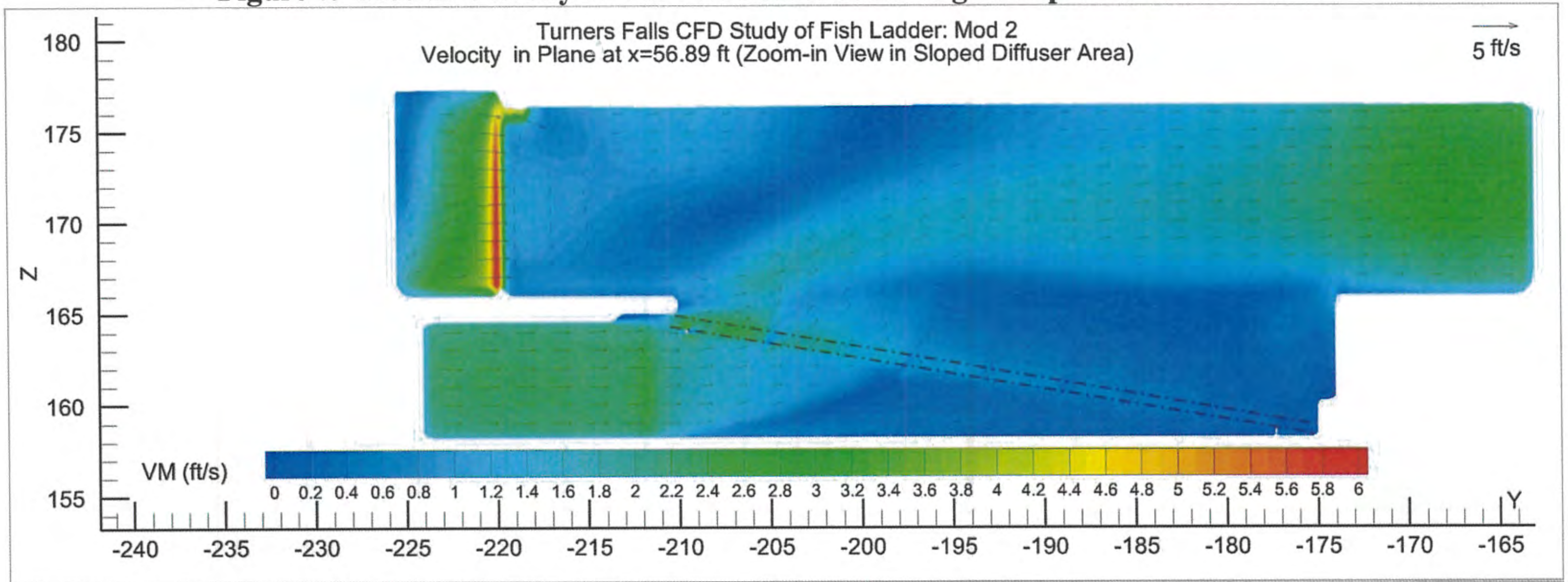

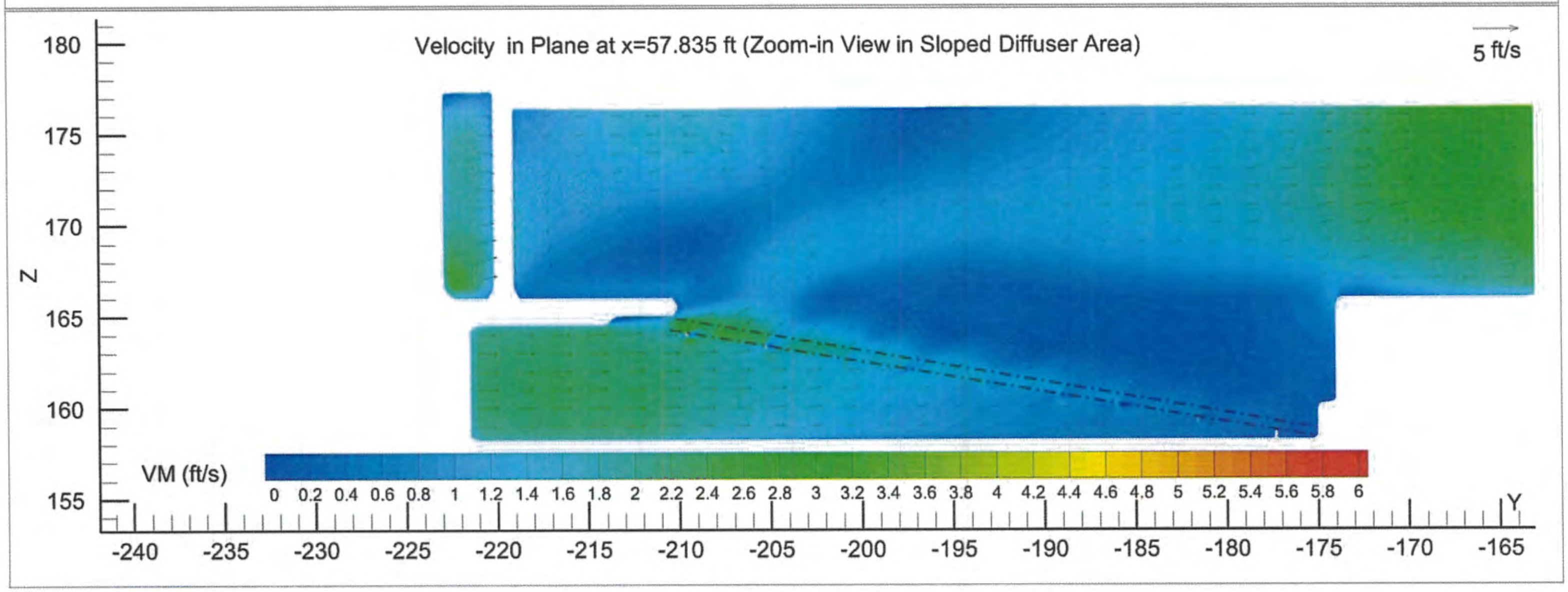

Figure 80 Mod 2: Velocity in Vertical Planes in the Right Sloped Diffuser Channel

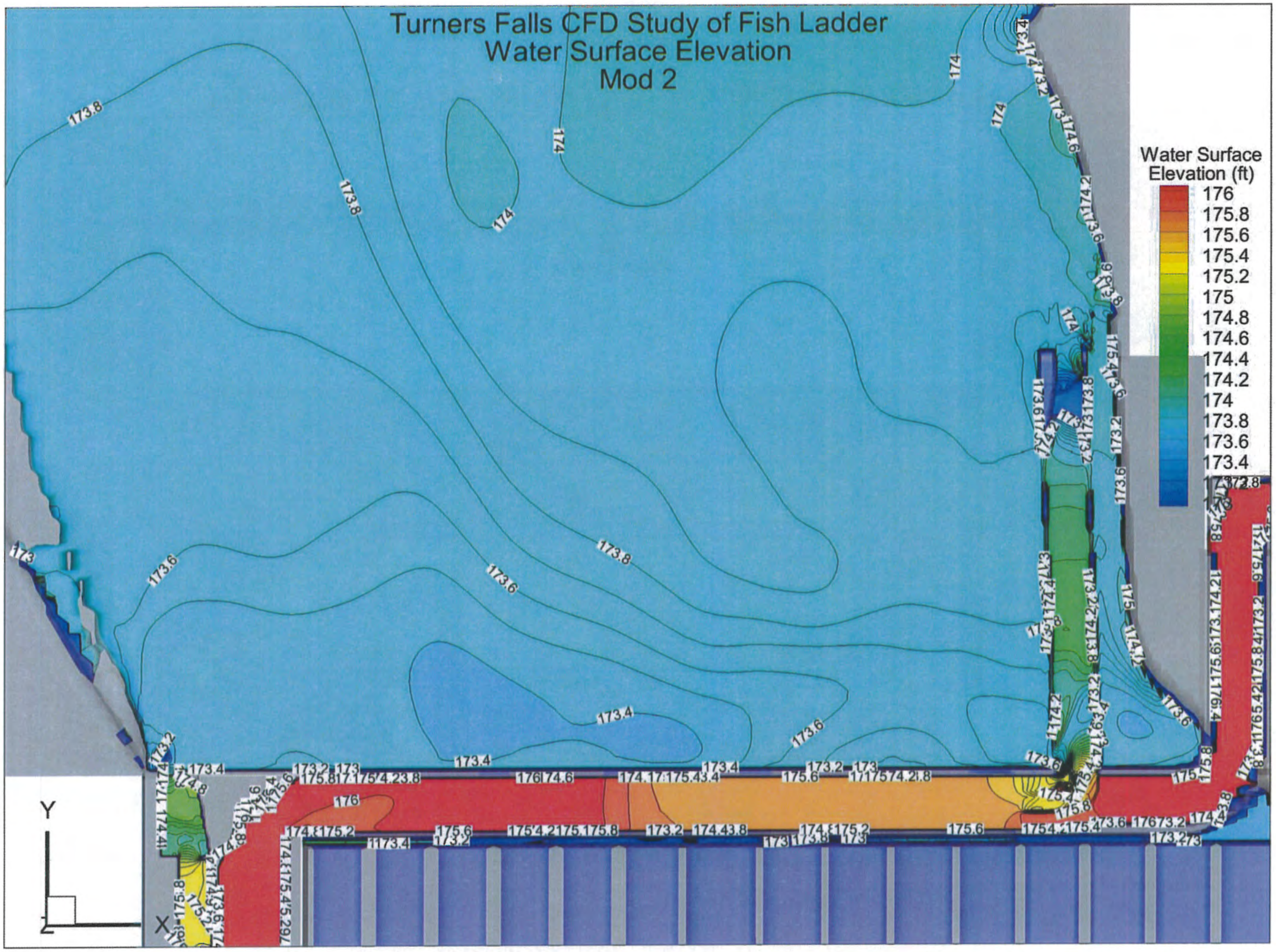

Figure 81 Mod 2: Water Surface Elevation in the Vicinity of Old and New Entrances in the Canal

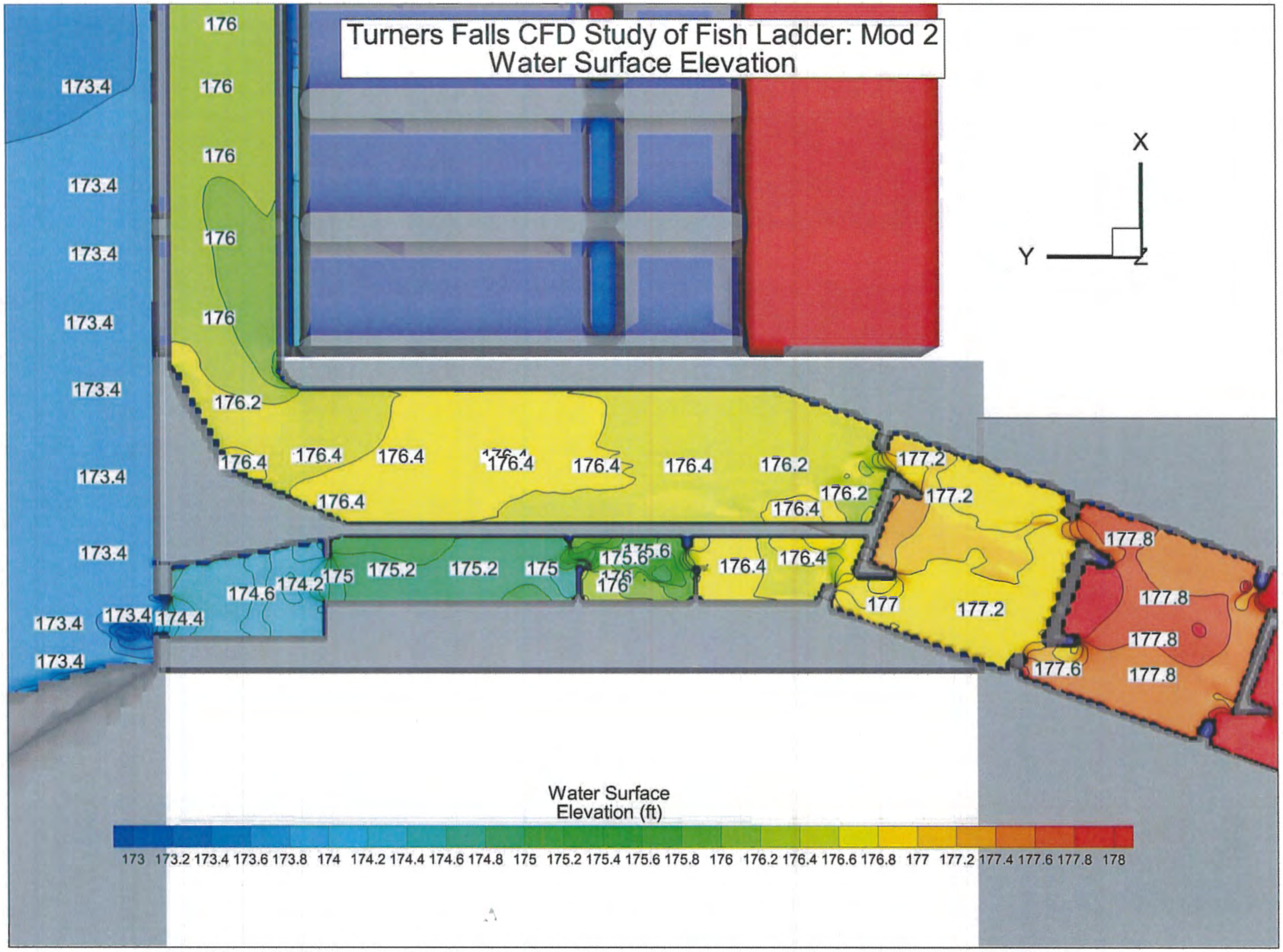

Figure 82 Mod 2: Water Surface Elevation in the Modified Area of Fish Way

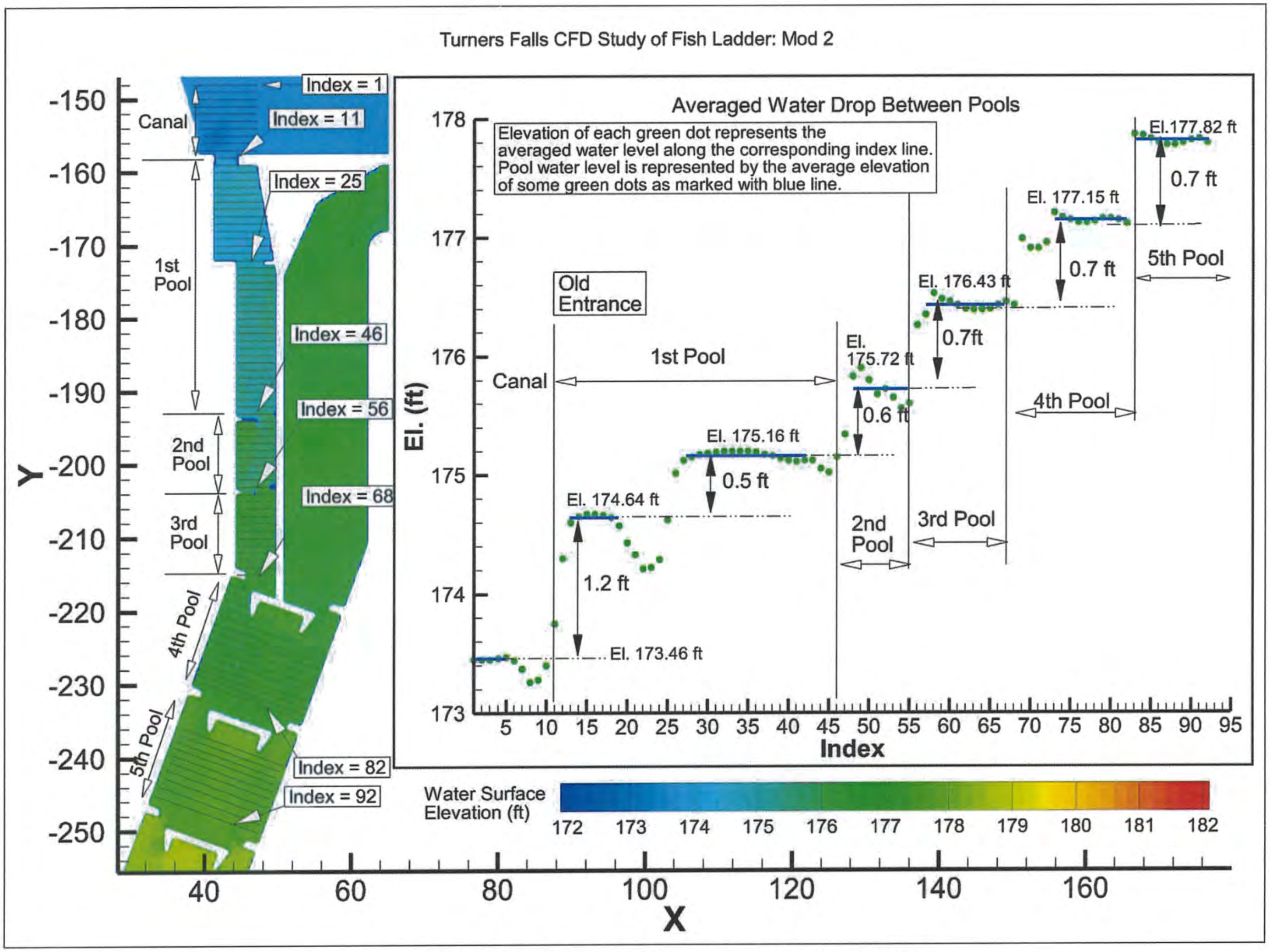

Figure 83 Mod 2: Averaged Water Drop between Pools

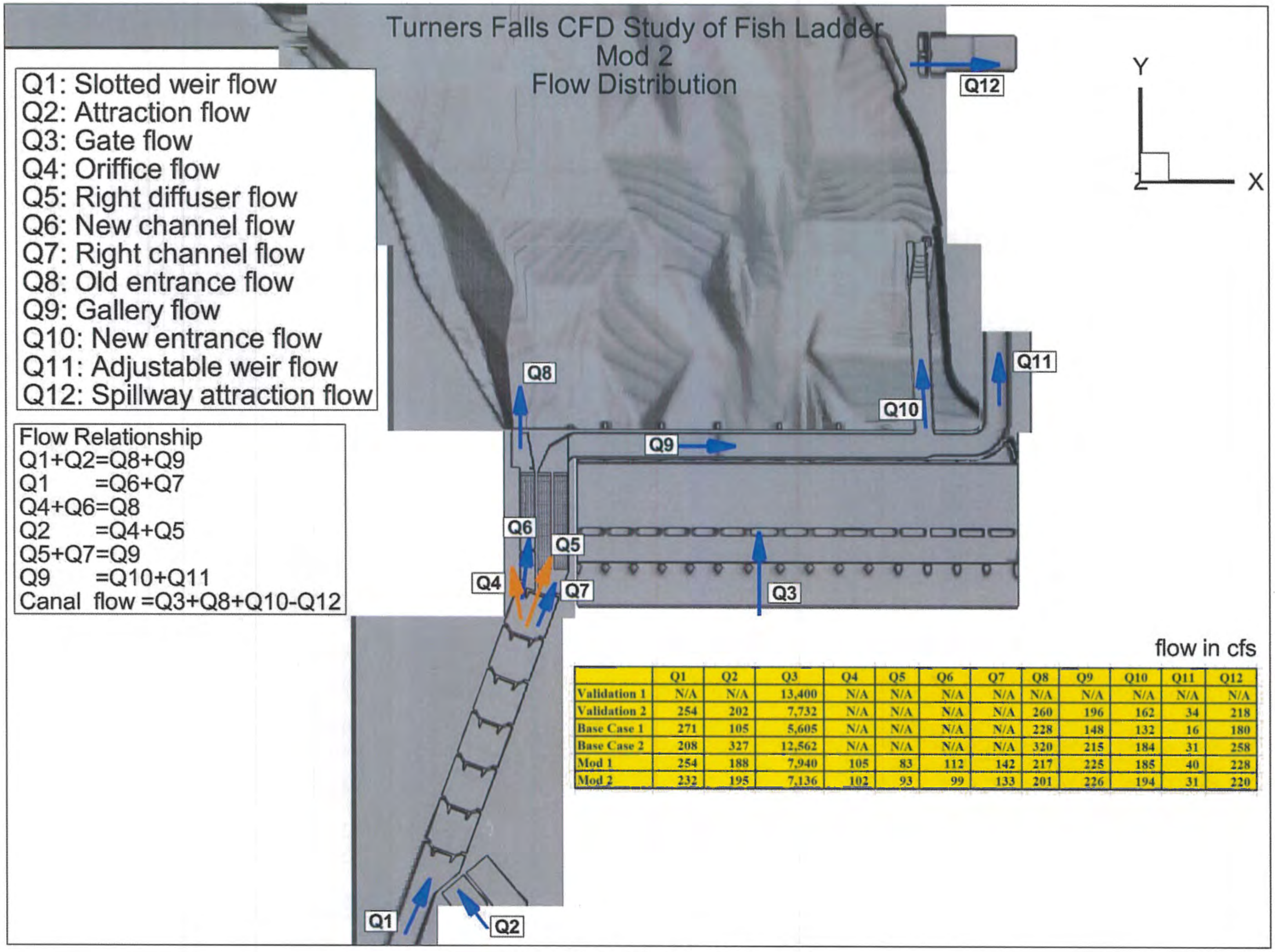

	Q1	Q2	Q3	Q4	Q5	Q6	Q7	Q8	Q9	Q10	Q11	Q12
Validation 1	N/A	N/A	13,400	N/A	N/A	N/A	N/A	N/A	N/A	N/A	N/A	N/A
Validation 2	254	202	7,732	N/A	N/A	N/A	N/A	260	196	162	34	218
Base Case 1	271	105	5,605	N/A	N/A	N/A	N/A	228	148	132	16	180
Base Case 2	208	327	12,562	N/A	N/A	N/A	N/A	320	215	184	31	258
Mod 1	254	188	7,940	105	83	112	142	217	225	185	40	228
Mod 2	232	195	7,136	102	93	99	133	201	226	194	31	220

Figure 84 Flow Distribution

Appendix G – 2011 Cabot Station Drawdown Juvenile American Shad Stranding Survey

MEMORANDUM

TO: FirstLight Power Resource Services, LLC

FROM: Chris Tomichek, Kleinschmidt Associates

DATE: September 16, 2011

RE: Cabot Station Drawdown Juvenile American Shad Stranding Survey

INTRODUCTION

FirstLight Power Resource Services, LLC (FirstLight) conducted a drawdown of the Cabot Station power canal on Saturday September 10, 2011 to facilitate station maintenance. FirstLight contracted with Kleinschmidt Associates (Kleinschmidt) to conduct a visual survey of the dewatered power canal to document stranded juvenile American shad. The survey was conducted by a team of three biologists from Kleinschmidt and two biologists from the Conte Anadromous Fish Lab. The survey documented no juvenile shad within the power canal, stranded or otherwise.

METHODS

Kleinschmidt segmented the canal into seven distinct zones. Zones 1-6 each about 1,000-ft long were located in the section of the power canal closest to Cabot Station. The final segment, Zone 7, was substantially longer as few shad were expected in the segment of the canal that runs through the village of Turners Falls. The zones were delineated in the field by the crew using a handheld Garmin Vista GPS. A map of the GPS data is available in Attachment A.

Each zone was surveyed and visually inspected for juvenile shad by survey teams consisting of at least two biologists. In addition to shad, the field crews collected data on other stranded or observed fish species, as well as information on the location of pooled areas. The data generated by this survey are available in Attachment A. The abundance of non-shad species was estimated.

RESULTS/DISCUSSION

No juvenile American shad were observed in the Cabot Station power canal. Several riverine species, including, various centrarchid and cyprinid species, chain pickerel, channel catfish, and carp were observed in most zones. Additionally, two diadromous species were observed, American eel and sea lamprey. The majority of stranding occurred in Zones 1-4. Areas of pooled water within the power canal, representative photos and the observed species, as well as an estimate of their abundance are available in Attachment A.

The results presented herein and within Attachment A represent those fish and canal features that were readily observable by field crews. Though the majority of the canal was observable, observations in areas where pools were inaccessible, relatively deep or highly turbid were limited.

Kleinschmidt
Energy & Water Resource Consultants

CONCLUSION

No juvenile American shad were observed in the dewatered Cabot Station power canal. Other riverine and diadromous species were observed especially in Zones 1-4. Kleinschmidt recommends reducing efforts in Zone 7 because leakage through the canal walls and gatehouse is apparently sufficient to maintain flow and depth through this section. The flow appears to be sufficient to support fish remaining in this section as it retains a relatively high proportion of water and will likely provide refugia for fish over the short term.

J:\1503\045\Docs\Report\001 Cabot Stranding Survey.9-16-11.docx

ATTACHMENT A

ID	Time	Coordinates
Zone 1	NA	N42 35 13.6 W72 34 42.2
Zone 2	9/10/2011 11:06	N42 35 23.2 W72 34 43.2
Zone 3	9/10/2011 11:25	N42 35 33.7 W72 34 43.5
Zone 4	9/10/2011 11:34	N42 35 40.8 W72 34 39.2
Zone 5	9/10/2011 11:41	N42 35 44.3 W72 34 32.8
Zone 6	9/10/2011 11:55	N42 35 48.7 W72 34 24.2
Zone 7	9/10/2011 12:03	N42 35 53.2 W72 34 11.3

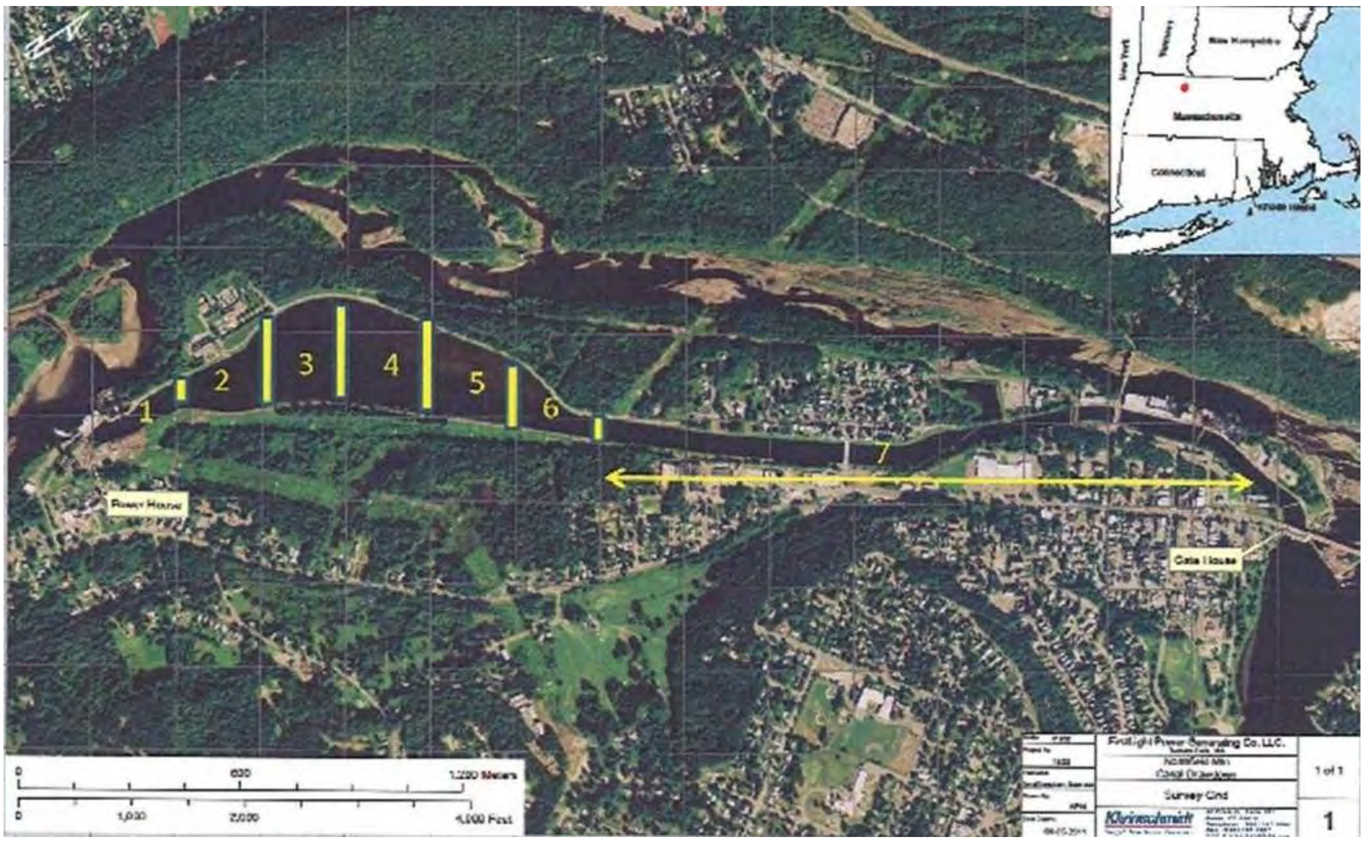

Location of Zones sampled during the survey. Coordinates are located on the west bank of canal and mark the edges of each section.

Zone 1

Observers	BRA,TM, KPN	
Survey Date	9/10/2011	
Survey Time	15:00	15:30

No Shad Observed

Species List	Estimate of Abundance
Sea Lamprey	600
Carp	1
Black Crappie	1
Centrarchids	
Sunfish Species	6
Smallmouth Bass	4
Chain pickerel	1
Cyprinids	
Spottail Shiner	Several 100
fall fish	Several 100
chubsucker	several

(a) 

 (b)

 (c)

Location of Zone 1 (a) and typical views of Zone 1 during the drawdown (b and c).

Zone 2

Observers	KPN, Matt (Conte)
Survey Date	9/10/2011
Survey Time	morning

No Shad Observed

Other Observed Species

Species List	Estimate of Abundance
Sea Lamprey	Several 1,000
Mussel Species	Several 1,000
Yellow Perch	Less than 1,000
Carp	Less than 100
Chain pickerel	Less than 100
Centrarchids	
Sunfish Species	Less than 1,000
Smallmouth Bass	Less than 100
Cyprinids	
Spottail Shiner	Less than 1,000
Fallfish	Less than 1,000
Daters	Less than 1,000

Zone 2 views during drawdown, photos taken along the West side of canal.

Zone 3

Observers	TM, Amy (Conte)	
Survey Date	9/10/2011	
Survey Time	11:30	12:10

No Shad Observed

Other Observed Species

Species List	Estimate of Abundance
Lamprey	Several 1,000
Mussel Species	Several 1,000
Yellow Perch	Less than 1,000
Carp	Less than 100
Chain pickerel	Less than 100
Centrarchids	
Sunfish Species	100's
blue gill and redbreast	
Smallmouth Bass	>50
Cyprinids	
Spottail Shiner	100's
Fallfish	100's
Daters	100's
common shiner	100's

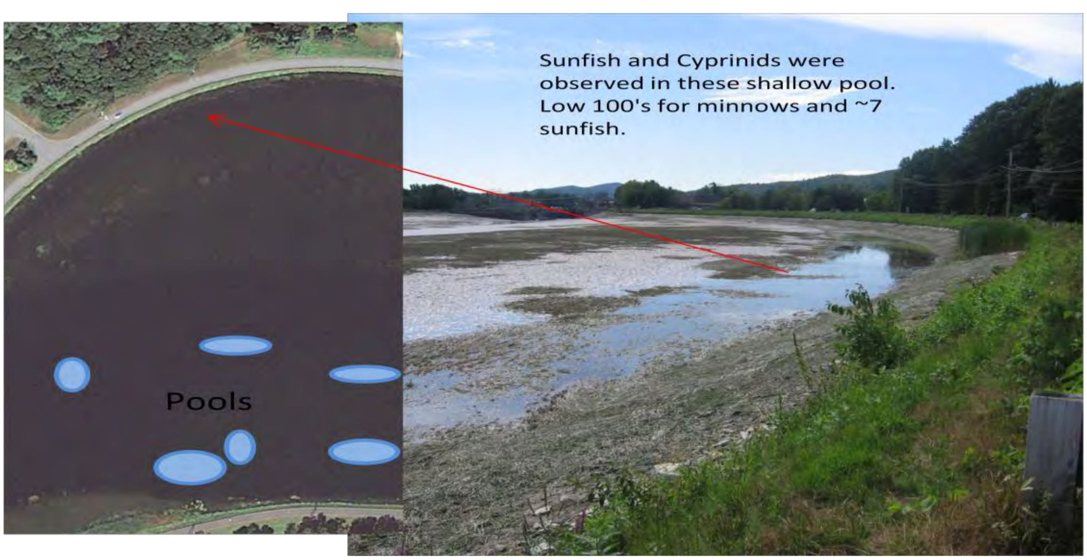

Zone 4

Observers	TM, Amy (Conte)
Survey Date	9/10/2011
Survey Time	12:10

No Shad Observed

Other Observed Species

Species List	Estimate of Abundance
Sea Lamprey	Several 1,000
Mussel Species	Several 1,000
Yellow Perch	Less than 1,000
American eel	2
Chain pickerel	6
mud puppy	1
Crayfish	Less than 1,000
Centrarchids	
Sunfish Species	Less than 1,000
Smallmouth Bass	Less than 50
Cyprinids	
Spottail Shiner	Less than 1,000
Fallfish	Less than 1,000
Daters	Less than 1,000
common shiner	Less than 1,000

Typical view of pools in Zone 4.

Zone 5 and 6

Observers	TM, Amy (Conte)
Survey Date	9/10/2011
Survey Time	12:35

No Shad Observed

Species List	Estimate of Abundance
Sea Lamprey	Several 1,000
Crayfish	10
Centrarchids	
Sunfish Species	20
Smallmouth Bass	10
Cyprinids	30

Typical view of Zone 5 and 6

Zone 7

Observers	TM, BRA, KPN
Survey Date	9/10/2011
Survey Time	13:30 15:00

No Shad Observed


Typical view of Zone 7. One small school of fish (species unknown) observed in Zone 7.

Document Content(s)